Polyurethane Rigid Foam from Soybean Oil-based Polyol

A THESIS
SUBMITTED TO THE FACULTY OF THE GRADUATE SCHOOL
OF THE UNIVERSITY OF MINNESOTA
BY

SUQIN TAN

IN PARTIAL FULFILLMENT OF THE REQUIREMENTS
FOR THE DEGREE OF
MASTER OF SCIENCE

Christopher Macosko, Tom Hoye, Advisors

Date: August 2010

Acknowledgements

I am indebted to many of my colleagues to support me during my master study at University of Minnesota. This thesis would not have been possible without all your help and encouragement. I owe my deepest gratitude to my advisors Professor Chris Macosko and Professor Tom Hoye for their long-term support. I still remember the time when Chris worked with me on the written preliminary exam and discussed with me about my iprogress. He provided me unflinching encouragement and support in various ways. His scientist intuition had made him as a constant source of ideas and passions in science, which exceptionally inspire and enrich my growth as a student and a researcher. I am indebted to him more than he knows. I would also like to thank Professor Tom Hoye and Professor Marc Hillmyer for reviewing my thesis and being the committee members of my thesis defense.

I am truly thankful for the financial supports from Cargill and Initiative for Renewable Energy and the Environment. I appreciate the chances to discuss my research progress with experts from Cargill. Tim Abraham, Don Ference and Dave Henton gave me a lot of good advice on the research.

I gratefully acknowledge many colleagues. Ling Zhang and Harikrishnan G were the first to guide me on the early stage of my research. I have learned a lot of polyurethane fundamentals from them. Dr. David Giles has helped me with rheometry and other polymer characterization techniques. Dr. Choi from Department of Mechanical Engineering has helped me a lot in developing the needle probe setup for k value measurement of polyurethane rigid foam. I owe my special thank to Bill in Machine Shop

who has helped me greatly in cutting samples. I thank Dr. Jinping Dong for his patience in discussing FTIR characterizations. I would also like to thank the staff in the University of Minnesota Characterization Facility have provided me their technical support for my research.

It is really a good time to spend my three-year graduate study in polymer group. Former and current group members Harikrishnan G, Ling Zhang, Carlos Lopez-Barron, Zhengxi Zhu, Hyunwoo Kim, Jie Song, Dawud Tan, Luca martinetti, Jing Han, Kirby Liao, Aaron Hedegaard, Darius Jaya and Randy Ewoldt are always here to give me support and encouragement. They make my lab life very enjoyable. Working with an undergraduate student is really a valuable experience. Jason Zhang is a very hard-working student, he is always full of enthusiasm and energy. The administrative staff in the Department of Chemical Engineering and Materials Science has made my study life here more convenient and organized.

I will never forget delivering my deepest love to my family and friends. Though in China, my dear parents are always there to encourage me. They are my greatest reason to live well and work hard. My boyfriend Weiwei Wu is always standing by my side ever since we met in China seven years ago. His love has supported me to conquer many difficulties.

Dedication

To my loved family and friends.

Abstract

Polyurethane rigid foams are widely used as thermal insulation materials. The general route to make polyurethane is through the reaction between polyol and isocyanate. Blowing agents are added to generate cell structure for foam applications. As people are becoming much more environmentally conscious, green products are becoming increasingly more mainstream. According to a life cycle comparison of soy-based polyol and petroleum-based polyol, the soy-based feedstocks showed 75% less total environmental impact than petroleum-based feedstocks with significant global warming reductions. Though some studies have shown that soy-based polyol has potential to replace petro polyol in rigid foam application, a systematic study is still needed. The goal of the thesis is to formulate polyurethane rigid foam from soy-based polyol, understand the mechanism behind the property deficiencies, and develop strategies to improve them.

Initially, a petroleum-based polyol with functionality of 4.4 and molecular weight of 690 g/mol was chosen as the control polyol. This was compared to a soy-based polyol (SBOP) with functionality of 4.4 and molecular weight of 1100 g/mol. It was found that soy-based foams had much higher density, k value (thermal conductivity), and poorer cell morphology. By adding glycerol, which can help to balance the gelling and blowing reaction, foam properties of density, k value, and cell morphology were greatly improved. Moreover, soy-based foams had a similar k value and k value aged with time, as control foams. Measurements of foam kinetic had shown that glycerol not only generated more heat for pentane evaporation to form cell structure, but also accelerated the build-up of crosslinks to support the cell structure.

Considering the structure difference between SBOP and petroleum-based polyol, the effect of surfactant on foam properties especially k value and its aging was investigated. Though soy-based foams from different surfactants did show different k value, only a small correlation between surfactant hydrophobicity and foam properties was observed. The average cell size increased slightly with increasing surfactant hydrophobicity.

Although glycerol improved foam properties significantly, foams with high glycerol addition had high flammability which was not favorable in industry. Additionally, due to the high polarity of glycerol, the reactive nature of soy foaming system was largely changed. Thus, a new formulation was highly desired in order to study the effect by solely replacing petroleum-based polyol with SBOP.

The second control polyol selected had lower molecular weight and lower functionality than SBOP, a glycerol free formulation was developed. In this formulation, exactly same type and amount of chemicals were used for both control polyol and SBOP. Soy-based foams had comparable density, initial k value, cell morphology, higher T_g, and compressive strength than petroleum-based foams. However, they showed much faster k value aging. The effect of solely replacing SBOP on foam k value aging was further studied. Foam k value aging was related to the permeability of CO_2, air and physical blowing agents. Permeability was measured through polyurethane thin films. Soy-based polyurethane thin films had much higher N_2 permeation than petroleum-based films, and N_2 had much higher k value than physical blowing agent pentane. Three different approaches were discussed to reduce N_2 permeation. They focused on the effect of

polymer intrinsic property (cohesive energy), polymer T_g (free volume theory) and the addition of physical gas barrier respectively.

Table of Contents

List of Tables

List of Figures

Chapter 1. Introduction: Polyurethane

1.1 Thesis Overview and Organization

The excellent insulating property combined with good adhesion, high strength-to-weight ratio and durability make polyurethane rigid foam an indispensible material in the construction industry. As consumers have increasing concerns on environmental impacts, it is highly desired to develop polyurethane feedstock from bio-renewable raw materials. Though some work has been done in developing soy-based polyurethane rigid foam, limited work has shown systematic study on the mechanism of soy-based foaming system. The research goal of the thesis is to develop polyurethane rigid foam system using only soy-based feedstock, investigate the mechanism behind the property deficiencies and develop strategies to improve them.

This chapter introduces the fundamentals of polyurethane chemistry and typical routes to synthesize natural oil-based polyol. Current progress in the literature on developing polyurethane rigid foam from soy polyol is deeply discussed.

In Chapter 2, Jeffol® SD-361 (commercially from Huntsman, denoted as Control A) was chosen as the control petroleum-based polyol and SBOP (experimental from Cargill) was chosen as the soy-based polyol. Aided with glycerol, soy-based polyurethane rigid foams had comparable density, k value (thermal conductivity), cell morphology and even higher compressive strength and T_g. Surfactant played an important role in foaming. The effect of surfactant on foam properties especially k value and its aging was studied in Chapter 3. However, high amount of added glycerol was not favorable in industry due to

the high foam flammability. Also, the control foams did not have glycerol, so we could not study the effect of solely replacing petroleum-based polyol with soy-based polyol if extra glycerol was added to aid in the soy system. Thus, it was desirable to develop a new system, which was more helpful in studying the limitation of SBOP in making polyurethane rigid foam.

In Chapter 4, Jeffol ® FX31-240 (commercial from Huntsman, denoted as Control B) was chosen as the second control petroleum-based polyol. A formulation was successfully developed to study the effect of SBOP on foam properties. Replacing only the petroleum-based polyol with soy-based polyol gave foams with comparable density, k value, cell morphology and higher T_g, compressive strength. However, k value of 100% soy-based foams aged much faster than that of petroleum-based foams. The mechanism behind the k value aging problem was proposed and studied in Chapter 5. Strategies were also discussed and developed to improve it.

1.2 Background

In 1849, Wurtzdhk Hoffman first reported the reaction of a hydroxyl-containing compound with an isocyanate.[1] But it was not until late 1930s that the polyurethane industry foundations were laid, and ever since then polyurethanes have been finding their places into different application fields and playing a more and more important role in many industries.[2] Polyurethane is a very versatile polymer and can be manufactured into different forms. In the U.S., the polyurethane market has been on a stable growth track

over the past few decades. Between 2002 and 2004, polyurethane production grew 10.8% per year. [3]

Polyurethane rigid foam accounts for about 23% among all polyurethane application. According to the U. S. Department of Energy, heating and cooling account for about 56% of the energy used in a typical U.S. home. Polyurethane rigid foam, which has high insulating value and high strength-to-weight ratio, is one of the most effective thermal insulation materials, usually used in construction and refrigerator industries. Polyurethane rigid foam is the primary concern in this research.

1.3 Polyurethane Chemistry

Polyurethane is the polymer that contains urethane links (-NH (CO) O-) in the chain. The general route to make polyurethane is by reacting a hydroxyl-containing compound with two or higher functionality ($f_n \geq 2$, functionality, f_n is the average number of OH groups in a molecule) with a diisocyanate or isocyanate with higher functionality. [2, 4] An oligomer containing multiple OH groups is called a polyol. Typically, there are two competing reactions during foaming: gelling and blowing. Figure 1.1 shows these two chemical reactions. Gelling is the process that isocyanate reacts with polyol to produce urethane links (-NH (CO) O-) for polymer networks. Blowing process is that isocyanate reacts with water to form urea links (-NH (CO) NH-) and release carbon dioxide. For simplicity, the reactions are shown in terms of monofunctional compounds. For water-blown polyurethane rigid foam, initially, the polyol is mixed with surfactant, catalysts, water, and physical blowing agent. Then isocyanate is added into the mixture and

reaction starts. Air bubbles are introduced into the mixture during mixing and served as the foam cell nuclei.[5] Water reacts with isocyanate and produces a carbamic acid, which quickly decomposes into amine and carbon dioxide. The added physical blowing agent evaporates due to the highly exothermic reaction. The diffusion of carbon dioxide and the evaporated physical blowing agent into the air bubbles causes the foam to rise. Meanwhile, the polyol reacts with isocyanate to form the cross-linking structure and produce polymer networks. [2, 4-6] Unlike flexible foams, which phase separate into urea-rich hard segments and polyol-rich soft segments, rigid foams are phase mixed and homogeneous. Under high temperature and the presence of catalyst, excess amount of isocyanate undergoes trimerization and forms isocyanurate rings (see Figure 1.1). Isocyanate index, which is used to indicate the excess of the isocyanate, is defined as the value of actual amount of isocyanate added over the stoichiometric amount of isocyanate required to just react all the active hydrogens in the polyol and water times 100. Polyurethane rigid foam can be separated into two types by their isocyanate index: polyurethane rigid foam (PUR) and polyisocyanurate rigid foam (PIR). Generally, isocyanate index is larger than 200 in PIR foam while smaller than 150 in PUR foam. The study in this thesis is focused on PUR foam with low isocyanate index.

1.4 Raw Materials for Polyurethane

In the manufacture of polyurethane foam, isocyanates and polyols are the most important raw materials. Their physical properties, such as structure and molecular weight, and their chemical properties, such as reactivity and stability, have a great effect on the polymerization process and properties of the final polyurethane products. Catalysts,

surfactants, blowing agents, and cross-linkers are used to modify the properties of the products.

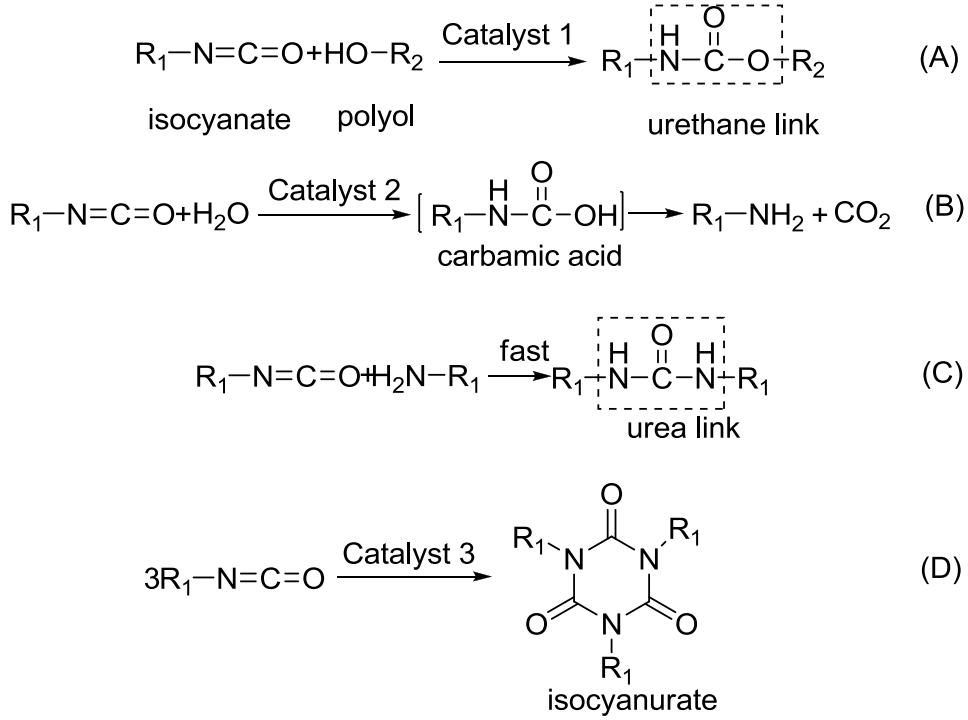

Figure 1. 1: General chemical reactions to synthesize polyurethane foam: (A) isocyanate reacts with polyol to produce urethane networks; (B) isocyanate reacts with water to produce amine and carbon dioxide; (C) isocyanate reacts with amine to produce urea links; (D) isocyanates trimerization.

1.4.1 Isocyanate

Different isocyanates are available to meet with different polyurethane applications. Molecular shape, functionality, and reactivity will all influence the properties of the derived polymer. Compared to aliphatic isocyanates, aromatic isocyanates are more reactive and economical accounting for the major use in polyurethane foam application.[2,4,6] Two most important aromatic isocyanates are toluene diisocyanate (TDI)

and methylenediphenyl diisocyanate (MDI). TDI is usually a mixture of 2, 4- and 2, 6- isomers. The number followed by TDI represents the percentage of the 2, 4- isomer. For example, the most important commercial isocyanate TDI-80 contains 80% 2, 4- isomer and 20% 2, 6- isomer. [2] Besides pure TDI isomers, crude TDI is also used. MDI has three isomers: 4, 4'-, 2, 4'- and 2, 2'-. The 4, 4'- isomer, which is much less volatile than the other two MDI isomers, is used most often to produce polyurethane rigid foam. The resulting foam has much higher compressive strength compared to TDI. [6] TDI is used extensively in flexible foam manufacture. Crude TDI and TDI/MDI blends can be used in rigid foam applications. Currently, polymeric MDI (pMDI), which is the oligomer of MDI, is the predominant isocyanate used in rigid foam due to its low viscosity, and higher functionality. [6] The structures of the typical isocyanates are shown in Figure 1.2.

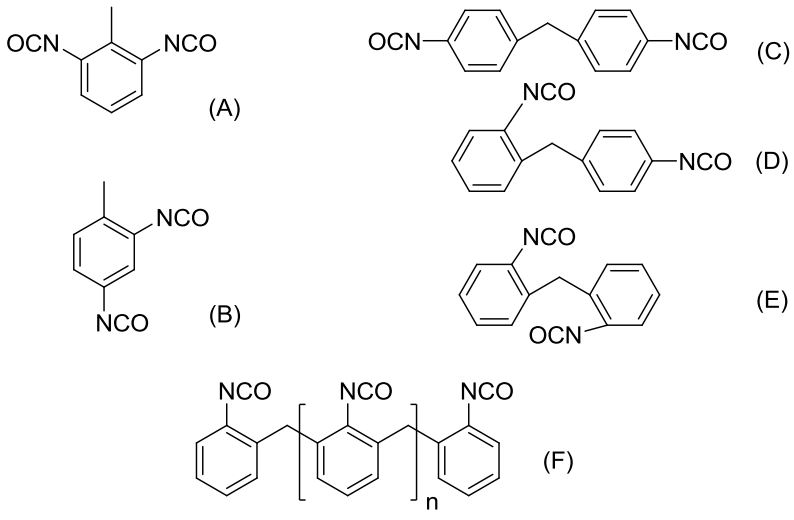

Figure 1.2: Isocyanates used in polyurethane foams: (A) 2,6-TDI; (B) 2,4-TDI; (C) 4,4'-MDI; (D)2,4'-MDI; (E) 2,2'-MDI; (F)pMDI.

1.4.2 Polyol

There are mainly two classes of polyol used in polyurethane manufacture: polyether and polyester. The molecular weight and functionality of the polyol plays an important role in determining the properties of the final polyurethane products.[2,7,8] Table 1.1 shows the characteristics of the polyols used in polyurethane rigid foams and flexible foams. The OH number is a measure of the concentration of OH groups per unit weight of the polyol and is expressed as mg KOH/g. The value of OH number is the ratio of functionality to the molecular weight of the polyol. Equation 1.1 shows this relationship.[9]

$$\text{OH number (mg KOH/g)} = \frac{56.1 \times \text{functionality}}{\text{molecular weight}} \times 1000 \qquad \text{Equation 1.1}$$

Table 1.1: Polyols for different polyurethane applications. [9]

Polyol Property	Flexible Foams	Rigid Foams
Molecular Weight (g/mol)	1000-6500	150-1600
Functionality (f_n)	2-3	3-8
OH number (mg KOH/g)	28-160	250-1000

The general route to synthesize polyether polyol is through anionic polymerization. An initiator with two or more active hydrogens is added to initiate ring opening and oxide addition of the alkylene oxides. Water or acids are used to terminate the polymerization.[11] Polyols for rigid foams use high functionality initiator such as sucrose

(f_n=8), sorbitol (f_n=6) or toluenediamine (f_n=4); polyols for flexible foam use low functionality initiator like glycerin (f_n=3). Ethylene oxide and propylene oxide are the most common alkylene oxide monomers. [4] In my experiment, I will use propylene oxide-based polyether type polyol as the control.

Conventional polyesters are synthesized from direct polyesterification of diacids and glycols, like adipic acid and 1, 4-butanediol. Other polyesters can be made by transesterification of poly (ethyleneterephthalate) (PET) or dimethylterephthalate (DMT) with glycols. [4, 7] Figure 1.3 shows the structure of the polyether and polyester.

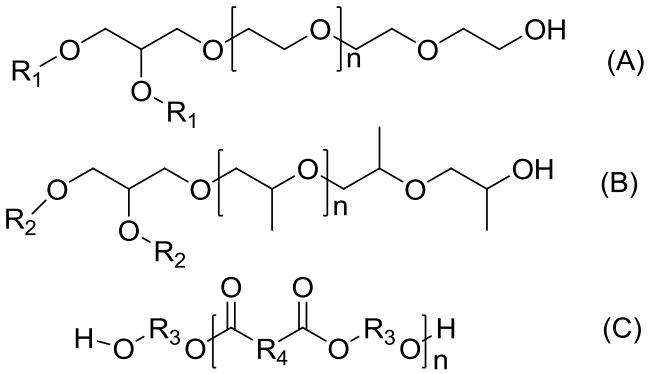

Figure 1.3: Polyether polyols made from ethylene oxide (A) and propylene oxide (B); and (C) linear polyester.

1.4.3 Blowing Agent

The blowing agent is essential in generating cell structure during the foaming process. Chemical blowing and physical blowing are two major blowing types.

Carbon dioxide generated from the reaction between water and isocyanate is a widely used chemical blowing agent. As discussed before, water reacts with isocyanate

and produces a carbamic acid, which quickly decomposes into amine and carbon dioxide.[2]

The most widely used physical blowing agents in polyurethane rigid foams used to be chlorofluorocarbons (CFCs) and hydrochlorofluorocarbons (HCFCs). They have low boiling points, low k value, and low flammability. They also have a suitable solubility in both the reaction mixture and the polyurethane foam. However, due to their depletion of the ozone layer, CFCs are banned now and HCFCs are being replaced by substitutes such as hydrofluorocarbons (HFCs) or hydrocarbons (HCs) (e.g., cyclopentane), which show much lower depletion of the ozone layer. However, many factors must be considered when choosing alternative physical blowing agents. Some important factors include environmental effects, such as ozone depletion and global warming, industrial processing feasibility, as well as product performance. Actually, these substitutes have various problems. For example, HFCs have a low boiling point and low solubility in reaction mixture. Some will even decompose to harmful substances. [2,4] Cyclopentane has high flammability and may cause explosion when mixed with air. Also, cyclopentane is immiscible in the foaming mixture. [2] Nevertheless, HFCs and HCs are still the predominant blowing agents being used. Effort has been devoted to improving their effectiveness. For instance, HCs can be mixed with halohydrocarbons to form a non-flammable mixture. [4] In my study, I will use n-pentane as the physical blowing agent.

1.4.4 Catalyst

Catalysts are used not only to control the overall reaction rate but also to balance the reactions between polymer network formation (polyol/isocyanate reactions) and blowing (H_2O/isocyanate reactions) in order to obtain the desire foam properties. Tertiary amines, and organometallics (mainly tin compounds) are two dominant catalysts used. Catalysts work through the formation of transient complexes between the catalyst and isocyanate.[2] Tertiary amines can catalyze both the gelling reaction and the blowing reaction, but they tend to catalyze blowing reactions and are usually considered as the blowing catalysts.[2] But the relative reaction rate of gelling and blowing processes depends greatly on the catalyst structure. Specific amine catalysts can be chosen to control those two reactions. Organometallic catalysts are more reactive than the amine catalysts, and are usually used in small amount. They mainly catalyze gelling reaction and are usually considered as the gelling catalysts. Thus, by selecting suitable types and amounts of catalysts, the rate of these two different reactions can be adjusted. Diazabicyclooctane (DABCO, Figure 1.4) is the most active amine catalyst. For example, if the blowing reaction is preferred, more tertiary amine can be added; while organometallic catalysts can be added to favor the gelling reaction.

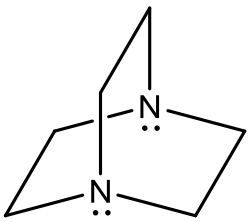

Figure 1.4: DABCO structure.

1.4.5 Surfactant

Surfactants are very important in polyurethane foaming. Good mixing among polyol, isocyanate, catalysts, water, blowing agent, and et al. is essential to get homogeneous

foams with low density. Surfactants can help to promote good mixing during foaming. More importantly, surfactants can reduce the work required to increase surface area, prevent bubbles from collapse, and stabilize cell structure. [5] Non-ionic organosilicon-polyether copolymers are currently used as the major surfactants. The effect of the surfactant in the foaming mixture can be widely adjusted by varying the molecular weight ratio of polyether and siloxane. The content of ethylene oxide and propylene oxide can be changed to alter the polarity and hydrophobicity of the polyether. Also, branching chains can be introduced to either silicone or polyether and different end groups can be capped into the chain end. [5] This flexibility makes it possible to adjust the properties of the silicon surfactants to meet different foam applications. The structure ranges of surfactants used in polyurethane rigid foams are shown in Table 1.5.

1.4.6 Chain Extenders and Cross-linkers

Chain extenders are difunctional glycols, diamines or hydroxyl amines. They are used in flexible foams, elastomers and reaction injection molding systems. Cross-linkers ($f_n \geq 3$) are low molecular weight compounds with a hydroxyl or amine terminus. Cross-linkers like glycerol have high functionality and act as the cross-linking or branching agents. [3] Cross linkers are used to adjust the mechanical properties of the polyurethane rigid foams. [11-13]

Table 1.2: Structure ranges of silicone surfactants for polyurethane rigid foam. [5]

Application	Surfactant MW (g/mol)	Silicone weight percent (%)	Polyether MW (g/mol)	Weight percent EO in polyether
Rigid foam	1500-15000	20-60	400-2000	60-100

1.5 Polyols from Vegetable Oils

Vegetable oils are triglycerides. There are five fatty acids dominant in vegetable oils, two saturated palmitic (C16:0) and stearic (C18:0), and three unsaturated: oleic (C18:1), linoleic (C18:2), and linolenic (C18:3). The first number is the number of carbon atoms in the fatty acid and the second is the number of double bonds. All three of these unsaturated acids have cis-double bonds, the first one locates between the 9^{th} and 10^{th} carbon, the second between 12^{th} and 13^{th} carbon, the third between 15^{th} and 16^{th}. Vegetable oils are very heterogeneous and consist of a number of triglycerides. Even with a given double bonds number, the structure of the oil may vary. For instance, a triglyceride with three double bonds can have three double bonds distributed evenly among three fatty acids, or have all these double bonds in just one of the fatty acids leaving the remaining two with no double bonds at all; or have fatty acids with two, one, and zero double bonds separately. The oil composition may also vary from the geographic area. Despite all these factors, the number average and weight average molecular weights of vegetable oils are quite constant with various compositions, which

make them nearly monodisperse materials. Vegetable oils are excellent renewable raw materials for polymers. As the concerns of the environment and sustainability keep growing, vegetable oils attract more and more attention. [11]

Like many other polymers, polyurethanes rely greatly on petroleum as their feedstock. Vegetable oils have great potential to compete with petroleum in producing polyol. However, except castor oil, vegetable oils do not have hydroxyl groups.[11, 13] The unsaturated sites in vegetable oils can be used to produce hydroxyl groups and a number of methods have been developed to synthesize vegetable oil-based polyols.

Oxidation of double bonds is the most direct way to introduce hydroxyl groups. However, the control of the direct oxidation is not satisfactory, many other oxidation products such as carboxyls, ketones, aldehydes and peroxides are also produced.[14, 15] Instead of direct oxidation, epoxidation is utilized in order to better control the oxidation reaction. During the epoxidation process, epoxy groups are inserted exactly into the double bonds and then hydroxyl groups are introduced by ring opening of the epoxy groups using alcohols, water, or acids (HCl, HBr et al) or by hydrogenation. [16-20] The halogen groups will be introduced into the polyol by using HCl or HBr as the ring opening agents. Figure 1.5 shows these reactions. In the figure, R_2 and R_3 represent the unsaturated fatty acid residues. The resultant polyol has a hydrocarbon backbone and hydroxyl groups locate in the middle of the chain, leaving dangling ends. Compared to petroleum-based polyols (Figure 1.3), which have primary hydroxyl groups or secondary hydroxyl groups at the chain end, soy-based polyols have secondary hydroxyl groups in the mid-chain, which react slower with isocyanate. At room temperature, halogenated

soy-based polyols are solid while the non-halogenated soy-based polyols are liquid. And the non-halogenated soy-based polyols still have higher viscosity than that of the petroleum-based polyols. [18]

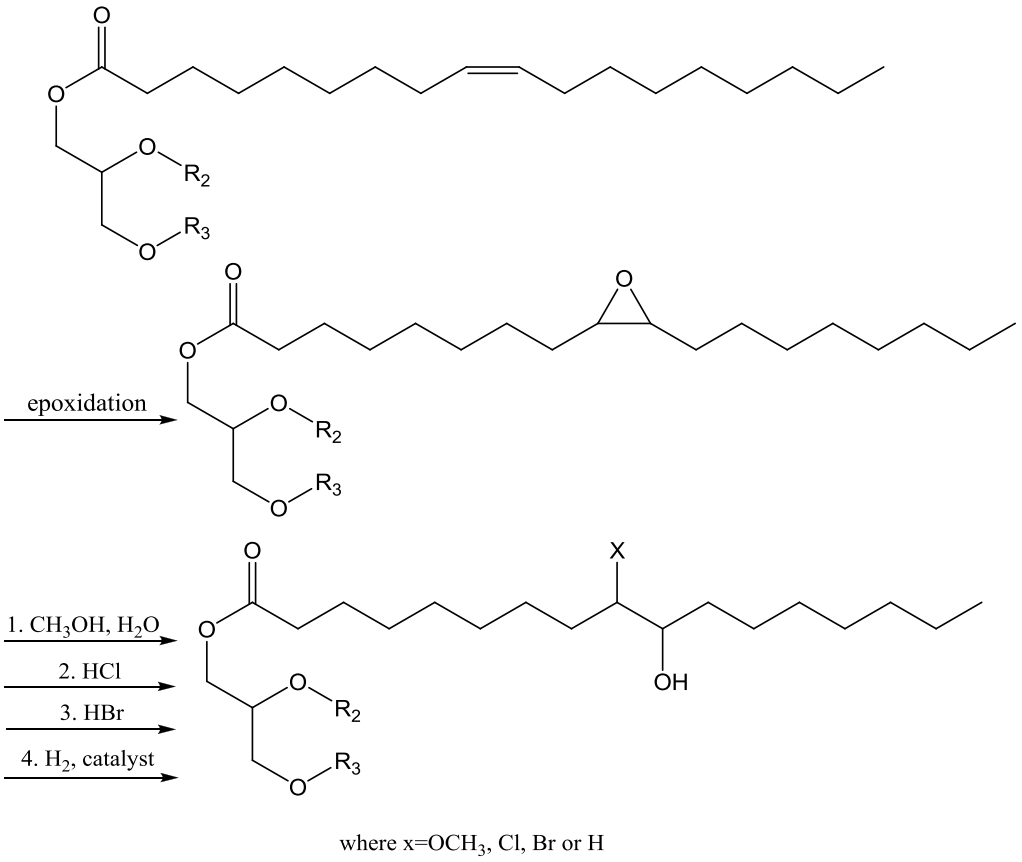

Figure 1.5: Formulation of polyol from epoxidized soybean oil.

Several methods have been developed to produce soy-based polyols with primary hydroxyls. Ozonolysis is a good way to cut double bonds and can be used to produce primary hydroxyls as well. [21-22] Figure 1.6 shows the soy-based polyols from ozonolysis route using O_3 as the ozonlysis agent. Ozonolysis is a clean and fast way to cut double bonds to produce hydroxyls at the 9 position since all major unsaturated fatty acids have

their first double bonds between 9 and 10 carbon. However, due to the heterogeneity of the vegetable oils, some fatty acids residues may have no unsaturated sites. As a result, the synthesized soy-based polyols from ozonolysis has the functionality no larger than 3.

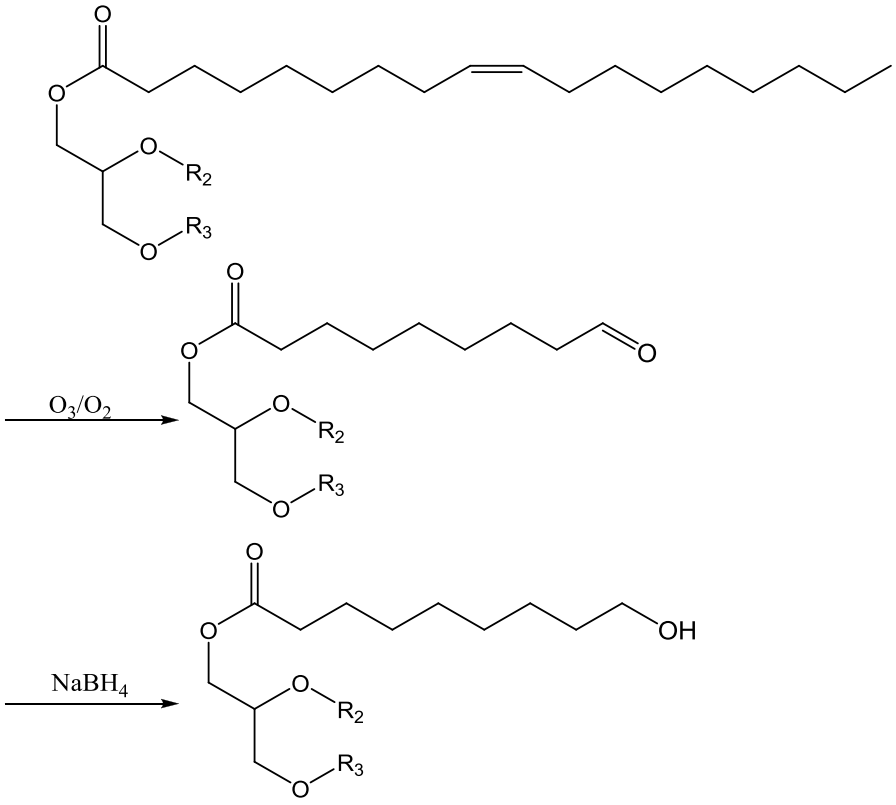

Figure 1.6: Synthesis of polyol from ozonolysis route.

Another method used to produce primary hydroxyls is hydroformylation (see Figure 1.7). During the hydroformylation process, double bonds react with synthetic gas (H_2/CO) in the presence of rhodium or cobalt carbonyls as the catalysts to give aldehyde groups. The aldehyde groups are then hydrogenated to hydroxyl groups.[23-25] An extra carbon atom is introduced at every double bond.

Soy-based polyols can also be synthesized from transesterification between vegetable oils and multifunctional alcohol such as glycerol.[26] Microbial conversion is another method using in the field of microbiology.[27,28] The epoxidation and hydroformylation are two routes that are mostly used in industry.

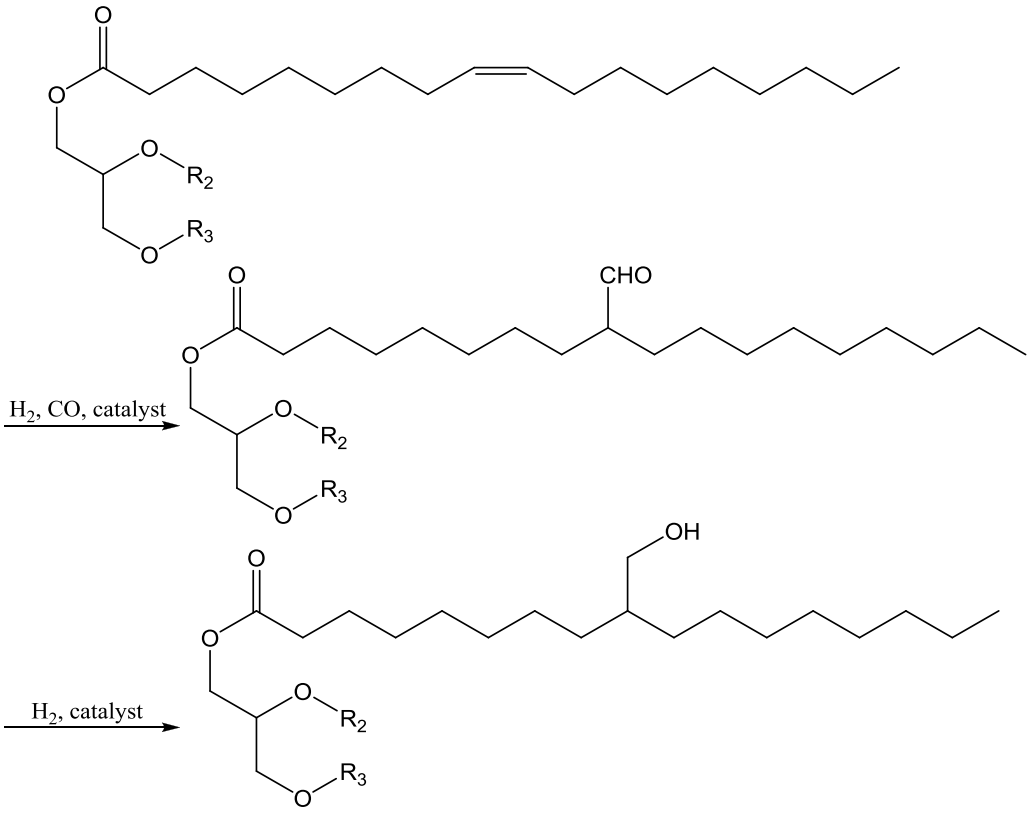

Figure 1.7: Synthesis of polyol from hydroformylation route.

1.6 Vegetable Oil–Based Polyurethane Rigid Foam

As early as 1974, Lyon had already successfully prepared polyurethane rigid foam from hydroxymethylated castor oil, safflower oil, and polyol esters of castor acids.[29] These foams had satisfactory compressive strength and good resistance to shrinkage.

Other polyols such as rape seed oil- and palm oil-based polyols had been used to make polyurethane rigid foams as well. [29, 30]

Research effort has been put into producing polyurethane foams using soy-based polyols. In 2000, Guo and co-workers prepared HCFC- and pentane- blown polyurethane rigid foams from soy-based polyols made from epoxidation followed by oxirane ring-opening.[31] Nevertheless, these foams were found to have inferior mechanical and thermal insulating properties though higher thermal degradation temperature (measured by TGA) than foams made from petroleum-based polyols (see Table 1.3, foam C). The effect of catalysts, surfactant, water, cross-linker, blowing agent and isocyanate on the foam properties were also studied. It was found that TEGOSTAB® B-8404(Goldschmidt, polyether-modified polysiloxane), which was a general purpose surfactant for rigid foams, turned out to be more effective than other surfactants. The k value of the material, did not change significantly when the amount of surfactant was above 1.0 pph. The compressive strength increased with increasing amount of water while the k value stayed constant when the amount of water was above 2 pph. Three cross-linkers were tested: triethanolamine, trimethanolylpropane, and glycerin. Glycerin was found to be the best cross-linker and the foam shrank the least at 5-10 pph of glycerin.

Since then, more research has been done to understand the properties of soy-based polyurethane foam. Guo et al. [32] continued to investigate the effect of soy-based polyol structure on the polyurethane rigid foam (see Table 1.3, foam B). The polyols made from hydroformylation followed by hydrogenation were compared to those by epoxidization followed by methanolysis. The former type polyol, having primary hydroxyls, reacted

faster and more completely than the latter one, which had secondary hydroxyls. The resulting polyurethanes from the latter type polyol had lower T_g. Since T_g is a measure of rigidity of plastics, foams from latter type polyol were less rigid. Unlike petroleum-based polyols, which were pure, soy polyols were mixtures due to the presence of different types of fatty acids in the soybean oil. Petrovic et al. [33] had examined the effect of heterogeneity of the soy-based polyol structures on the foam properties. They found that this heterogeneity actually had no obvious effect on the mechanical properties of glassy polyurethane (glassy polyurethanes had high modulus), but a negative effect on rubbery polyurethane (rubbery polyurethanes had low elongation).

Narine et al. [34] prepared polyurethane rigid foam using three polyols: soy-based polyol, canola oil-based polyol, and crude castor oil (see Table 1.3, foam D). The reactivity of canola oils-based polyol was found to be higher than that of both soy-based polyol and castor oil-based polyol. Importantly, they appeared to be the first to probe the dynamic mechanical properties of bio-based polyurethane rigid foam.

Tu et al.[35] prepared fifty natural oil-based polyols and replaced up to 50% of the petroleum-based polyol in water blown polyurethane rigid foam to study their potential for replacement of the petroleum-based polyol (see Table 1.3, foam A). They characterized the OH number of the synthesized vegetable oil-based polyols and investigated the density, k value, and compressive strength of the foams. Though most of the foams had inferior properties compared to those made from 100% petroleum-based polyol, some foams made from 50% hydroxyl soybean oil, epoxidized soybean oil

reacted with acetol, and oxidized epoxidized diglyceride of soybean oil can have relatively better k value and compressive strength.

Table 1.3: Comparisons of the formulations of polyurethane rigid foams made from petroleum-based polyol and soy polyol.

Formulation	Petroleum oil-based	Soybean oil-based			
	Control[36]	A[35]	B[32]	C[31]	D[34]
Polyol (parts)	100	50/50	100	100	100
Polyol OH number	450-500	250-500	212	~190	185.5
Gelation Catalyst (parts)	0.5	0.84	1.0	1.0	1.0
Blowing Catalyst (parts)	2.1	1.26	1.0	1.0	1.0
Surfactant (parts)	2.5	2.5	2.0	2.0	2.0
Physical blowing agent (parts)	9.6 (n-pentane)	--	11-14 (HCFC)	Vary (c-pentane)	--
Glycerin (parts)	--	--	29	10-25	15
DI water (parts)	1.9	3.0	2.0	1-5	2.0
MDI index	110 (polymeric)	110 (polymeric)	120 (crude)	130 (crude)	120 (crude)

Table 1.4: Comparisons of the properties of polyurethane rigid foams made from petroleum-based polyol and soy polyol.

Properties	Petroleum oil-based	Soybean oil-based			
	Control[9]	A[35]	B[32]	C[31]	D[34]
Density (kg/m^3)	24-32	35-45	--	31.6	163±3
Compressive Strength (kPa) (parallel to foam rise)	138-310	80-300	130	140	~300
Tensile Strength (kPa)	207-276	--	--	--	--
Closed Cells Content (%)	92-98	--		--	9±1
Glass Transition Temperature(℃)	100*	--	--	--	67
k value (m ŧK/W)	0.025-0.033	0.027-0.039	--	0.037	--
E' (Pa)	10^9**	--	--	--	$10^{8.5}$
E" (Pa)	$10^{7.5}$**	--	--	--	10^7

* Data from the maximum usage temperature of the typical polyurethane rigid foam

** Data from reference [37]

Table 1.3 and 1.4 summarizes the formulations and properties of polyurethane rigid foam from soy-based polyol in details. Formulation and properties of typical polyurethane rigid foam from petroleum-based polyols are also listed for comparison.

Comparing the formulations of the polyurethane rigid foams between the petroleum-based and soy-based, the amount of the catalysts, surfactant, water, and isocyanate index was close but the amount of physical blowing agent and glycerin varies. The biggest difference came from the OH number of the polyol. Petroleum-based polyol had a much higher OH number at 450-500 than that of the soy-based polyol, which was about 200. This turned out to be an important issue and will be discussed further. Soy-based polyurethane rigid foams had comparable density with that of petroleum-based polyurethane rigid foams (except B). Foam A and D seemed to have good compressive strength. Nevertheless, the fact was that foam A was made from a polyol blend of 50% soy polyol and 50% petroleum-based polyol, and the measured compressive strength values had a big error bar as well. Foam D had much higher density, which made it stiffer. Very few studies on soy-based polyurethane rigid foam had reported the closed cell content, the only reported measured value was about 9%, which was extremely low.[32] And in this study, the T_g of the soy-based polyurethane rigid foam was found to be lower than the typical maximum usage temperature of the commercial petroleum-based polyurethane foam. Thermal insulation property is a very important property for the polyurethane rigid foam. Foams made from substituting 50% petroleum-based polyol with soy polyol had a wider range and about 10% higher k value than the petroleum-based foam. Foams made from solely soy polyol also had at least 10% higher k value. [35]

In summary, some work has been done on developing soy-based polyurethane rigid foams. Though they had comparable density to petroleum-based foams, their k value and compressive strength were inferior to the commercial products to different extents. A systematic and complete study on polyurethane rigid foams from soy polyol is needed to fully understand the potential limitation of soy polyol in producing polyurethane rigid foams. The goal of my research is to formulate polyurethane rigid foam from soy-based polyols, characterize and compare foam properties with those from petro-based foams, and then study the mechanism behind the property deficiencies and develop strategies to improve them.

Chapter 2. Glycerol Aided Route of Making Polyurethane Rigid Foam from Soybean Oil-based Polyol

2.1 Introduction

Polyurethane rigid foam is largely used in thermal insulation. Its superior long-term insulation property combined with good adhesion, good thermal stability and high strength make it an indispensible construction material.

Soy-based polyols have high functionality (f_n=3-5) and low molecular weight (M_w=1000-1200 g/mol), thus they have the potential to replace petroleum-base polyols for polyurethane rigid foam application.[2,4, 8] However, previous work was solely focused on making polyurethane rigid foam from soy-based polyol, there does not appear to be a systematic study on replacing petroleum-based polyol with soy-based polyol.[31] Thus, a complete study on the properties comparison between petroleum-based foams and soy-based foams and strategies to improve property deficiencies is highly desired.

In this chapter, a commonly used petroleum-based polyol (Jeffol® SD-361) and a soy-based polyol (SBOP) are chosen to study. A complete study on the foam properties, which include foam density, T_g (glass transition temperature) cell morphology, k value (thermal conductivity), aging and compressive strength, was performed. The mechanism behind the property deficiencies and strategies to improve them will be discussed.

2.2 Experimental

2.2.1 Materials

The polyols used in polyurethane rigid foams are generally short chain oligomers with functionality of OH groups between three and eight. Petroleum-based polyol Jeffol® SD-361 and an experimental soybean oil-based polyol (SBOP) are selected. SBOP is synthesized from the route of epoxidation followed by the ring opening using water and methanol (synthesis details can be seen in section 1.4). Figure 2.1 shows the structure of major component of soybean oil and SBOP. The properties of the two polyols are listed in Table 2.1.

Table 2.1: Properties of polyols used.

Polyol	Jeffol SD 361	SBOP
OH # (mg KOH/g)	360	240
Molecular Weight (g/mol)	690	1100
Functionality	4.4	4.4
Viscosity (mPa·s)	2500	8900
Acid Value (mg KOH/g)	--	1.7
Water content (ppm)	--	3000
Manufacture /Resource	Huntsman	Experimental (Cargill)

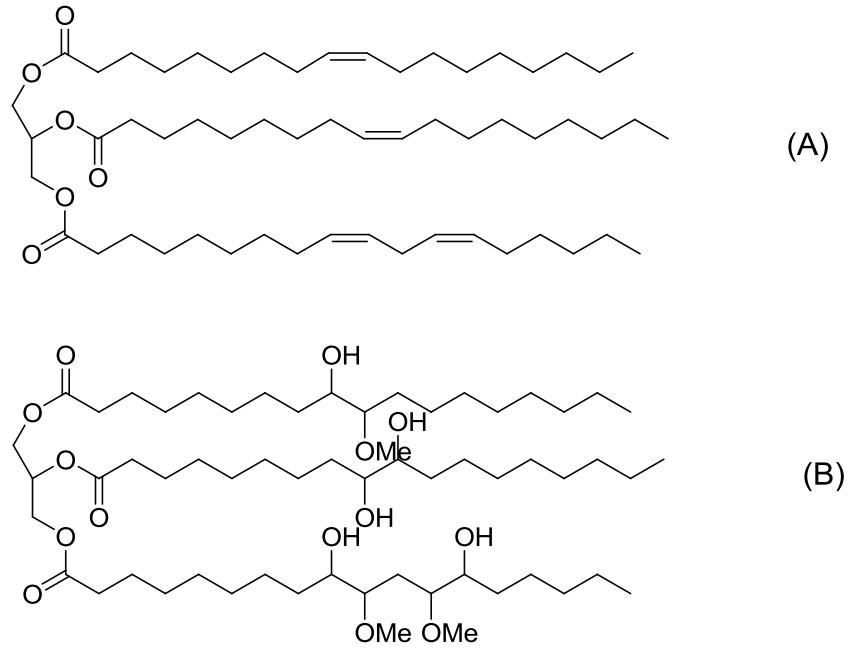

Figure 2.1: (A) Structure of the soybean oil; (B) Structure of the major component of soy-based polyol synthesized via epoxidation followed by oxirane ring-opening using methanol and water (SBOP).

The sucrose-based polypropylene polyether polyol (Jeffol® SD-361) (see Figure 1.3 B for structure,) and polymeric MDI (pMDI, Rubinate®M, CAS 9016-87-9) were obtained from Huntsman International. Jeffol® SD-361 polyol contains propoxylated sucrose (CAS 9049-71-2) and propoxylated diethylene glycol. *N*,*N*-Dimethylcyclohexylamine (Polycat®8, AirProducts, CAS 98-94-2) was used as the gelation catalyst. Pentamethyldiethylenetriamine (Polycat®5, AirProducts) was used as the blowing catalyst. Polyether-modified polysiloxane (TEGOSTAB B-8404, Goldschmidt Chemical Corporation) was used as the surfactant. TEGOSTAB B-8404 is a general-purpose silicone surfactant used in polyurethane rigid foam formulation. It was found to work satisfactorily for the SBOP system compared to other surfactants. [31] n-

pentane (Anhydrous, 99%, Aldrich®) is the physical blowing agent. Distilled water was obtained in our laboratory. All the chemicals were used as received.

2.2.2 Foam Synthesis

Table 2.2: Foam formulation.

Chemical (pbw)	Control A	SBOP A (w/o glycerol)	SBOP A (w/ glycerol)
Jeffol ®SD-361	100	--	--
SBOP	--	100	100
DI water	1.9	1.9	1.9
Glycerol	--	--	16
Polycat ®8	2.1	2.1	3.7
Polycat ®5	0.5	0.5	1.1
Surfactant	1.6	1.6	2.2
n-pentane	9.6	9.6	16
PMDI (index=110)	126.7	87.39	140.8

A low isocyanate index formulation for freely rise foam was selected. Table 2.2 lists the formulation details. The synthesized foams were made based on the total mixture weight of about 90g. Foams were synthesized from Jeffol® SD-361 alone, SBOP without glycerol and SBOP with glycerol added.

Polyols, surfactants, distilled water, n-pentane, and catalysts were weighed and put into an 800 mL plastic cup. pMDI was weighed and put into another cup. The mixture was mixed using a 10-mm drill (Delta VSR Drill, D21008) equipped with a 2.8-in diameter mixing blade for 40-50 seconds at the speed of 2500 rpm. The pre-weighed pMDI was then added into the mixture, and mixing was continued for another 10 seconds. The foam was then allowed to rise freely at room temperature. The foams were cut one week later and the properties of the foams including density, cell morphology, k value, and dynamic mechanical properties were measured.

2.2.3 Foam Characterization

2.2.3.1 Foam Density

Foam density is an important parameter to determine k value. Foams from the core of the outside-cup portion were cut into cube shape with dimension of 1”×1”×1”. The mass of the foams was measured and their volume can be calculated from their dimensions. The apparent density of the foam was calculated from dividing the mass by the volume. The data represented an average of foams from three different batches. Three to four pieces were cut from each foam for density measurement.

2.2.3.2 Scanning Electron Microscope (SEM)

SEM requires the sample to be electrically conductive, at least at the surface, to prevent electrostatic charging effect. Thus, nonconductive samples should be coated with an ultrathin electrically conductive material, like gold, platinum or carbon. The coating also helps to maximize the signal and improve spatial resolution. Conductive carbon tape

was used to fix the sample on the sample stub. The stub was then put in the sample holder to maintain the appropriate position. [38, 39]

A JEOL 6500 field emission scanning electron microscope was used to examine the cell morphology. It operated from 0.5 kV to 30 kV with a resolution of 1.5 nm, and with a magnification range from 10 to 400, 000. [40] The foams were cut into 4 mm cubes using a razor blade. The sample was then attached to the stub using the conductive carbon tape. Each sample was coated with a layer of 5 nm platinum. The sample was placed into the instrument and imaged under the accelerating voltage of 10 kV with 50x. The cellular structure of the foam was observed parallel to the free-rising direction.

Analysis of cell size is the first step in seeking structure-property relationships. There were several methods to measure cell diameter which were shown in Figure 2.2. In this study, apparent long axis which was the maximum chord length of a cell [41] was measured using ImageJ. In the software, the scale was set firstly, a straight line was dragged to measure the apparent long axis as the cell size. The average cell size and cell size distribution was based on 100-150 cells totally.

2.2.3.3 Compressive Strength Measurement

The compressive strength measures the degree of deformation of polyurethane rigid foam. Compressive strength was measured on foam samples with dimensions of 2.0”×2.0”×1.0”. The samples were placed between two parallel plates with a larger area than the specimen and the force required to compress the foam at the rate of 0.1”/min was measured. The test recorded the applied force and the sample displacement to obtain a

stress-strain curve. The compressive strength was the value of the maximum applied force divided by the initial sample surface area when the maximum applied force occurred before the strain reached 10%. Otherwise, the compression applied force was taken when the strain was 10%.

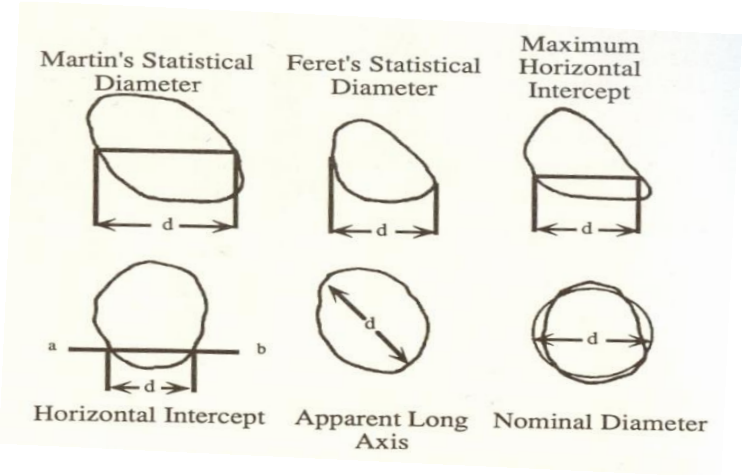

Figure 2.2: Typical methods by which particle diameters have been measured. [41]

2.2.3.4 Differential Scanning Calorimetry (DSC)

The value of heat capacity is another important parameter to the thermal conductivity measurement. [42] DSC (Q1000, TA Instruments) was used to measure the heat capacity of the foams. About 7-10 mg of compressed foam sample was loaded into an aluminum standard inverted pan and sealed. The sample was first heated at 10 ℃/min to 150 ℃ and equilibrated for 2 min, cooled to -120 ℃ and held for 10 min, and finally heated at 10 ℃/min to 220 ℃. The value of the heat capacity at room temperature was determined on the second heating cycle. [43] The specific heat capacity of foam is used to calculate k value.

2.2.3.5 Thermal Conductivity Measurement

Thermal conductivity or k value is the most important property for polyurethane rigid foam. [2,4,8] A typical k value measurement is based on the rate of steady state heat transfer across a foam with known thickness, which is induced by two different known temperatures between two opposite surfaces of the foam.[2,8] However, the current steady state method requires large sample size with 1 foot by 1 foot surface and thickness varying. This method is not suitable for lab scale samples. An attempt to measure k value based on steady state method using AR-G2 rheometer was discussed in Appendix B. Recently, Harikrishnan et. al have reported a simple and rapid technique based on a transient measurement using a needle probe. [42] The needle probe is widely used in the measurement of k value and thermal diffusivity of liquids and solids. [42] Using a needle probe, the time required to get the data is very short and the data accuracy is within 5%.[42] The details on needle probe method are seen in Appendix A. Figure 2.3 is the typical k value profile obtained from the needle probe method. Because the k value of the thermistor is larger than that of the foam, the k value decreases as the pulse penetrates into the entire foam. Once the penetration of the pulse reaches a sufficient extent, the k value will stabilize to a plateau. And the k value from this plateau represents the k value of the foam at room temperature. Table 2.3 shows the data reproducibility of k value from needle probe method. Four different commercial polyurethane rigid foams were chosen and five measurements were performed in different spots in the foam. The data had a very good reproducibility with the standard deviation within 0.2%.

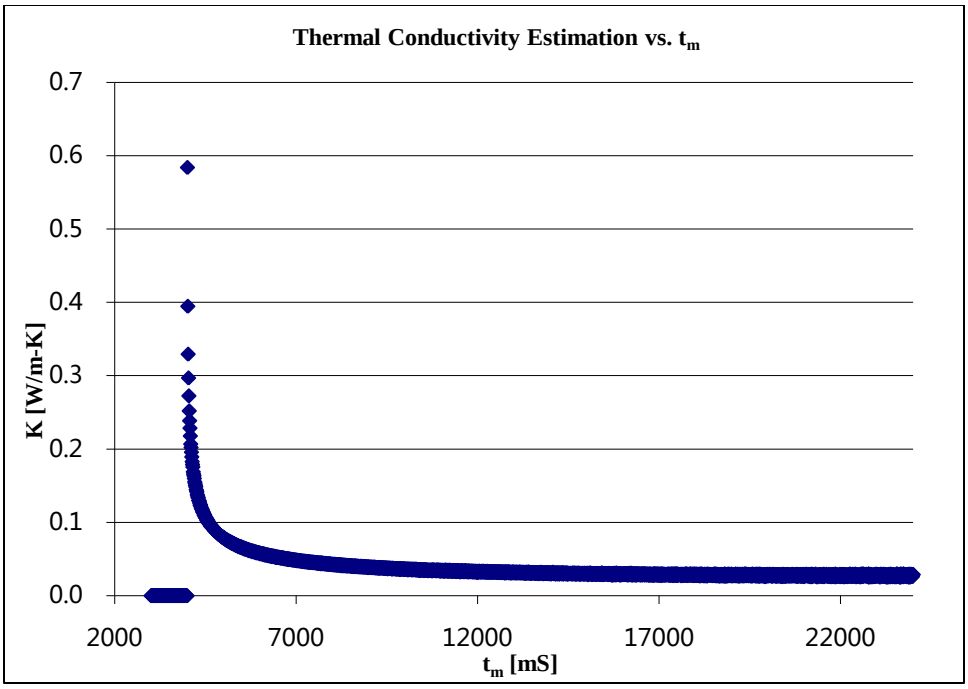

Figure 2.3: k value versus time curve from needle probe measurement.

Table 2.3: Data reproducibility of k value from needle probe method.

Foam	Thermal Conductivity (mW/(mK))						
	Run 1	Run 2	Run 3	Run 4	Run 5	average	Standard deviation
A	22.26	22.43	22.06	22.00	22.21	22.19	0.015
B	22.19	21.56	21.97	22.22	22.22	22.01	0.027
C	22.84	23.07	22.96	22.86	22.86	22.93	0.009
D	22.89	22.58	22.36	22.59	22.59	22.66	0.023

Foam k value aging test was tested at elevated temperature. Foam cubes with dimensions 2.5”×2.5”×2.5” were cut from the top of the cup foam. The foams were put into the oven and heated up at 70 ℃ to be cured. The foams were taken out of the oven after certain days and the k value measurements were taken.

2.2.3.6 Dynamic Mechanical Analysis (DMA)

DMA characterizes the mechanical properties of the material as a function of frequency, time or temperature. The most common method is to apply a sinusoidal strain (or stress) and measure the sinusoidal stress (or strain). Damping properties (tan delta) of the material can be analyzed by measuring the time lag between the deformation and the applied stress. The modulus of the material is calculated. DMA is especially useful to characterize viscoelastic materials like polymers. Polymers usually have two important properties, viscosity and elasticity, which greatly affect their applications. [44, 45] By scanning the temperature at a fixed frequency, the material may undergo state changes from glass to rubber. DMA is sensitive to the glass transition and acts as a good technique to measure the glass transition temperature.

A disk (8mm (diameter) × 8mm (thickness)) was cut from the foam and tested in sinusoidal oscillation mode between two 8-mm diameter serrated parallel plates (ARES, Rheometric Scientific^{TM}). Contact was maintained by loading sample at the plate temperature of 160 ℃ and applying a constant normal force of 16±8 g throughout the experiment. Strain sweep test was performed first to determine the linear viscoelastic region of the sample. Storage modulus (G’) and loss modulus (G”) were recorded at 1 Hz

over the temperature range from 0 to 220 ℃. The temperature ramp rate was controlled at 3 ℃ /min and the strain applied was 0.1%. The strain was within the linear viscoelastic region of the foam in the corresponding temperature ranges. Both temperature ramp up and ramp down measurements were taken.

2.2.3.7 Foam Kinetics Study

In order to understand the effect of the added glycerol, foam kinetics study is performed. Adiabatic temperature rise is a simple and quick method. [46] As reaction goes on, since polyurethane rigid foams are good insulating materials, a good adiabatic condition is obtained. Typically, any container with the diameter over 5-10 cm is enough to maintain adiabatic condition in the center of the reacting mixture.[47] Given the adiabatic condition, the temperature change during reaction is closely related to the gelling and blowing reactions and isocyanate conversion is calculated from the temperature profile. Equation 2.1 and 2.2 shows the relationship between temperature change and isocyanate conversion and are used to calculate isocyanate conversion from the obtained temperature profile. [46]

$$p(NCO) = \frac{r\Delta T_m}{\Delta T_{rxn}} \qquad \text{Equation 2.1}$$

$$\Delta T_{rxn} = \frac{Q}{C_p m_T} = \frac{\Delta H_{r,u}\frac{m_w}{M_w} + \Delta H_{r,r}\frac{m_{OH}}{M_{OH}} f_n}{C_p m_T} \qquad \text{Equation 2.2}$$

In the equations above, p is the isocyanate conversion; r is the stoichiometric ratio of functional groups, which is kept to 1 in the experiment; ΔT_m is the temperature rise during foaming; ΔT_{rxn} is the maximum temperature rise; Q is the total amount of heat generated during foaming in the unit of J; C_p is the specific heat capacity of foam, which is taken as 1.5 J/(g·°C) according to the DSC results; m is the reactant mass; ΔH_r is the heat of reaction; M is the molecular weight of reactant in the unit of g/mol; f_n is the functionality of polyol, subscripts, u, r, w, T and OH represent urea, urethane, water, total and polyol, respectively. $\Delta H_{r,u}$ and $\Delta H_{r,r}$ are taken as -125.5 kJ/mol and -93.9 kJ/mol.[48,49]

An insulating plastic cup with a diameter of about 10cm was used as the reacting mixture container. Reaction mixture based on total weight of about 25g was prepared according to the formulation below. Temperature profiles during foaming are monitored using type J thermo-couples (Omega®), which connected to a thermometer. An adapter was used to connect this whole setup to a computer and the temperature reading was recorded with software. Table 2.2 showed the formulation for foaming kinetic study except that the isocyanate index was kept at 100 to make the reaction stoichiometrically balanced because the isocyanate conversion calculation only depended on the gelling and blowing reaction. Excess amount of isocyanate would lead to other reactions such as isocyanate trimerization and further reaction between isocyanate and urethane. In order to study the effect by adding pentane or glycerol, formulation without pentane or glycerol was also used.

2.3 Results and Discussion

Table 2.4: Summary of foam properties.

Foam	Jeffol ® SD-361 Control A	SBOP A (w/o glycerol)	SBOP A (w/ glycerol)
Density (kg/m^3)	40.3 ±0.6	61.2 ±7.9	41.8 ±0.2
T_g (℃)	140 ±4.4	144 ±2.4	216 ±4.4
k value (mW/m·K)	24.1 ±0.5	36.3 ±3.5	25.9 ±1.4
K_{60}-k_0 (mW/m·K)	2.60	N/A	4.62
Compressive strength (kPa)	208	190	206
Plateau G' at glassy state (MPa)	2.5	2.5	1.0
Cell size (um)	342 ±46	poor	300 ±81

Figure 2.4 showed the foam appearance. The height of foam from SBOP without glycerol was much lower than that of control foam. By adding glycerol, foam from SBOP had a comparable appearance to that of control foam. Table 2.4 summarizes the foam properties. The property measurements of density, k value, T_g and cell size were based on three to five different foam samples. Without adding glycerol, although soy-based polyurethane rigid foam had comparable T_g and compressive strength but much higher density, k value and poorer cell structure. By adding glycerol, soy-based polyurethane

rigid foam's density, compressive strength especially k value and cell morphology were greatly improved, which were comparable to those of petroleum-based polyurethane foams.

Figure 2.4: Foam appearance, from left to right: Control A, SBOP A (with glycerol), SBOP A (without glycerol).

2.3.1 Foam Cellular Morphology

Foam's k value is closely related to foam density and cell morphology. Foams with high density have lower $\lambda_{radiation}$, but higher solid non cellular polyurethane portion leads to higher λ_{solid}. Though polyurethane solid only accounts for a small percentage, it has a much higher k value (220 mW/ (mK)) than the blowing agent gas (13.7 mW/(mK)). At a fixed foam density, $\lambda_{radiation}$ will decrease with decreasing cell diameter. Figure 2.5 shows the relationship between cell size and k value. It shows that the k value increases substantially, nearly 50%, as cell size increases from 0.25 mm to 0.6 mm. [50] The level of closed cell content should be kept as high as possible too. Open cells allow more

convection and even air to enter the foam, which has much higher k value (24.9 mW/(mK)) than that of typical physical blowing agent like n-pentane (13.7 mW/(mK)).[2]

Analysis of cell morphology is the first step to study the correlations between cell geometry and foam behavior. Though specific cell characters such as cell windows, cell struts and strut window junction can all be characterized, cell size are and its distribution are the most commonly measured features. Figure 2.6 shows SEM images of foams. Three SEM images for control foam and SBOP A (with glycerol) were chosen respectively and analyzed using ImageJ and the average cell size and cell size distribution were shown in Figure 2.7. The control foam had regular cell structure, with the average cell size about 342 um and standard deviation about 48 um. SBOP A (without glycerol) foam sample had very poor cell structure and well-shaped cells were hardly seen. By adding glycerol, SBOP foam's cell structure had greatly improved. Well-shaped cells were obtained although some large cells were still observed. Average cell size dropped to 300 um but with larger standard deviation about 81 um. Detail discussions on cell morphology and its effect on foam k value are in chapter 3.

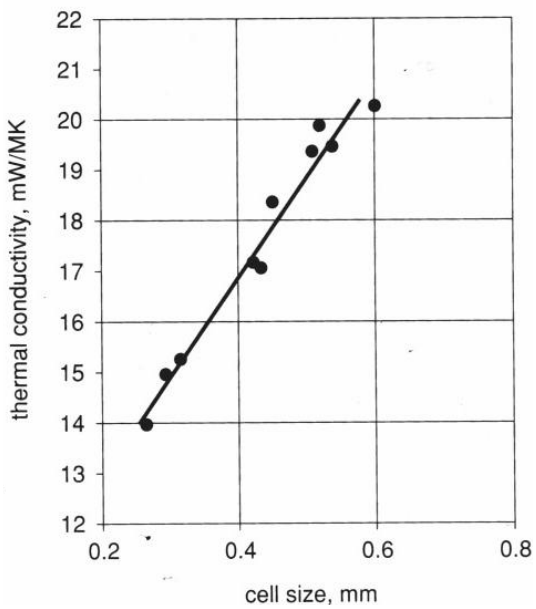

Figure 2.5: k value of polyurethane rigid foam vs. cell size. Cells were filled with trichlorofluoromethane (CFC-11) and fs=0.8, fs is the fraction of polymer in struts. [51]

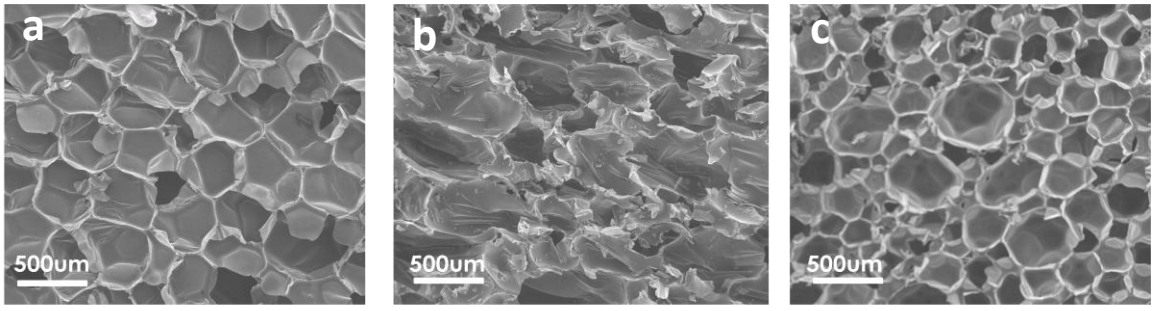

Figure 2.6: SEM images of the foams samples: (a) control A, (b) SBOP A(w/o glycerol), (c) SBOP A(w/ glycerol).

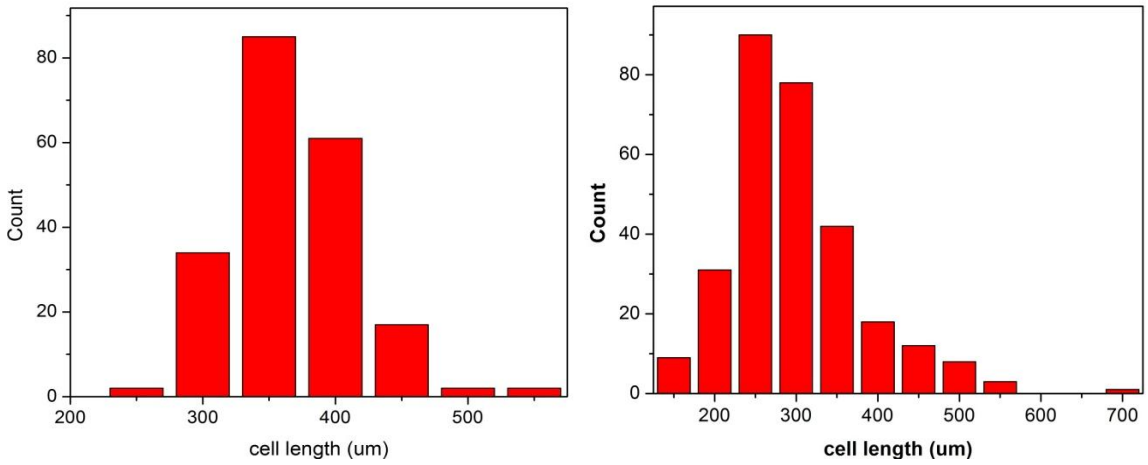

Figure 2.7: Cell size distribution analysis (a) control A, (b) SBOP A (with glycerol).

2.3.2 Compressive Strength Measurement

Figure 2.8 showed the typical stress-strain curve of foam samples in compressive strength measurement. Foams from Control A had maximum compressive stress right before the strain reached 10%. Soy-based foams did not have maximum compression stress before 10% strain and the stress at 10% strain was taken to calculate compression strength.

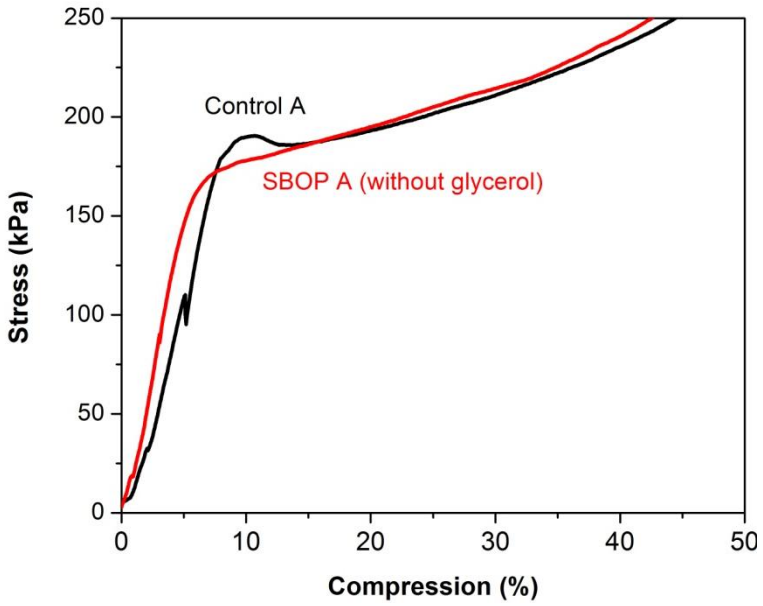

Figure 2.8: Stress-strain curves of polyurethane rigid foam samples.

2.3.3 Thermal Conductivity Measurement

Since same physical blowing agent was used in both control foams and SBOP A foams, cell morphology became a crucial factor. As discussed in section 2.3.1, foams with low density, small cell size and narrow cell size distribution have low k value. It was shown that the control foam had a low k value which was understandable from cell morphology. Foams from SBOP had very poor cell morphology and high density leading to a very high k value. By adding glycerol, SBOP A foams maintained good cell morphology and small average cell size though they had slightly higher density than control foams. Thus, these foams had a low k value, which was very close to that of the control foam.

Polyurethane rigid foams will undergo changes of k value over time. Actually, since foams are used as the insulating materials in construction and refrigerator industry, the aged k value will be declared rather than the initial one. [2] Foam k value aging is a very slow process, the most frequently used methods in obtaining aged k value are experimental aging of thin slices or aging at elevated temperature. Accelerated foam aging at elevated temperature was performed in this study.

Figure 2.9 showed the foam aging test results. Considering the measurement uncertainty, it showed that SBOP A foams with glycerol had similar k value aging process as control foams in the first 30 days, but a little faster after 30 days. The effect of surfactant on k value will further be discussed in Chapter 3, the mechanism behind k value aging will be discussed in Chapter 5.

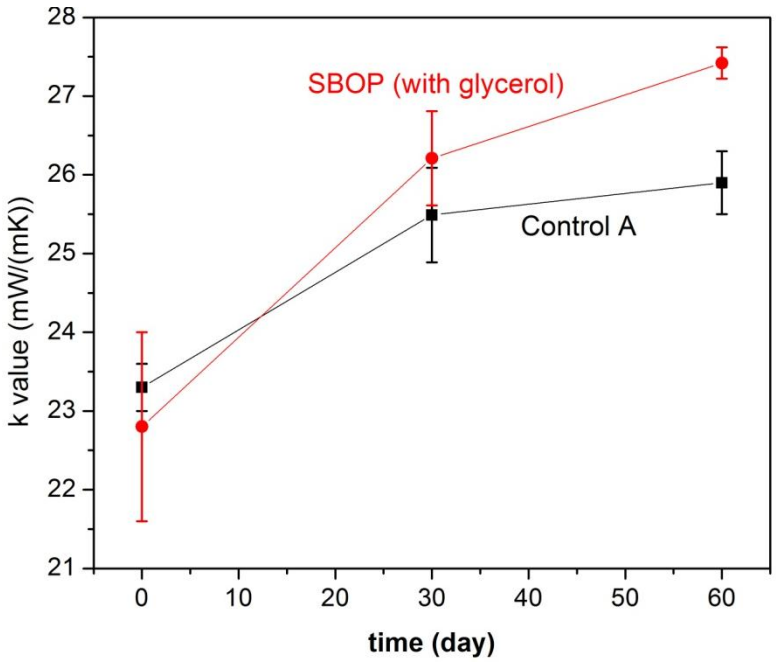

Figure 2.9: Foam k value aging.

2.3.4 Dynamic Mechanical Properties

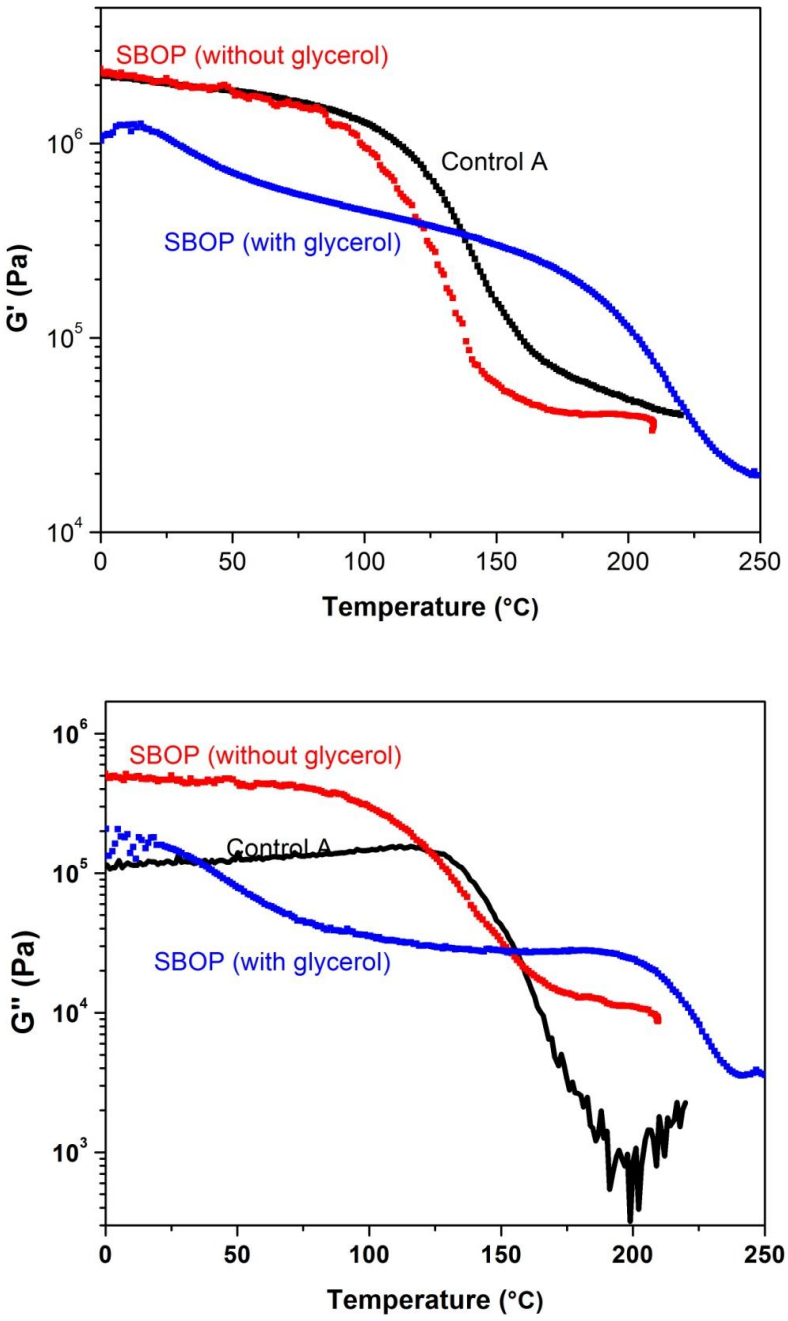

Figure 2.10: DMA curves of G' (top) and G" (bottom) as a function of temperature.

DMA was employed to determine the temperature dependence of modulus and thermal transition behavior of polyurethane rigid foams. [45, 52] Both G' and G" were plotted for the foam samples. The curve shape was similar for all these three foams. At temperature lower than T_g, the foams were at the glassy state and behaved as a solid and had a high G' about 2×10^6 Pa. When the temperature went through T_g, G' drops dramatically to $2\text{-}5\times10^5$ Pa. In the glassy state, control A foam had comparable G' to that of SBOP foam which was around 2.5×10^6 Pa. By adding glycerol, SBOP A foams had a lower G' about 1.0×10^6 Pa. In the rubbery state, foams of SBOP A also had comparable G' to Control A which was about 3×10^5 Pa; and with glycerol added, SBOP A had lower G' at about 2×10^4 Pa. The plot of G" had the same phenomena. T_g also changed greatly between foams from Control A and SBOP A with glycerol added. Foams from Control A and SBOP without glycerol had similar T_g around 140 ℃. By adding glycerol, T_g of foams from SBOP increased to 210 ℃. (See Figure 2.11) This was understandable from the polyol structure. Polymer T_g increases as the chain length between cross links decreases. [52] From Figure 1.3, since petroleum-based polyol have OH groups at the chain end, the average molecular weight between OH groups of Control A is about 230 g/mol. While from Figure 2.1, SBOP A has the molecular weight between OH groups ranging from 150 g/mol to 200 g/mol. But considering the plastizising effect of the dangling chain, it was still reasonable that foam from SBOP A without glycerol had comparable T_g with that from Control A. Due to much shorter chain length between OH groups of glycerol which was only about 25 g/mol, the average chain length between cross links decreased which led to a higher T_g for foams from SBOP A with glycerol. However, the width of the peak did not change significantly. Actually, Control A was a

mixture containing both sucrose-based and diethylene glycol-based polypropylene polyether. This heterogeneity varies the molecular weight between crosslinks.

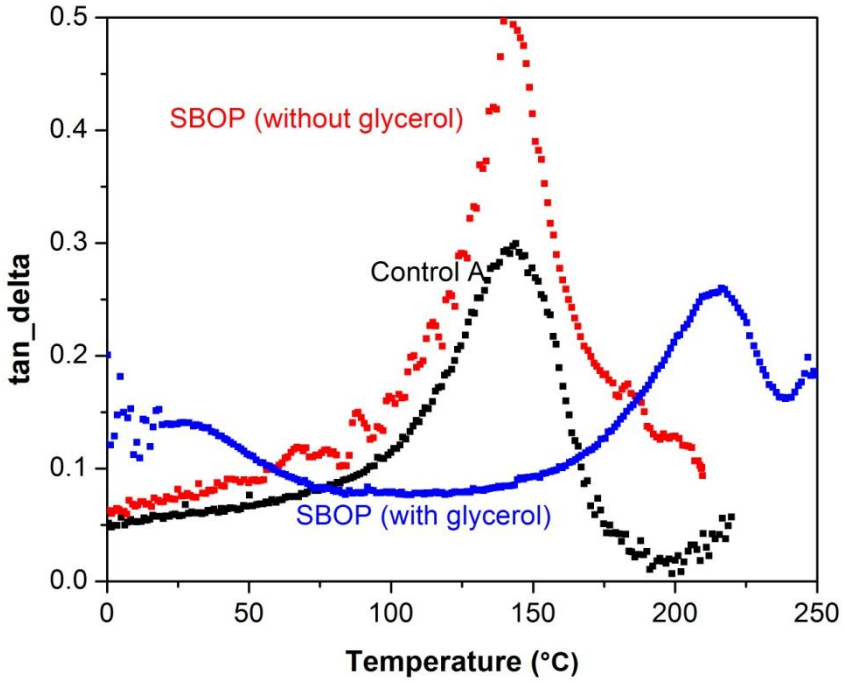

Figure 2.11: tan_delta curves for T_g determination.

2.3.5 Foam Kinetics

Figure 2.12 showed the original temperature profile obtained from the adiabatic temperature rise experiment (Control A without pentane) and Figure 2.13 showed the calculated isocyanate conversion from the temperature profile (Control A without pentane, SBOP without glycerol and SBOP with glycerol). In the first 10s, all these three foaming reactions had similar isocyanate conversion profile. Since the blowing reaction (H_2O/isocyanate) happened much faster than the gelling reaction (polyol/isocyanate), [49, 50] it was expected that the temperature profile in the first 10s was due to the blowing

reaction. For the control sample, foaming reaction still took place fast even after the first 10s. Until after 40s, the reaction slowed down and reached a plateau gradually. Without glycerol, SBOP sample reacted fast in the first 10s but slowed down afterwards due to the lower reactivity of SBOP than Control A. By adding glycerol, SBOP sample reacted much faster in the first 25s; reaction kinetics profile became closer to that of the Control A. It had also been noticed that the final isocyanate conversion of the SBOP reaction kinetics profile, no matter with or without adding glycerol, was lower than that of Control A. Figure 2.14 showed the temperature profile of Control A foaming with and without pentane. By adding pentane, temperature became lower compared to the reaction without pentane in the first 30s. After the first 30s, the temperature profile was parallel to that of the reaction without pentane then reached the same plateau at about 30s later. This indicated that the pentane evaporation took place during the first 30s.

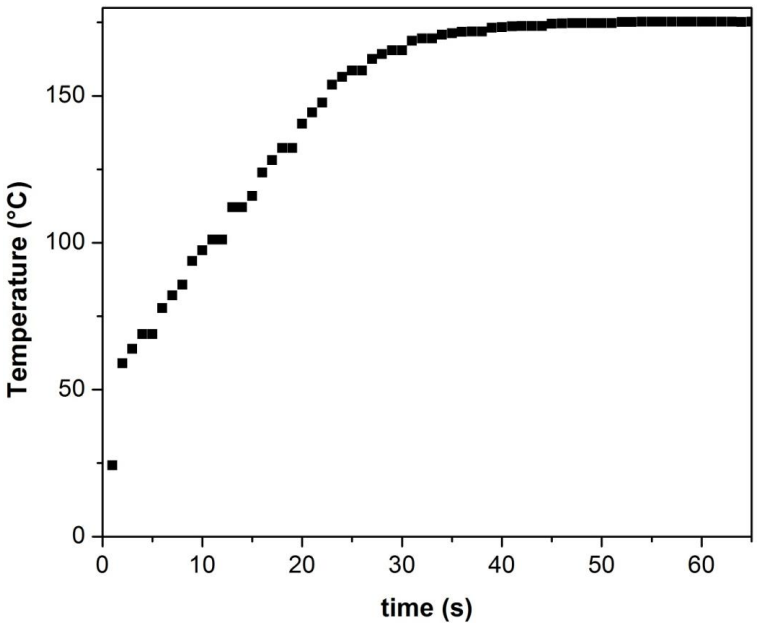

Figure 2.12: Original temperature profile (formulation without pentane added).

As discussed in Chapter 1, foaming process included gelling and blowing reactions. Polymer networks built up through the reactions between polyol/H_2O and isocyanate. The heat released from the exothermic reactions would evaporate pentane into gas phase. Pentane gas as well as CO_2 (generated from the reaction between H_2O and isocyanate) diffused into the air bubbles which were introduced during mixing. If the initial gelling reaction was not fast enough, less heat was generated for pentane evaporation. Thus, less pentane gas was available to be trapped inside the cells. On the other hand, slow gelling process also indicated slow polymer network build-up which could not provide enough strength to maintain cell structure. By adding glycerol, gelling reaction was greatly accelerated, which gave enough heat to generate pentane gas and enough polymer network strength to hold cell structure. So the cell morphology of soy foams was greatly improved by adding glycerol.

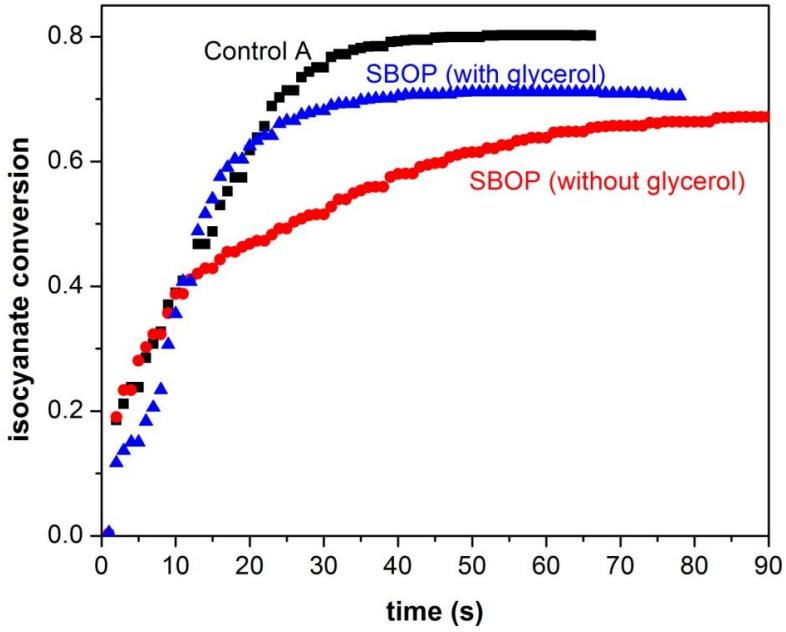

Figure 2.13: The calculated isocyanate conversion profile (formulation without pentane).

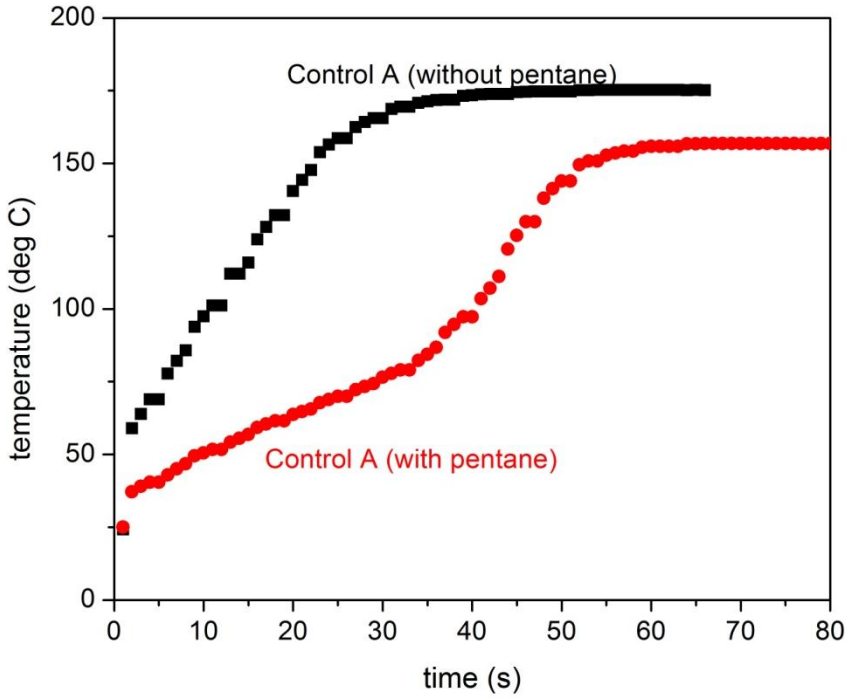

Figure 2.14: Temperature profile comparison for Control A foaming with or without pentane added.

2.4 Summary

A petroleum-based polyol with higher OH number and comparable functionality with SBOP was chosen in this study. Polyurethane rigid foam was made from SBOP. But those foams had much higher density and k value as well as poor cell morphology though comparable compressive strength and T_g. The property deficiencies were due to the lower reactivity of SBOP. By adding small molecule glycerol as a cross-linker, gelling and blowing reaction was balanced. Therefore, foams' density and k value were found to be reduced by as much as 40%. Good cell morphology, with much higher T_g and a slightly increased compressive strength were also observed. Foam kinetic study had showed that glycerol had accelerated the gelling reaction which not only gave out enough heat for

pentane evaporation to blow up, but also built up enough polymer strength to hold the cell structure. The k value aging is a very important property of polyurethane rigid foams. Foams from SBOP with glycerol had similar k value aging in the first 30 days, but aged faster after 30 days. Chapter 3 will be focused on further exploring the effect of surfactant on k value and its aging. Chapter 5 will discuss the mechanism behind k value aging phenomena.

However, due to higher foam flammability, large amount of glycerol in foam formulation is not favorable in industry.[53] Also we would like to evaluate the effect of replacing petroleum-based polyol with only SBOP without the presence of large amount of high polarity compound like glycerol. Thus in Chapter 4 a new formulation which was exactly the same for and petroleum-based polyol and SBOP was introduced.

Chapter 3. Effect of Surfactant on Soy-based Foaming System

3.1 Background

Surfactant is very crucial in foaming process and carries two major functions during foaming in polyurethane rigid foam manufacturing. [2, 5]One is the emulsification in mixing the incompatible components, since raw materials for making polyurethane rigid foam are incompatible. [54, 55]Another one is cell stabilization, which provides a well-shaped cell structure and narrow cell size distribution. [54-57] Figure 2.5 shows a nice relationship between k value and cell size. Thus, surfactant is important for foam k value.

Details in foaming process are discussed in section 1.2. During foaming, pentane and CO_2 diffuse into the tiny bubbles which are generated during the mixing. Cells grow and crowd together to give polyhedral shapes. The cell walls consist of lamellae which are two-sided films. The lamellae are curved where three or more cells meet, the triangle area is called Plateau border. According to Laplace equation, the pressure difference across a curved interface is given by:

$$\Delta P = \gamma(\frac{1}{R_1} + \frac{1}{R_2})$$

where R_1 and R_2 are the interface curvature. Due to the greater curvature in the Plateau border, greater pressure crosses the interface here. According to the equation above, the liquid pressure inside the highly curved Plateau border region is lower than the general lamella region. So the liquid will drain from the lower curved lamella region to Plateau border which results in cell wall thinning. When the thickness of the cell wall reaches a

critical value (usually 50-100 Å), they break and cells will be destroyed and foam will collapse. Thus, in order to stabilize cell structure, excess liquid drainage during foaming process must be prevented. The presence of a surfactant is necessary. A monomolecular layer of surfactant is absorbed on both sides of the lamellae at the liquid/gas interface. The resulted films are capable in resisting excessive film thinning which greatly help to stabilize cell structure. [58]

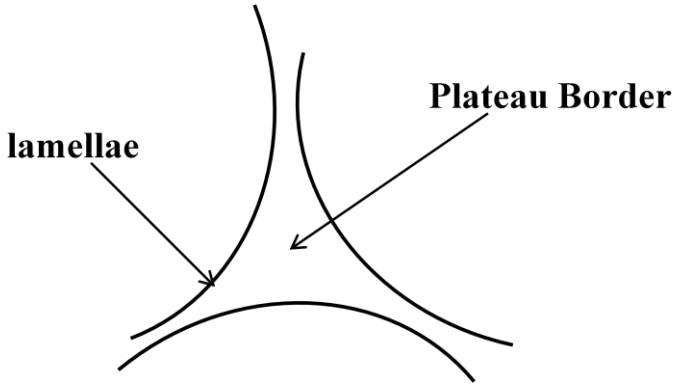

Figure 3.1: Scheme of lamellae and Plateau border of cell structure.

Polydimethysiloxane polyether copolymers are largely used in polyurethane rigid foam. Due to the flexibility of silicone chemistry, surfactant structure can be tailored in a wide range. The degree of polymerization of polydimethysiloxane and polyether can be controlled. The ratio the molecular weight of polydimethysiloxane over that of polyether can then be adjusted to tailor the hydrophobicity and surface reactivity in order to meet different polyurethane applications.[5,58]

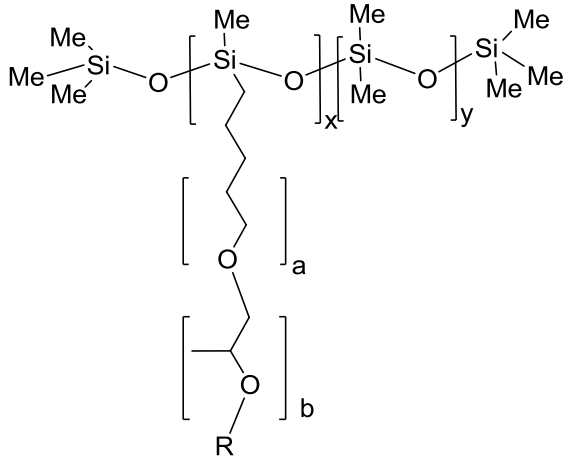

Figure 3.2: Surfactant structure: polydimethysiloxane polyether graft copolymer.

The purpose of this chapter is to investigate the effect of surfactants on foam properties. Since there is an increasing trend to use bio-renewable raw materials as the feedstock for polyurethanes, effort has been put to develop new surfactant for bio-based polyurethane system. Four surfactants used in this study include: TEGOSTAB® B 8404 (Goldschmidt Chemical Corporation, a general-purpose surfactant for polyurethane rigid foam, denoted as 8404), Silbyk-TP 3805, BYK-LPX 7105 and Silbyk-9204 are recommended by BYK Additives & Instruments for soy-based foaming system (denoted as 3805, 7105 and 9204 respectively).

3.2 Surfactant Characterization

The characterization of surfactant structure is the first step to study the effect of surfactant on foam properties. However, due to the complexities of commercial

surfactants, structure information is very limited. FTIR, NMR and cloud point measurement are employed to study the surfactant structure.

3.2.1 FTIR

Infrared spectroscopy is a technique for identification of compounds, determination of functional groups in organic materials. Attenuated total reflectance (ATR) mode is internal reflection spectroscopy. The sample is brought in contact with the reflecting surface. The evanescent wave, which is produced by the light introduced into the prism exceeding the critical angle, interacts with the sample and gives the spectrum. [59, 60]

According to Figure 3.4, the peak around 3000 cm^{-1} was C-H stretching of CH_3, the sharp peak at 1260 cm^{-1} was CH_3 symmetric deformation of Si- CH_3, the doublelet peak at around 1100 cm^{-1} was Si-O-Si stretching vibrations, another sharp peak at about 800 cm^{-1} was for Si-C stretching and CH_3 rocking. These are characteristic peaks of polydimethylsiloxane. [61] However, as for the polyether, the stretching of C-O-C was also in the range of 1000-1300 cm^{-1}. [61] Thus, the absorption of the C-O-C stretching overlapped with the stretching of Si-O-Si and Si-CH_3. The absorbance at 1450 cm^{-1} was the vibration absorption of –CH_3 of the polypropylene and the 1350 cm^{-1} was for the CH_2-O absorption.[61] Additionally, surfactant 8404 and 3805 also showed a small broad peak at around 3500 cm^{-1}, which was due to O-H stretching. Therefore, surfactants of 8404 and 3805 had OH groups which will make them more hydrophilic than 7105 and 9204. However, surfactant structure difference was still unknown.

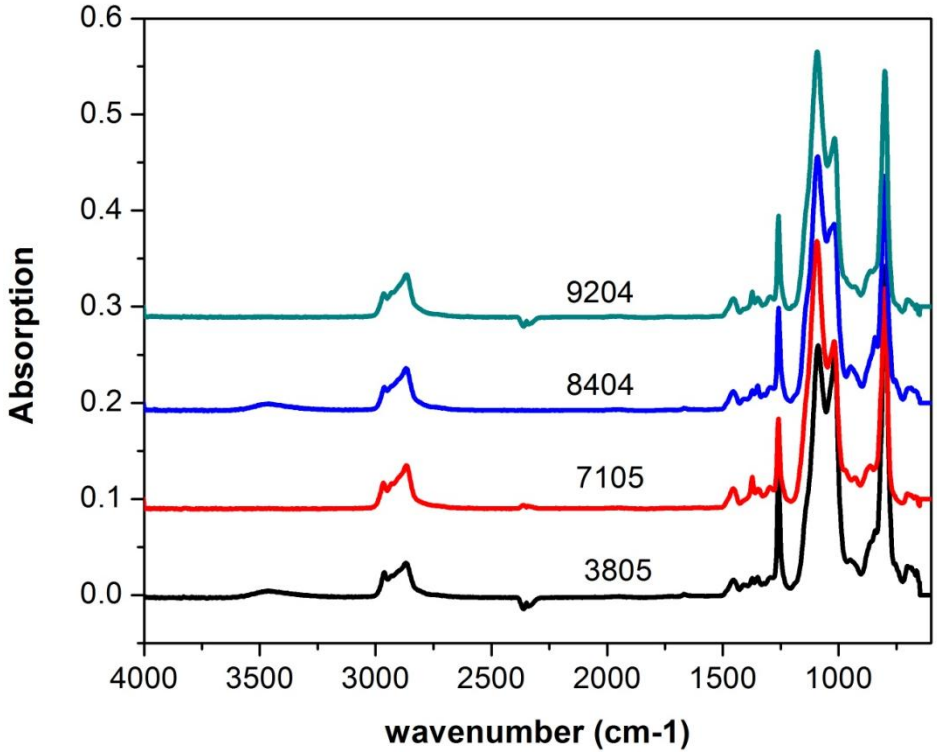

Figure 3.3: FTIR spectrum of four surfactants.

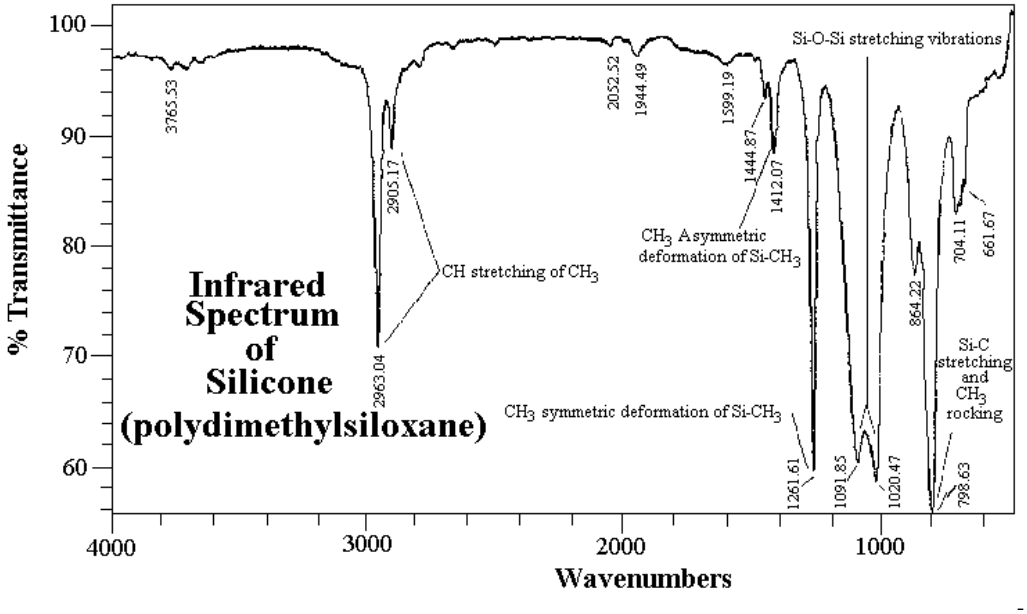

Figure 3.4: Infrared spectrum of silicone (polydimethylsiloxane). [62]

3.2.2 Nuclear Magnetic Resonance (NMR)

In a magnetic field, when electromagnetic pulses are applied to the magnetic nuclei, the nuclei will absorb energy from the pulse and radiate the energy out. The radiated energy is at specific resonance frequency which depends on the strength of the magnetic field and the electron density around the nuclei. [61] ^{1}H NMR is used to locate H atom in different chemical environment. Han and co-workers [56] have used ^{1}H NMR to investigate the silicone/polyether ratio in the surfactant.

In this study, ^{1}H NMR was used to characterize silicone surfactant. Figure 3.5 showed a typical ^{1}H NMR spectrum for the silicone surfactant. The signal at δ=0.1 ppm was due to the protons of Si-CH_3, The signals at δ=3.3 ppm, δ=1.1 ppm and δ=3.5 ppm were attributed to the protons of O-CH (CH_3)-CH_2 respectively.[5,56,63,64] Figure 3.6 showed the chemical shift of different protons of the surfactant.

However, due to the heterogeneity of the commercial surfactant mixture, peaks at the chemical shifts around 3.3-3.6 were hard to distinguish. Accurate integral of the peak area was challenging. Three integral analyses were taken by setting peak area baseline differently. Table 3.1 showed the calculated silicone/polyether ratio and the standard deviation was taken from three different analyses from a spectrum. It was found that, the standard deviation was huge even for just adjusting the peak area baseline slightly different. Surfactant structure was still unknown from ^{1}H NMR characterization.

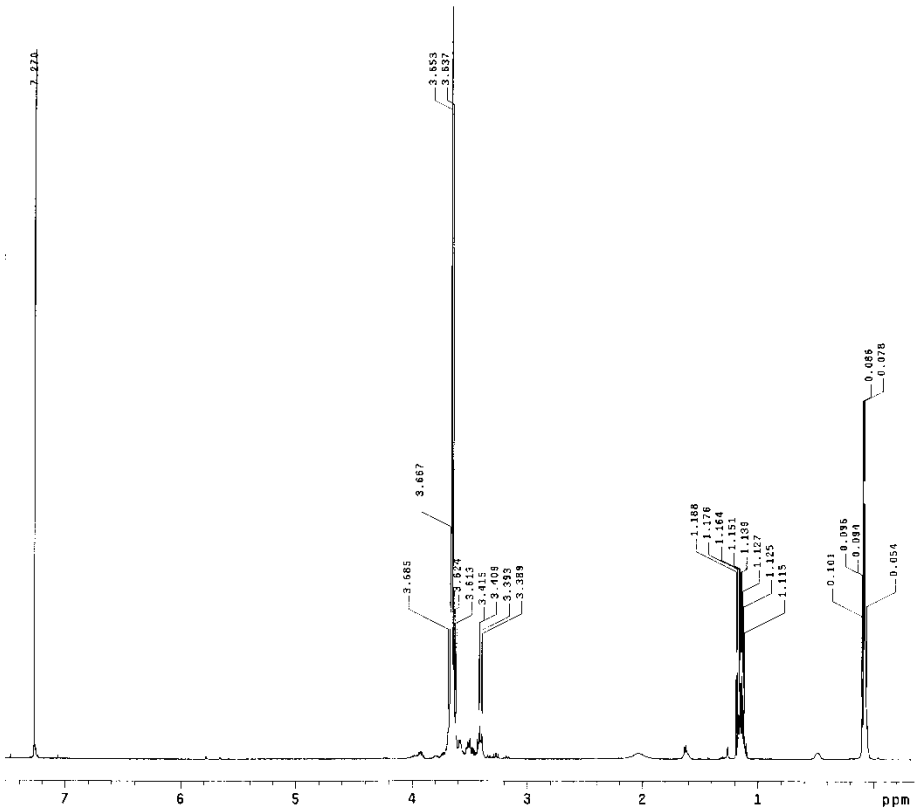

Figure 3.5: ^{1}H NMR spectrum of silicone surfactant.

Table 3.1: Calculated silicone/polyether ratio from ^{1}H NMR spectrum.

Surfactant type	3805	7105	8404	9204
Calculated silicone/polyether ratio (%)	33.6 ±13.4	22.2 ±15.7	36.6 ±10.8	29.2 ±13.0

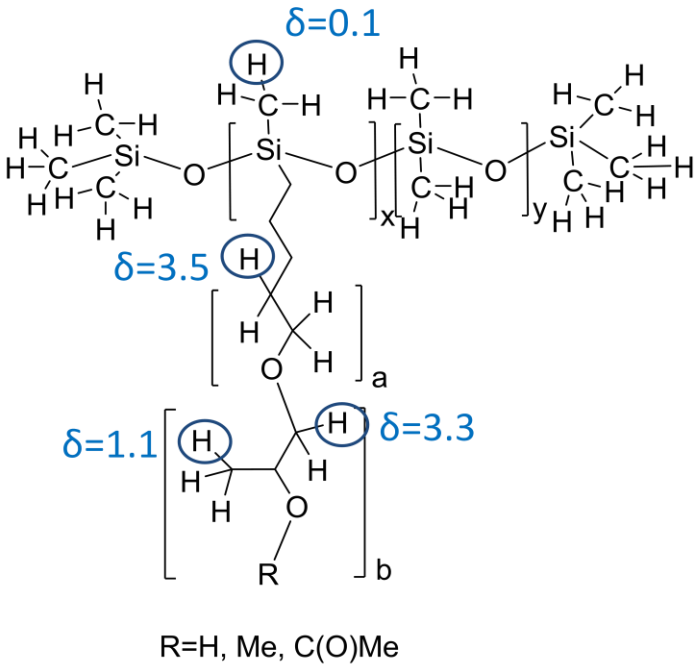

Figure 3.6: Chemical shift of different protons in silicone surfactant.

3.2.3 Cloud Point Test

Cloud point is an important property of nonionic surfactants. The dilute surfactant solution appears to be a single phase below the cloud point temperature, above it the hydrogen bonding between water and surfactant became weaker, so the water solubility of surfactant greatly decreases, the solution becomes turbid. [65-67] Thus, cloud point is the temperature above which a homogeneous surfactant solution becomes phase separates. It is a simple indication of surfactant relative hydrophobicity. Cloud point of four surfactants was measured in a home-built setup (See Figure 3.7)

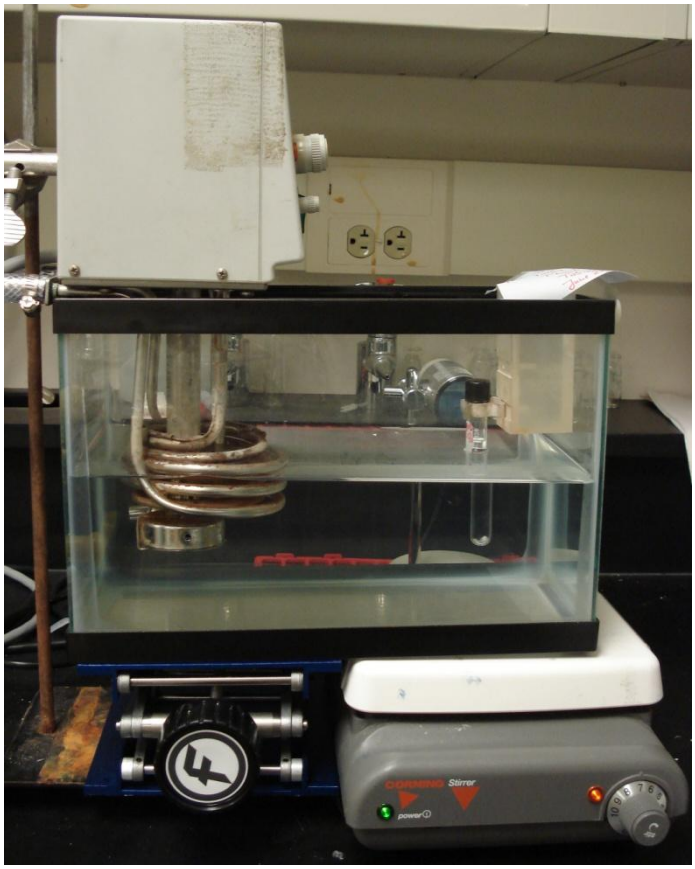

Figure 3.7: Home-built setup for cloud point measurement.

Surfactant water solutions with different concentrations were prepared. The solution was then immersed into the water bath and stirred with a magnetic stir bar. Heating was turned on and the temperature of water bath increased gradually. The lamp behind helped to monitor solution changes with a clearer and brighter sight. The temperature was kept increasing until 80 ℃ or the surfactant solution became turbid, the heating was turned off. The temperature of the water bath decreased naturally. The cloud point was recorded when the solution turbid just disappeared. Three measurements were taken for each solution.

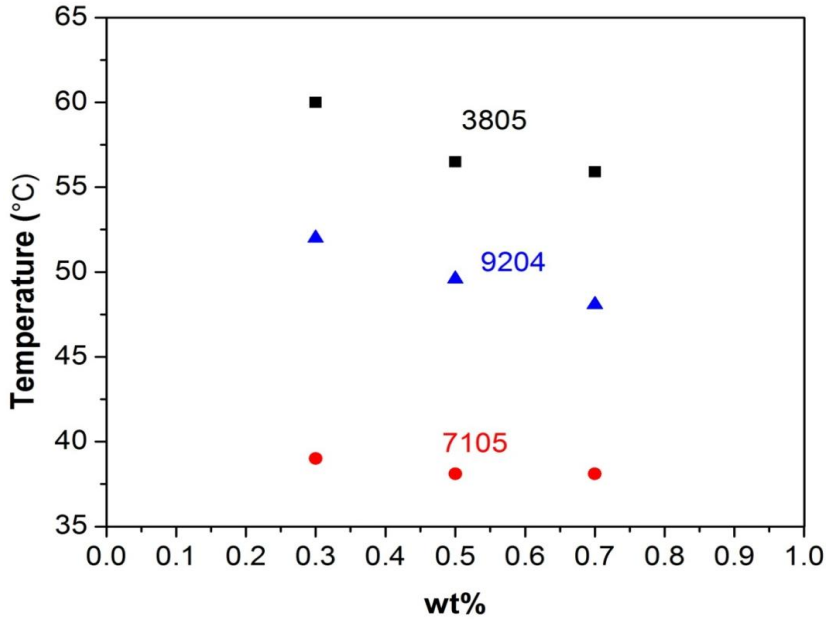

Figure 3.8: Surfactant cloud point measurement results.

Figure 3.8 showed the cloud point of different surfactant solutions for four surfactants. Surfactant 8404 was not shown in the graph because its solution was still clear upon 80 ℃, which was the maximum temperature limited by the home-built setup. Namely, 8404 was the most hydrophilic among these four surfactants. Surfactant 3805 was less hydrophilic with a cloud point at about 58 ℃. Surfactant 9204 was even less hydrophilic whose cloud point was around 50 ℃. Surfactant 7105 was most hydrophobic, the cloud point of which was only around 38 ℃. Therefore, according to the cloud point data, the hydrophobicity order is: 7105> 9204> 3805> 8404.

3.2.4 B-side Compatibility Test

B-side is the mixture of polyol, catalyst, surfactant and other necessary chemicals except isocyanate for foaming. One of two roles surfactant carrying out is helping in

mixing incompatible components. To study the emulsification effect of surfactant, B-side compatibility test was done in the mixture of polyol, water catalyst, surfactant, n-pentane and glycerol for four different surfactants. Different components were added into a small glass bottle and mixed well with the stir rod. The mixtures were then placed at room temperature until all bubbles were gone and the mixtures were stable (about three days after the mixtures were prepared). Pictures were then taken.

Figure 3.9: B-side Compatibility tests of four different surfactants, from left to right: control A, SBOP A_3805, SBOP A_7105, SBOP A_8404, SBOP A_9204 (top) mixture of polyol, water, catalyst, surfactant and n-pentane; (bottom) mixture of (top) with addition of glycerol for SBOP A mixtures.

It had been shown that all the mixtures were opaque and homogeneous even after adding glycerol into SBOP A mixtures. Thus, all these four surfactants were effective in emulsifying incompatible components in B-side mixtures.

3.3 Foam Synthesis and Characterization

Details on the foam synthesis procedures and characterization see section 2.2.2 and section 2.2.3.

3.4 Results and Discussions

Figure 3.10: Appearance of foams from different surfactants, from left to right: Control A, SBOP A_3805, SBOP A_7105, SBOP A_8404, and SBOP A_9204.

Table 3.2: Summary of foam properties from different surfactants.

Foam property	Control A	SBOP A_3805	SBOP A_7105	SBOP A_8404	SBOP A_9204
Density (kg/m^3)	40.3±0.6	43.2±0.1	47.0±0.2	41.8±0.2	46.7±0.1
T_g (℃)	144	206	193	218	208
k value (mW/mK)	23.3±0.3	25.5±0.5	27.8±0.6	25.9±1.4	24.9±0.7
k_{60}-k_0 (mW/m·K)	2.6	3.55	2.49	4.62	5.38
Compressive Strength (kPa)	208	173	206	206	245
Cell size (um)	342±46	271±72	302±108	301±81	227±59

From Figure 3.10 we could see that foams from different surfactants had comparable appearance including foam shape and height. Foams from surfactants of 3805 and 8404 had comparable density to control foams (within 7% difference); foams from surfactants of 7105 and 9204 had a density about 15% higher than control foams. All SBOP A from different surfactants had comparable compressive strength within 15% difference, 30-40% higher T_g and 10-35% smaller average cell size though 20-130% larger cell size distribution. However, foams from different surfactants did show different initial k value.

Considering the measurement uncertainty, foams of SBOP A_8404 had comparable k value (within 4% difference) while the rest three foams had higher k value than control foams to different extents (8- 16% difference). The relationship between surfactants' cloud point and foam density as well as k value was shown in Figure 3.11. It was observed that density and k value decreased with increasing cloud point (decreasing surfactant hydrophobicity).

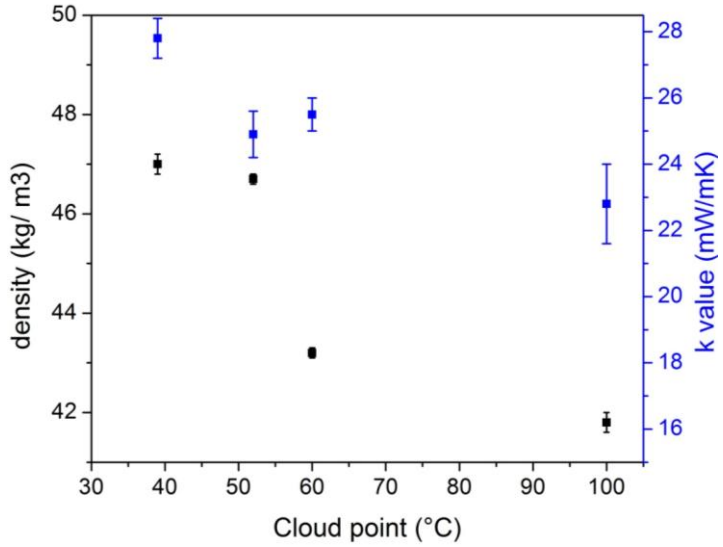

Figure 3.11: Foam density and k value as a function of surfactants' cloud point.

3.4.1 Foam Cellular Morphology

SEM images showed the foam cellular morphology from different surfactants. Cell size analysis and its distribution were shown in Figure 3.12.

As we can see the SEM images and the cell size analysis that soy-based foams from different surfactants all had smaller average cell. This can be explained from the surfactant aided foaming mechanism.

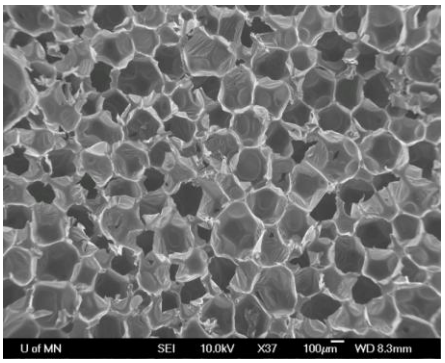

Control B

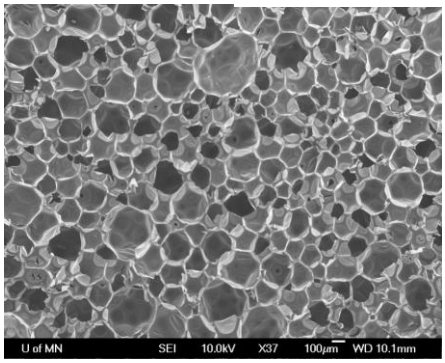

SBOP A_3805

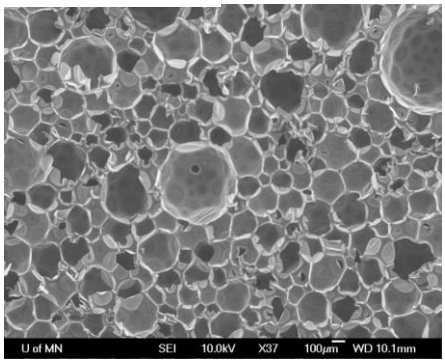

SBOP A_7105

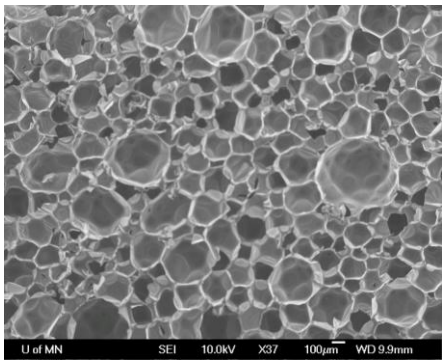

SBOP_8404

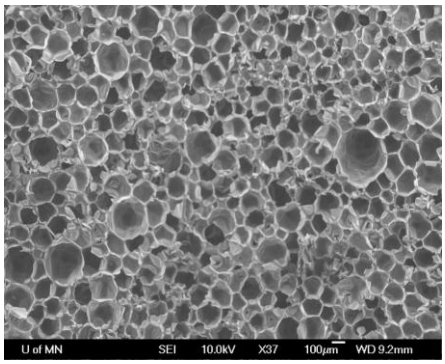

SBOP A_9204

Figure 3.12: SEM images of foams from different surfactants.

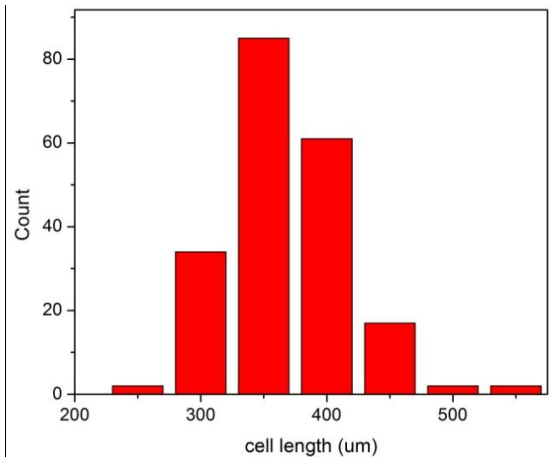

Control A

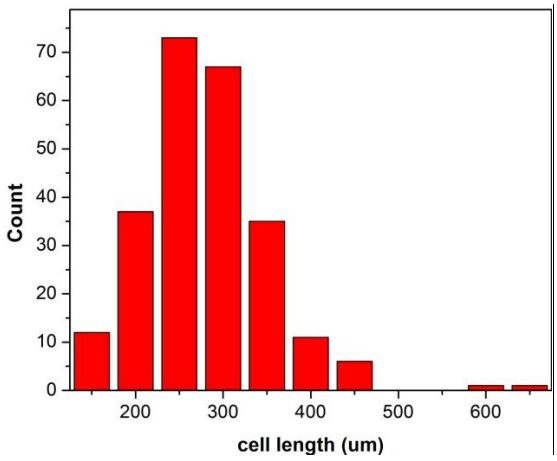

SBOP A_3805

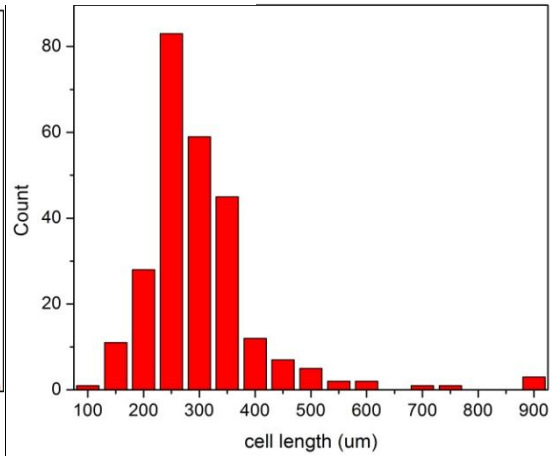

SBOP A_7105

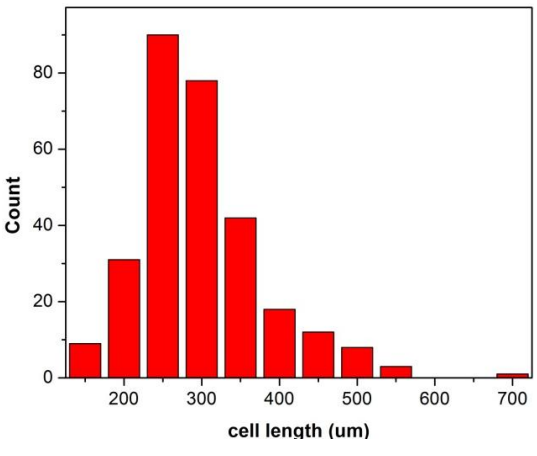

SBOP A_8404

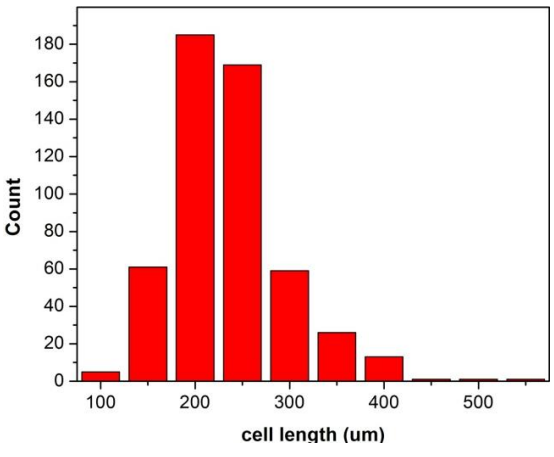

SBOP A_9204

Figure 3.13: Cell size distribution analysis.

The rate and extent of drainage of liquid in the lamellae is very important in determining foam cellular morphology. There are two different types of drainage: by gravity and by and by pressure. At the initial stage of foaming, when the bulk viscosity is very high and the lamellae are still very thick, drainage by gravity is dominant. The drainage caused by gravity is retarded when the bulk viscosity of the foaming solution is high.[58] SBOP has much higher viscosity than Control A (see Table 2.1), so drainage by gravity at the initial foaming stage in soy-based foaming system was greatly retarded, which made foams from SBOP have slightly smaller average cell size than Control A. However, this drainage retardant also slightly suppressed the blowing process, due to which soy-based foams all have higher density than Control A. As the reaction underwent, the lamellae were becoming thinner, when drainage by pressure difference became critical and surfactant started to play the role in stabilizing cell structure. The orienting effects caused by the surfactant monolayer in the interface between gas and liquid increase the viscosity of the remaining liquid, which reduced the rate and extent of the drainage by pressure difference. Cell size distribution was related to the diffusion of gas through the lamellae. Since the gas pressure in small bubbles was higher than that in large bubbles, gas tended to permeate from small bubbles to large bubbles. As will be discussed in Chapter 4, soy-based foaming system had higher gas permeation than petroleum-based system. The faster gas permeation in soy-based foaming system caused broader cell size distribution. The data in Table 2.5 showed that all soy-based foams had larger cell size distribution. It was found that the gas permeated through the bubbles between the surfactant monolayer in the lamellae interface. Therefore, the packing of the surfactant molecules can also decreased the gas permeation rate. [58] However, when the

solution temperature reached the surfactant's cloud point, surfactant molecules aggregated. This will weakened the barrier function of the surfactant molecules.[65,66] The cloud point test showed that, surfactant 7105 had low cloud point, while surfactant 3805, 9204 and 8404 have higher and close cloud point. Accordingly, foams from surfactant 7105 had larger cell size distribution (302±108 um), foams from surfactant 3805, 9204 and 8404 had narrow cell size distribution (271±72 um, 227±59 um and 301±81 um respectively). It should be noticed that foams from surfactant 9204 had exceptionally small cell size and cell size distribution. It seemed that surfactant 9204 was more effective in controlling cell size although causing higher foam density. Due to the complexity of the commercial surfactant (extra additives, surfactant mixture, limited information on surfactant structure, etc.), further study was still needed in order to know more about the mechanism using surfactant 9204.

3.4.2 Foam Aging Test

Foam cubes with dimensions 2.5"×2.5"×2.5' were cut from the top of the cup foam. The foams were put into the oven and heated up at 70 ℃ to be cured. The foams were taken out of the oven after certain days and the k value measurements are taken. Figure 3.14 showed the foam aging test results.

Soy-based foams from different surfactants had different k values. Although λ_{solid} just accounts for 3-4% of total k value of foam, the effect of foam density could not be ignored since the k value of polyurethane solid was much larger than that of pentane. [8, 50] Figure 3.15 showed the apparent relationship between k value and foam density. Taking

into account of k value measurement uncertainty, there was a trend that k value increased with increasing density with the exception of SBOP A _9204. Although SBOP A_9204 had higher density, the exceptional small cell size had compensated it. Table 3.2 also showed the k value change between the initial k value and the k value at 60th day. SBOP foams from 7105 had smaller k value change than Control foams. Foams from 9204 had largest k value change, followed by foams from 8404 and then 3805. Although foams from different surfactants did show different k value changes, no good correlation was found between k value change during aging and surfactant hydrophobicity.

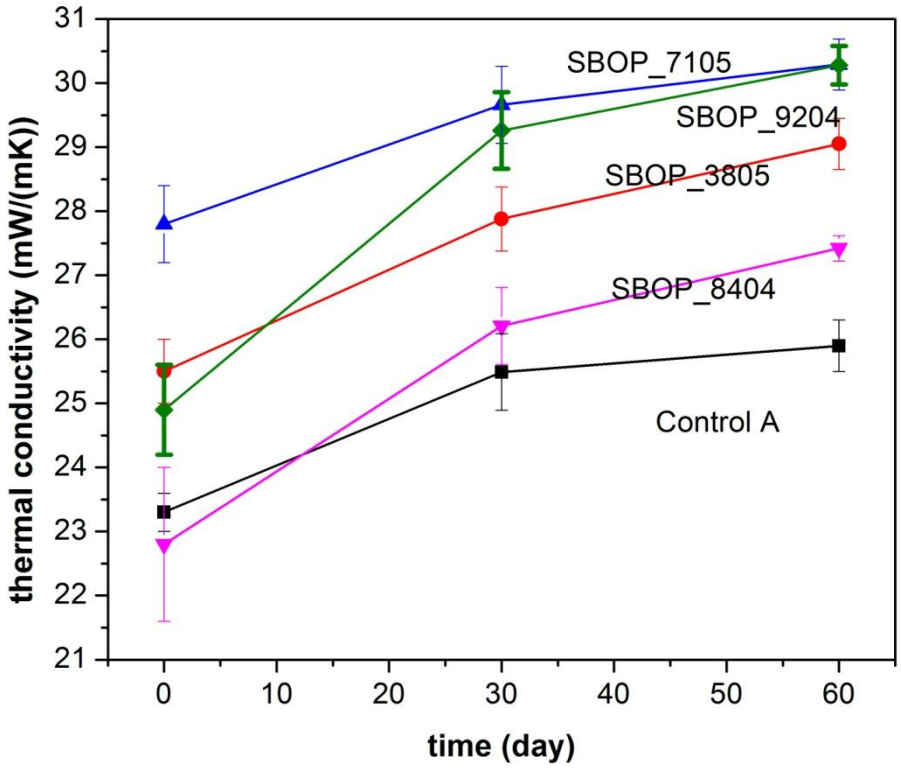

Figure 3.14: Foam aging test of foams from Control A, SBOP A_3805, SBOP A_7105, SBOP A_8404, SBOP A_9204.

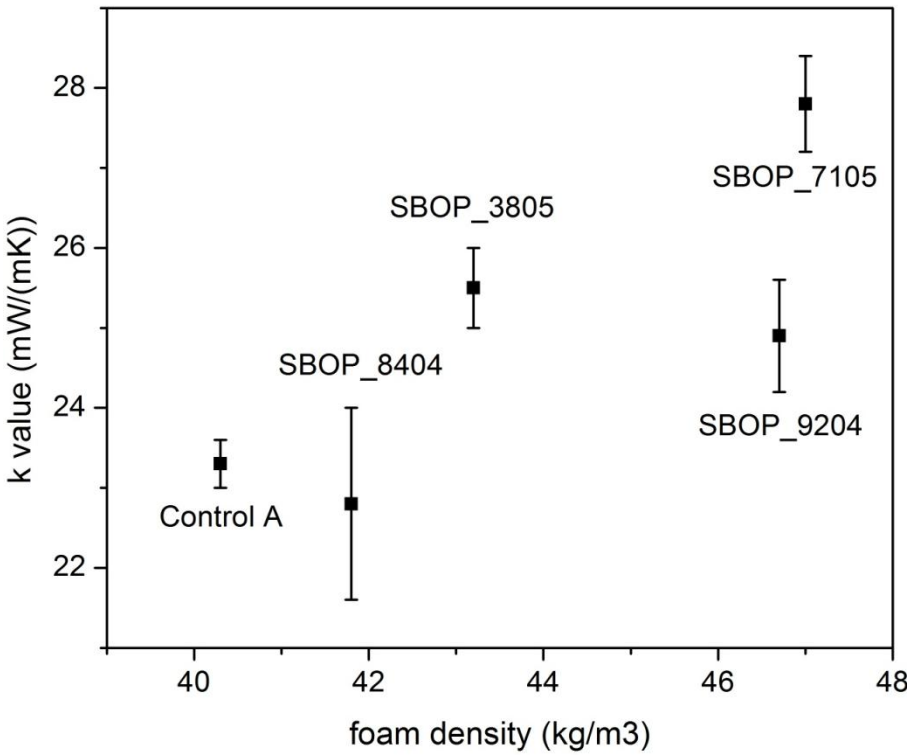

Figure 3.15: Apparent relationship between foam k value and density of foams from Control A, SBOP A_3805, SBOP A_7105, SBOP A_8404, SBOP A_9204.

3.5 Summary

The effect of four surfactants on soy-based foaming system was investigated. The results from FTIR and NMR showed that the surfactants were polydimethylsiloxane polyether copolymer .But the surfactant structure was still unknown. According to the cloud point test, the surfactants showed the following relative hydrophobicity: 7105> 9204> 3805> 8404. Although soy-based foams from different surfactant did have different cell size (distribution) and k value, only a weak correlation between surfactant hydrophobicity and k value and foam density was observed. However, the nature of the reaction mixture had changed a lot by adding glycerol since glycerol was a very polar

small molecule. In order to study the effect of SBOP itself on the foam properties, a new formulation will be developed and discussed in Chapter 4.

Chapter 4. Glycerol Free Route of Making Polyurethane Rigid Foam from Soybean Oil-based Polyol

4.1 Introduction

In Chapter 2, petroleum-based polyol Jeffol® SD-361 was chosen as the control polyol (Control A). But this control polyol had a larger OH number and smaller viscosity than SBOP which made it react much faster. Due to the imbalance between gelling and blowing reactions, foams from solely SBOP had much higher density, k value and poorer cell morphology though comparable T_g and compressive strength. In order to compensate this problem, cross-linker glycerol was added into soy-based foaming system. By adding glycerol, the gelling reaction was greatly accelerated, which gave enough heat to generate pentane gas and enough polymer network strength to hold cell structure. Thus, the cell morphology of soy-based foams was greatly improved. These foams had comparable density, k value and cell size, higher T_g and compressive strength. However, high level of glycerol was not favored due to high foam flammability. In Chapter 3 the effect of surfactant types was further investigated. A small correlation was found that with increasing surfactant hydrophobicity foam density and k value increased.

In this chapter, another petroleum-based polyol Jeffol® FX31-240 which had lower functionality and same OH number as SBOP was selected as the control polyol. Accordingly, a new formulation was successfully developed to study the effect of SBOP on polyurethane rigid foam properties. Following results and discussions revealed that

this was a very helpful formulation to study the limitation of SBOP in the application of polyurethane rigid foam.

4.2 Experimental

4.2.1 Materials

Petroleum-based polyol Jeffol® FX31-240 (Huntsman International) and an experimental soybean oil-based polyol (SBOP) were selected. SBOP was synthesized from the route of epoxidation followed by the ring opening using water and methanol (synthesis details seen section 1.4, Figure 2.1 in section 2.3 shows the major component in soybean oil and SBOP). The properties of two polyols were listed in Table 4.1. For comparison, the properties of Jeffol® SD-361 which was used in Chapter 2 also listed in the table.

From the table we see that Control A and Control B have a comparable molecular weight which was about 700 g/mol. But Control A had higher functionality and viscosity than Control B. The most significant difference between Control B and SBOP was that, unlike Control A, which had higher OH number, Control B had same OH number as SBOP. Control B had a lower functionality than SBOP as well. Moreover, SBOP had large amount of water content.

The water, catalysts, surfactant and physical blowing agent used in this chapter were the same as those used in Chapter 2; materials details can be found in section 2.3.1. In this formulation, diethylene glycol (Huntsman International) was used as a chain-extender to avoid foam shrinkage.

Table 4.1: Properties of polyols used (Control A, Control B and SBOP).

Polyol	Jeffol ® SD-361 (Control A)	Jeffol® FX31-240 (Control B)	SBOP
OH # (mg KOH/g)	360	240	240
Molecular Weight (g/mol)	690	700	1100
Functionality	4.4	3.0	4.4
Viscosity@25 ℃ (mPa·s)	2500	250	8900
Acid Value (mg KOH/g)	--	--	1.7
Water content (ppm)	--	--	3000
Manufacture /Resource	Huntsman	Huntsman	Experimental (Cargill)

4.2.2 Foam Synthesis

Table 4.2 showed the new formulation. It could be seen from the table that this formulation (including the amount of water, catalysts, surfactant, diethylene glycol and n-pentane) was exactly the same for both petroleum-based polyol and SBOP. The amount of water was adjusted according the water content in SBOP (see Table 4.1 for water content in SBOP). This formulation was very helpful in studying the effect of substituting SBOP. For the first attempt, SBOP substituted Control B from 25% to 100% in 25% increment. Details on the foam procedures were seen in section 2.3.2.

Table 4.2: Foam formulation (Control B, SBOP B).

Chemical	Control B	25% SBOP B	50% SBOP B	75% SBOP B	100% SBOP B
Jeffol ®FX31-240	100	75	50	25	--
SBOP	--	25	50	75	100
DI water	2.6	2.5	2.5	2.4	2.3
Diethylene glycol	6.0	6.0	6.0	6.0	6.0
Polycat ®8	4.0	4.0	4.0	4.0	4.0
Polycat ®5	1.0	1.0	1.0	1.0	1.0
Surfactant (TB 8404)	2.0	2.0	2.0	2.0	2.0
n-pentane	8.0	8.0	8.0	8.0	8.0
pMDI (index=125)	130	130	130	130	130

Figure 4.1: Foam appearance, from left to right: Control B, 25% SBOP B, 50% SBOP B, 75% SBOP B and 100% SBOP B.

It was shown in Figure 4.1 that by substituting SBOP from 25% to 100% of the total polyol used, the foam appearance did not have significant changes. All foams had similar shape and height.

4.2.3 Foam Characterization

Details on characterizations of foam density, cell morphology, k value, dynamic mechanical analysis, foaming kinetics study and foam aging test were seen in section 2.3.3.

4.3 Results and Discussion

4.3.1 Foam Property Summary

Table 4.3: Summary of foam properties (Control B, SBOP B).

Foam type	Control B	25% SBOP B	50% SBOP B	75% SBOP B	100% SBOP B
Density (kg/m^3)	39.5 ±0.8	39.7 ±0.9	39.8 ±1.1	41.3 ±1.3	46.4 ±2.0
T_g (℃)	98	107	123	134	142
k value (mW/m·K)	24.4 ±0.04	--	24.5 ±0.14	--	24.7 ±0.07
K_{45}-k_0 (mW/m·K)	2.38	--	1.59	--	3.64
Compressive strength (kPa)	115	--	138	--	170
Cell size (um)	431 ±91	392 ±84	390 ±102	375 ±128	386 ±102

4.3.2 Foam Cellular Morphology

SEM images showed that all foams had good cell morphology, maintained well-shaped cell structure. Figure 4.3 showed the cell size distribution analysis, data was listed in Table 4.3. Full discussion on foam cell morphology can be found in section 3.4.1. High bulk viscosity of the SBOP reaction mixture helped to reduce cell drainage by gravity at the initial foaming stage which led to a smaller average cell size. The viscosity of reaction mixture increased with SBOP substitution or replacement. Thus, foams from SBOP had smaller average cell size than Control B. Comparing the average cell size difference between control foams and 100% SBOP in two formulations, it was found that such difference was larger for the second formulation. It was understandable that the viscosity difference between petroleum-based and soy-based foaming mixture was larger in the second formulation than that in the first formulation (See Table 2.1 and 4.1 for viscosity data).

4.3.3 Thermal Conductivity Measurement

k value measurement was done on samples from Control B, 50% SBOP B and 100% SBOP B. All these samples showed comparable k value with the difference within 1 mW/(mK) (about 4% difference). As discussed in Chapter 3, k value greatly depended on foam density and cell morphology. Foams from 50% SBOP B had comparable density and 10% smaller cell size, though 100% SBOP B foams had 17% higher density while 11% smaller cell size which still led to low foam k value. Thus, freshly-made foams from SBOP B had comparable thermal insulating properties with those from Control B.

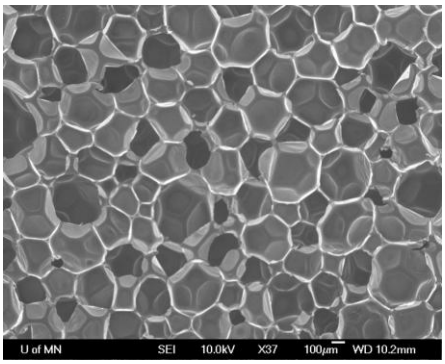

Control B

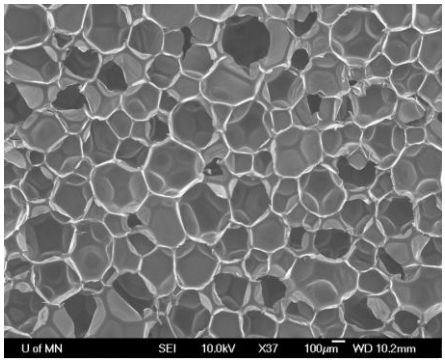

25% SBOP B

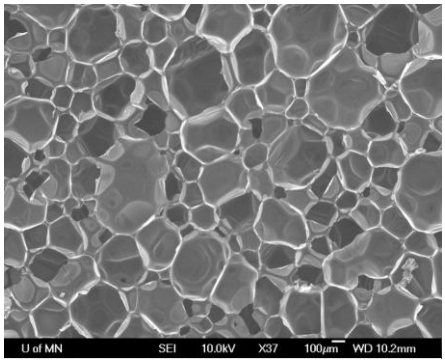

50% SBOP B

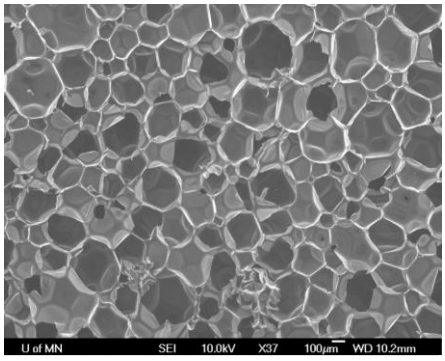

75% SBOP B

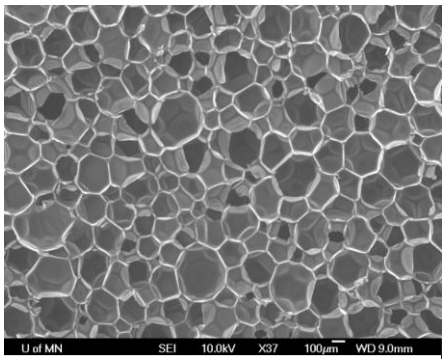

100% SBOP B

Figure 4.2: SEM images of foam samples (Control B, SBOP B).

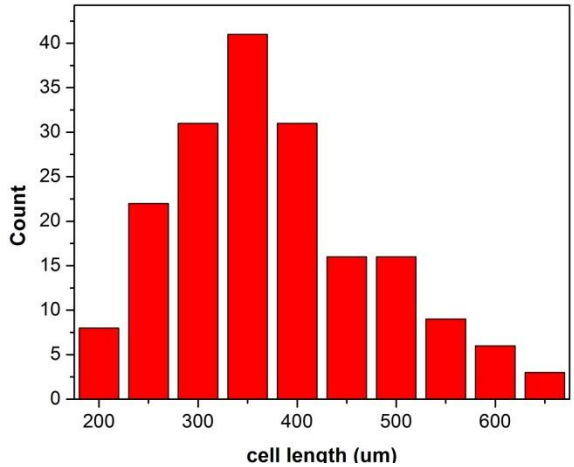

Control B

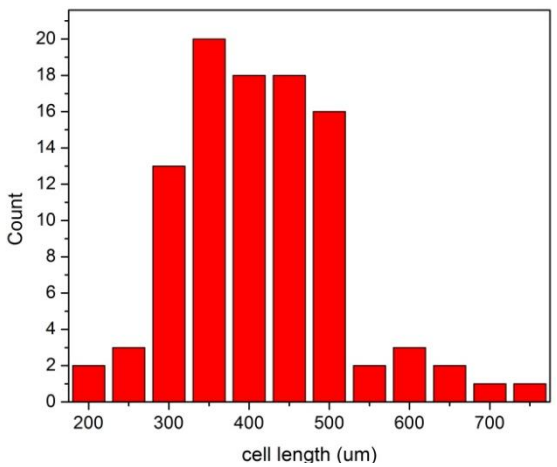

25% SBOP B

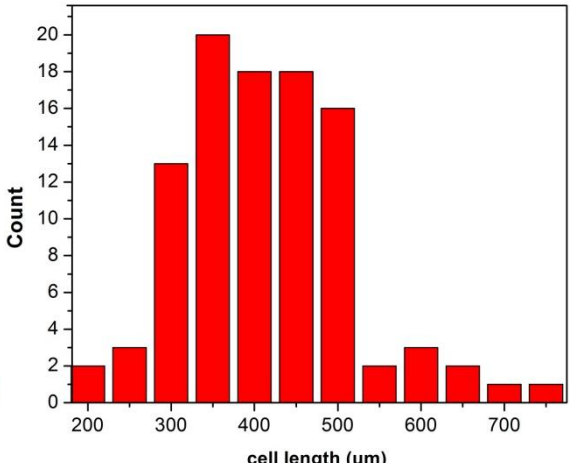

50% SBOP B

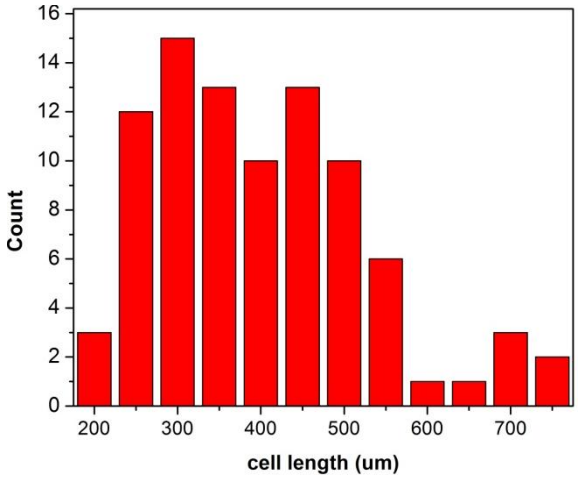

75% SBOP B

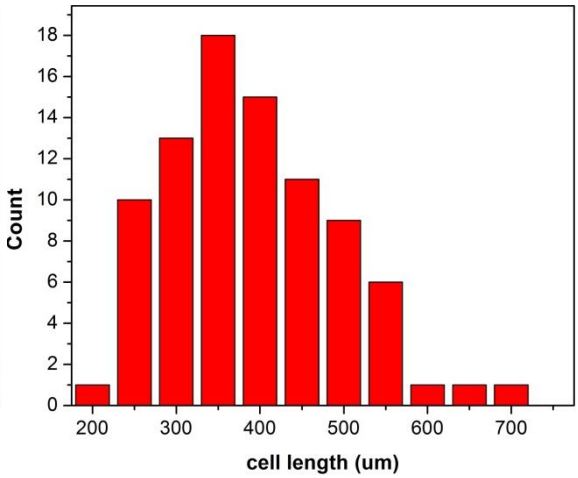

100% SBOP B

Figure 4.3: Cell size distribution analysis (Control B, SBOP B).

4.3.4 Dynamic Mechanical Properties

In Figure 4.4, both G' and G" data were plotted for the foams from Control B, 50% SBOP and 100% SBOP. At glassy state, all samples had comparable plateau G' values at about 2×10^6 Pa. As the SBOP substitution increased, the drop of G' from glassy to rubbery state shifted to higher temperature. At rubbery state, foams from Control B and 50% SBOP B had comparable G' which was about 2×10^6 Pa. The plot of G" shared the similar trend. Figure 4.5 showed the determination of T_g from tan_delta curve, T_g value was picked from the peak value of the tan_delta curve. Foams from Control B had T_g at about 98 ℃, with 50% SBOP substitution, T_g increased to 123 ℃, with 100% SBOP replacement, T_g reached as high as 142 ℃. As discussed in section 2.3.3, shorter chain length between cross links of SBOP led to a higher T_g. It was observed that the peak of tan_delta curve of SBOP B foams was not as sharp as Control foams. With increasing SBOP substitution, the peak became increasingly broader.

Compared the G' and G" plateau value at glassy state that, foams from the second formulation had lower G' and G" value than the foams from the first formulation. Thus, foams from the second formulation were less rigid than the foams from the first formulation. This characteristic made a better contact between foams and parallel plates during the measurement. So, compared to the plots of G' and G" in Chapter 2, G' and G" graph in this chapter is much better.

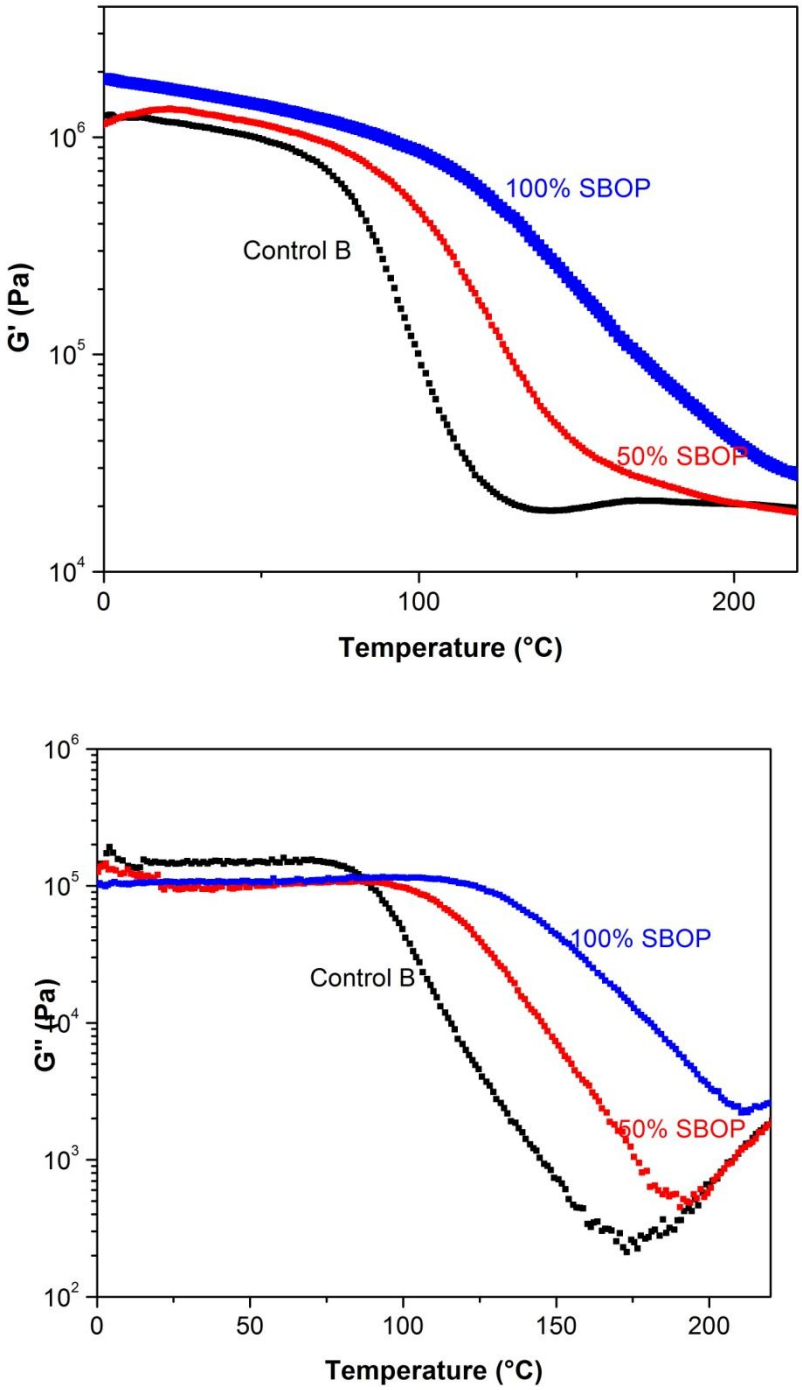

Figure 4.4: DMA curves showing G' (top) and G" (bottom) as a function of temperature (Control B, SBOP B).

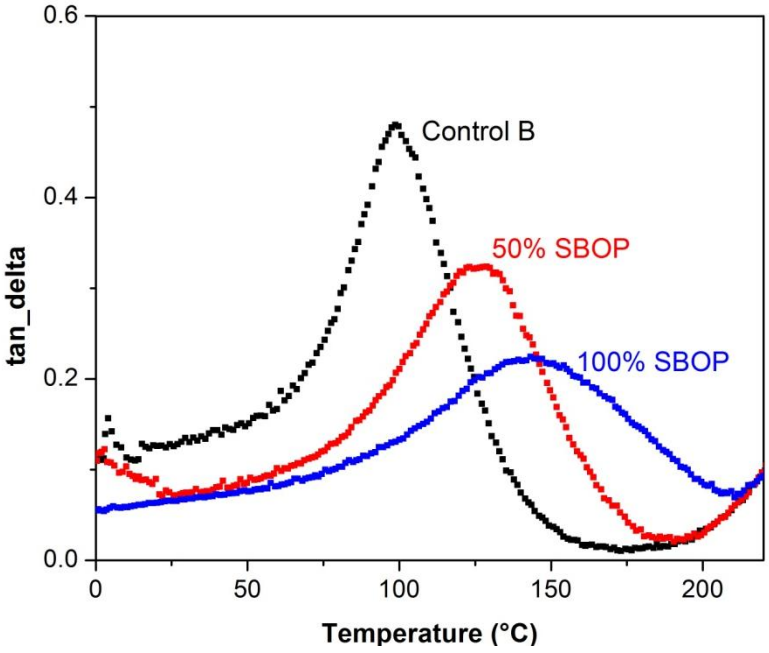

Figure 4.5: tan_delta curves for T_g determination (Control B, SBOP B).

4.3.5 Foam Kinetics

It was shown in Figure 4.6 that reaction mixture of 100% SBOP B shared very similar isocyanate conversion profile to that of Control B. The isocyanate conversion profile showed that foaming from Control B and 100% SBOP B had same isocyanate conversion in the first 20s. After the initial 20s, foaming of 100% SBOP B reacted only slightly slower than that of Control, and reached a slightly higher plateau value of isocyanate conversion. There were mainly three reactions involved in this study, reactions of isocyantes with water, diethylene glycol and polyol respectively. According to the reactivity of water, diethylene glycol and polyol, the first 20s was mainly due to the reactions of isocyanate with water and diethylene glycol. After 20s, the reaction in soy-based foaming system was slower than that in petroleum-based foaming system. For

petroleum-based system, the reactions reached the plateau value at about 50s, while soy-based system start to reach the plateau value at about 100s.

Figure 4.7 showed the calculated isocyanate conversion profile of Control A and Control B. From the graph we could see that the isocyanate conversion of Control A and Control B was the same in the first 20s. After 20s, the reaction of Control B had slowed down, but reached the plateau at an approximate same time about 40s as that of Control A.

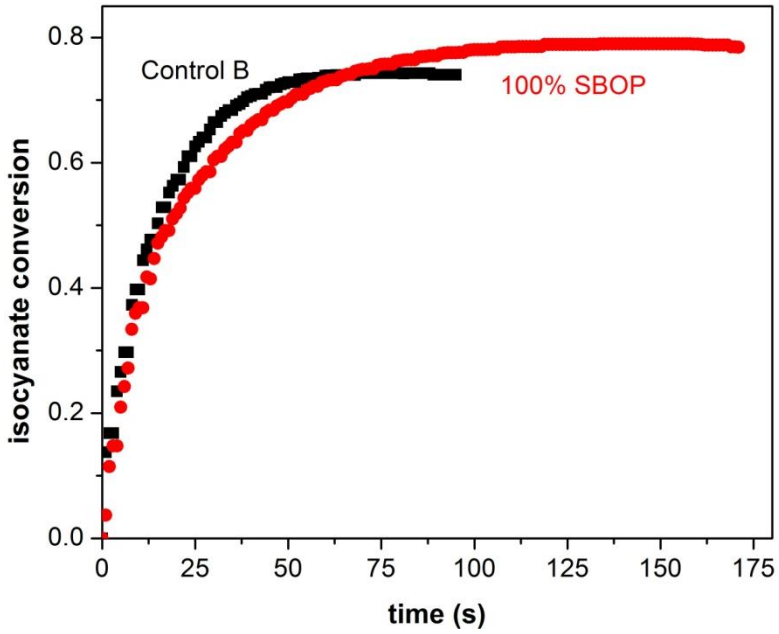

Figure 4.6: The isocyanate conversion profile calculated from adiabatic temperature rise experiment during foaming (Control B, SBOP B).

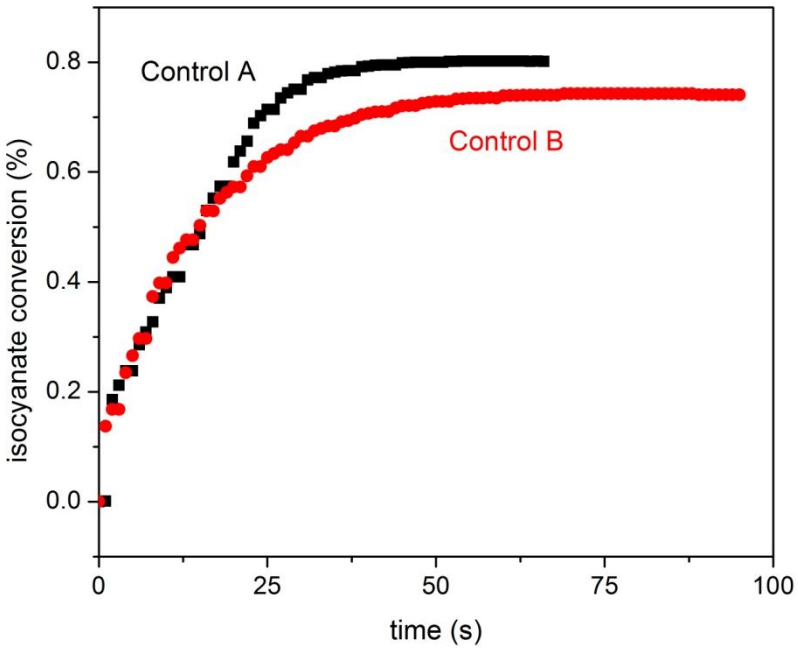

Figure 4.7: Temperature profile of foaming systems of Control A and Control B (formulation without n-pentane).

4.3.6 Foam Aging Test

Details on the procedures see section 2.3.2. The foam k value aging profile was very different from that of the first formulation. For the first formulation in Chapter 2, foams from 100% SBOP had similar k value aging profile with foams from Control A. Figure 4.8 showed the foam aging results for foams from Control B, 50% SBOP B and 100% SBOP B. Foam from 50% SBOP B had very similar k value aging process as that foam from Control B, while foam from 100% SBOP B aged much faster. Comparing these two k value aging profile, foams from the second formulation had different profile from those from the first formulation. As discussed in Chapter 2, glycerol was added into soy-based foaming system in order to improve foam properties. However, the nature of the reaction mixture had greatly changed by adding a polar additive. Unlike the formulation used in

Chapter 2, the formulation in Table 4.2 was exactly the same for petroleum-based polyol Control B and SBOP B. Thus, the resulted foam property deficiency was only due to SBOP substitution. The mechanism of the foam aging will be further discussed in Chapter 5 shortly.

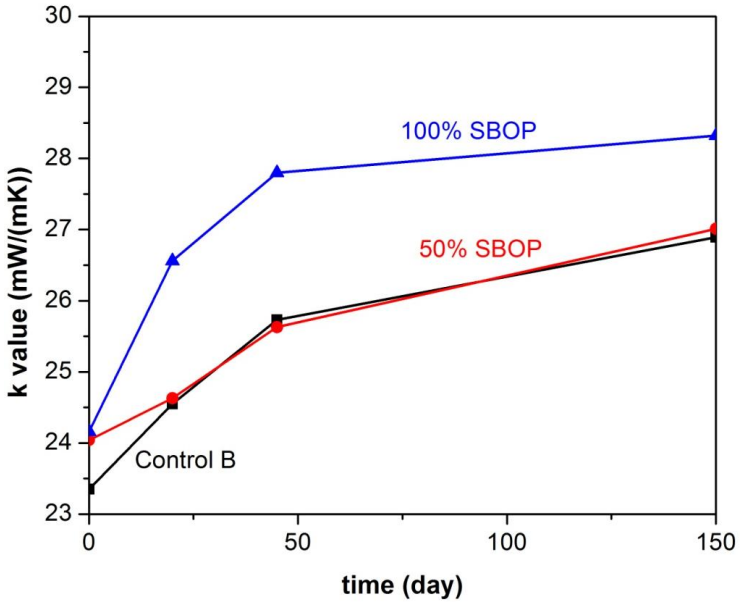

Figure 4.8: Foam k value aging curve (Control B, SBOP B).

4.4 Summary

In this chapter, a petroleum-based polyol with comparable OH number but lower functionality was chosen, a formulation was developed to study the effect on foam properties caused only by substituting SBOP. In this formulation, soy-based foaming system had exactly the same amount of components as petroleum-based foaming system. Table 4.3 summarized foam properties. Soy-based foams had comparable density with Control B within 5% difference, except that the density of foams from 100% SBOP B

was 17% larger which was still in the acceptable range for low density polyurethane rigid foam. [2,4] Soy-based foams also had comparable k value (within 4% difference) and higher T_g (10%, 25%, 37% and 45% higher respectively), compressive strength (20% higher for 50% SBOP and 48% higher for 100% SBOP respectively). As for the cell morphology, all the soy-based foams also had maintained regular cell structure and even slightly smaller average cell size (9%, 10%, 13% and 11% respectively). Therefore, the soy-based polyurethane rigid foams had comparable or even superior properties to petroleum-based foams. Although soy-based foams had comparable initial k value to petroleum-based foams, foams from 100% SBOP aged much faster while foams from 50% SBOP had similar k value aging. Comparing the results from Chapter 2 and this chapter, a similar trend was found that, foams had slightly higher density, comparable k value, much higher compressive strength and T_g by replacing petroleum-based polyol with SBOP. However, foams from SBOP in two different formulations showed different k value aging process. Unlike the soy-based foams from the first formulation which showed similar k value aging process to that of Control A, soy-based foams from the second formulation aged much faster than Control B. Because the second formulation was exactly the same for both SBOP and Control B, the resulted property deficiency was only due to the intrinsic property of SBOP. In order to study the limitation of soy-based polyurethane foaming system, the mechanism behind the faster foam aging problem and strategies for k value aging improvement were further investigated in Chapter 5.

Chapter 5. Foam Aging Mechanism Study

5.1 Introduction

Over time, polyurethane rigid foam will undergo k value changes due to the change in gas composition. For freshly made polyurethane rigid foam, gas trapped inside the cell is a mixture of mostly physical blowing agent (n-pentane in this study), some CO_2 and small amount of air. Driven by the partial pressure difference between foam cells and atmosphere, air will gradually diffuse into the cells. Similarly, CO_2 and pentane will diffuse out of the cells. [2, 67-70] Figure 5.1 show the mean cell gas pressure of 245fa (HFC type physical blowing agent), CO_2 and air and total cell pressure from the measured gas effective diffusion coefficient during aging.

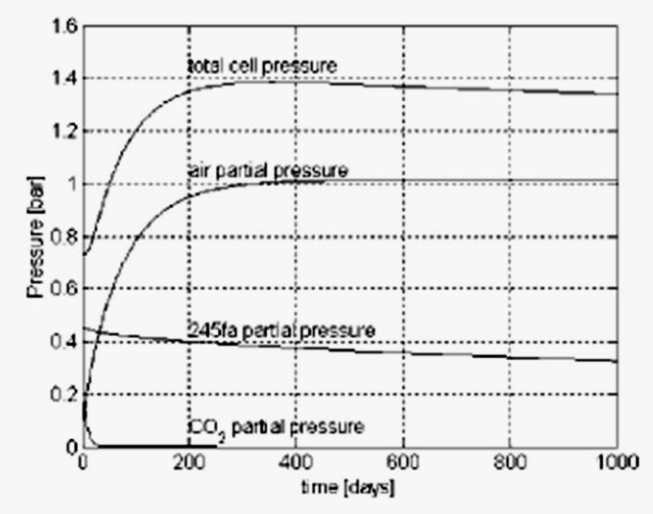

Figure 5.1: Mean cell gas pressure of 245fa, CO_2 and air and total cell pressure during aging. [68]

Generally, CO_2 diffuses out much faster than other gases. The process of air diffusion is slower than CO_2, its partial pressure increases quickly initially but will gradually reach a plateau. N_2 builds up faster than O_2. For physical blowing agent like CFC and HFC type physical blowing agents and pentane, the diffusion is really slow.

Table 5.1: k value of some cell gases. [67]

Gas	N_2	O_2	CO_2	n-C_5H_{12}
k value @ 10 ℃ (mW/(mK))	24.6	24.9	15.3	13.7

Bogdan et al. [59] summarizes the factors that influence the thermal performance in terms of the cell structure, physical properties of the blowing agents such as their k value, boiling point, solubility in the reaction mixture and diffusion rate.

Total foam k value consists of four parts: [72]

$$\lambda_{foam} = \lambda_{gas} + \lambda_{radiation} + \lambda_{solid} + \lambda_{convection} \qquad \text{Equation 5.1}$$

λ_{gas} is the k value of the gas trapped inside the cell, it counts for 60-65% of λ_{foam} (about 15-16 mW/(mK)); $\lambda_{radiation}$ is the heat radiated across the cells of the foam, it is proportional to the cell diameter and its proportion increases with decreasing density, it contributes about 30% of λ_{foam} (about 7-8 mW/(mK)); λ_{solid} is the heat conducted through the walls of the cell, it counts for only 3-4% of the λ_{foam} in low density foam (about 0.7-1

mW/(mK)); $\lambda_{convection}$ only matters when the diameter of the cells is larger than 10mm, and is usually treated to be effectively zero in the polyurethane rigid foam.

Table 5.1 shows the k value of the representative cell gases. Air has much higher k value than CO_2 and pentane, while CO_2 has slightly higher k value than pentane. Theoretically, the outgassing of CO_2 should lead to a lower k value. But the k value difference between CO_2 and pentane is not large enough to cause significant k value change for foam samples. Additionally, the ingress of the air also takes place during the same time, and air has much higher k value which also compensates the outgassing of CO_2. Compared to the pentane outgassing process, air ingress is much faster which dominates in the k value change process.

Figure 5.2 showed the comparison between experimental and predicted foam aging. The k value aging was predicted based on equation 5.1. λ_{solid} was calculated from the expression proposed by Gilcksman and Schuetz; λ_{gas} was calculated using the gas composition and the contribution of different gases; $\lambda_{radiation}$ was calculated from the extinction coefficient which could be measured from FTIR. The predicted foam aging curve had a good agreement with the experimental data.[68] The foam aging curve had similar shape with air partial pressure change curve. The diffusion of CO_2 out and air into the cells happened during foam aging. The experimental accelerated foam aging curve in my study (Figure 5.3) also shows similar shape which indicate air ingress problem.

Actually, there are many factors that will influence foam aging, some important parameters include: density and its distribution, average cell size and cell size distribution,

cell elongation and orientation, material distribution within the individual cells between struts and windows. [67]As discussed in Chapter 3, surfactants can be designed and chosen to control cell morphology according to different foaming systems to some extent. Data in both Chapter 2 and Chapter 4 has shown that, all soy-based foams have comparable cell morphology. The study in Chapter 5 is focus on investigating the effect of the intrinsic property of SBOP on foam aging.

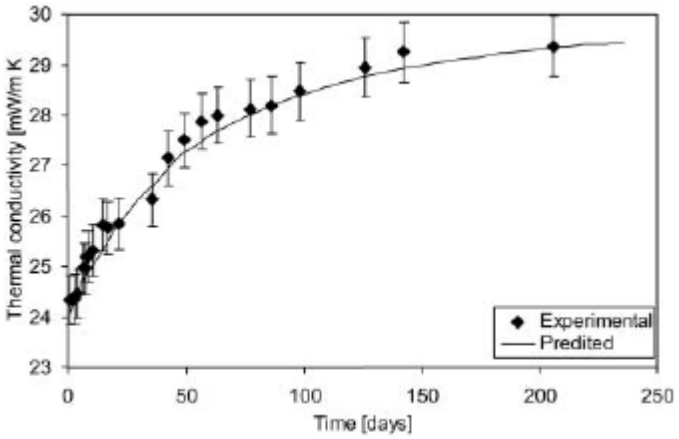

Figure 5.2: Comparison between experimental and predicted foam aging. [68]

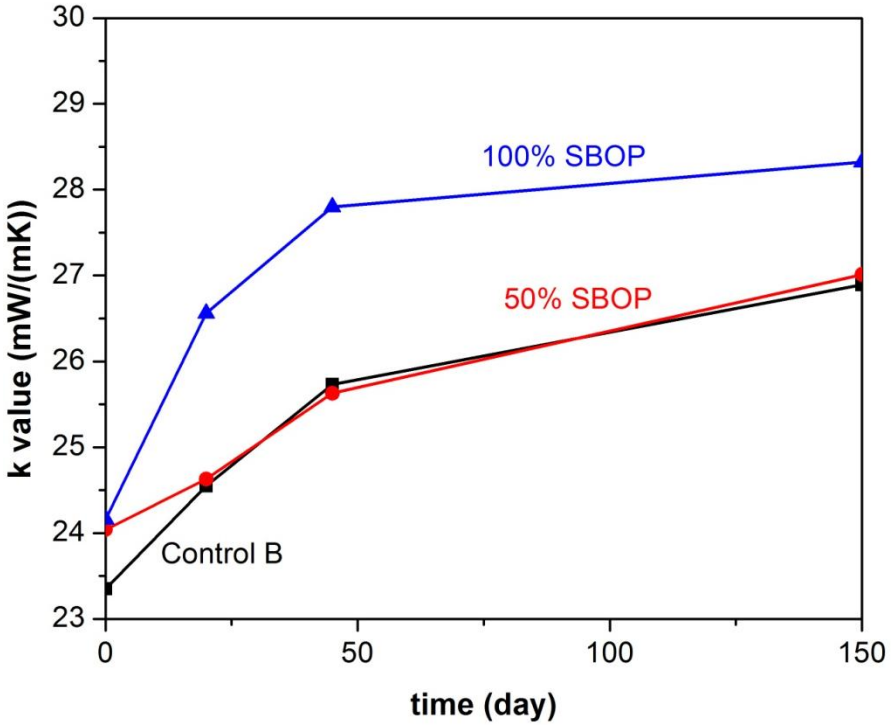

Figure 5.3: Experimental accelerated foam aging (Control B, SBOP B).

5.2 Experimental

5.2.1 Choice of Technique

Table 4.2 has already provided a very good formulation to study the effect of substituting petroleum-based polyol with SBOP. In the literature, there are mainly two methods to study the gas permeation. The first approach is to use the actual foam samples directly. However, due to the complexities of cell morphology, it's very complicated to get precise comparison only between two polyols. The second method is to measure gas permeation through a polyurethane thin film which can represent the polymer in the polyurethane rigid foam. This method eliminates the influence of foam cell morphology.

Therefore, gas permeation measurement is performed using the second approach in this study.

5.2.2 Materials

Two polyols used in this study were one petroleum-based polyol Jeffol® FX31-240 (Control B) and SBOP. Polymeric MDI (pMDI, Rubinate®M, CAS 9016-87-9) was obtained from Huntsman International. *N, N*-Dimethylcyclohexylamine (Polycat®8, AirProducts, CAS 98-94-2) was used as the gelation catalyst. Diethlyene glycol was used as the chain extender. Organic solvent acetone was also used.

5.2.3 Film Preparation

Table 5.2 listed the formulation to prepare polyurethane thin film. Since isocyanate can easily react with water including the moisture in the air, the most difficult part was to avoid producing bubbles during the preparation procedure. Water was not added because urea linkages in the polymers only slightly affect the gas permeation. [71] Polyols were dried under high vacuum, high temperature (110 ℃) and high speed stirring for 3-4 hours before use. Acetone was used to dilute the reaction mixture. This not only helped to make a thin and homogeneous film, but also helped to avoid trapping bubbles. Decreasing the bulk viscosity of the solution can help to increase the bubble drainage by gravity, which had been discussed in Chapter 3. The amount of catalyst was also adjusted to balance the gelling reaction and acetone evaporation. The gelling reaction should be fast enough to avoid the reaction between isocyante and moisture as much as possible, but should be slow enough for most of the acetone to evaporate.

Table 5.2: Polyurethane thin film formulation.

Chemical	Control B	50% SBOP	100% SBOP
Control B	20	10	--
SBOP	--	10	20
DEG	1.2	1.2	1.2
Polycat ® 8	0.05	0.2	0.2
Acetone	25	25	25
pMDI	14.24	14.24	14.24
ISO index	105	105	105

Polyurethane thin films of about 300-500 um thickness were prepared in an open-face film casting mold. [71]The mold was made from a 14"×14" high density polyethylene (HDPE) sheet with an aluminum picture frame with 1" sides on top. Prior to casting the films, the mold was carefully leveled in order to get even film thickness.

Polyol, DEG, catalyst and isocyanate were blended with acetone in a 200 ml polypropylene plastic cup. The mixture was stirred gently until a homogeneous solution was formed. The solution was then poured into the mold carefully. Another HDPE sheet was covered over the mold to prevent direct contact with air flow. The film was kept at room temperature for 24 hours, during which the solution gradually solidified and most of the acetone had evaporated. The film was removed from the HDPE sheet and cut into disk with 4.2 cm diameter. The films were placed between sheets of Mylar® films for

further curing at room temperature for 120 hours, a heavy bulk steel was placed on top to ensure film flatness. The films were then put into the vacuum oven for final cure for 48 hours. Figure 5.4 represented the film making procedures.

5.2.4 Gas Permeation Measurement

Gas permeation tests based on a constant volume-variable pressure method [72, 73] were performed on a home-built apparatus. [73] The film was fit and sealed into the gas transmission cell to form a semibarrier between two chambers. The apparatus was evacuated overnight. N_2 flow was fed to one side of the chamber and the pressure change in the opposite chamber which has been evacuated was monitored as a function of time. Gas permeation constants were obtained from the pressure change normalized with the pressure gradient across the sample, film area and thickness. [74]

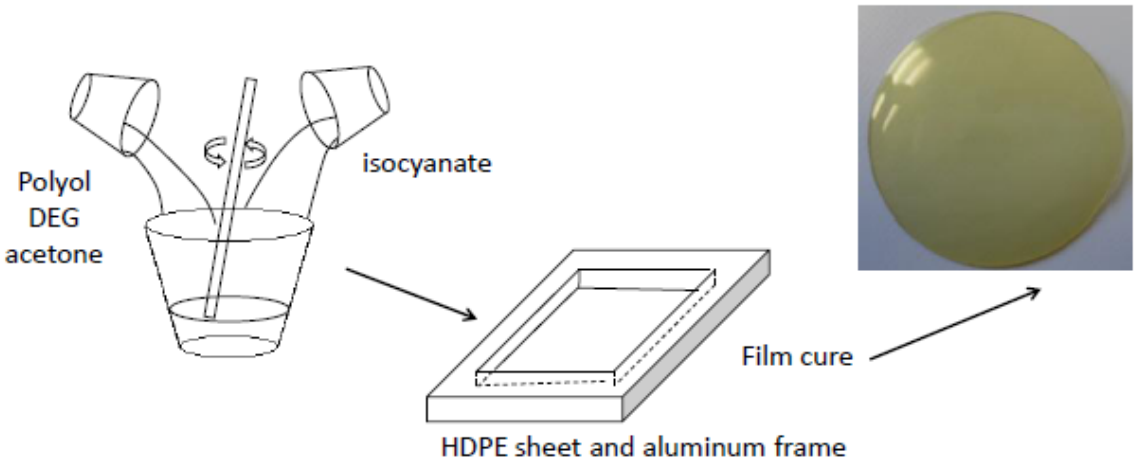

Figure 5.4: Polyurethane thin film making procedure.

5.2.5 Results and Discussion

Figure 5.5 showed the N_2 permeation results for polyurethane thin films from Control B, 50% SBOP and 100% SBOP. It was shown that by substituting 50% SBOP into Control B, N_2 permeation did not change significantly. However, films from 100% SBOP had much higher N_2 permeation, almost as twice as films from Control B. The N_2 permeation results showed good agreement with the foam aging results. The much higher N_2 permeation of the soy-based polyurethane thin film led to faster k value aging than petroleum-based or partially petroleum-based polyurethane thin film. The mechanism behind the faster k value aging for soy-based foams was revealed. Possible approaches were discussed to reduce N_2 permeation of soy-based polyurethane thin film.

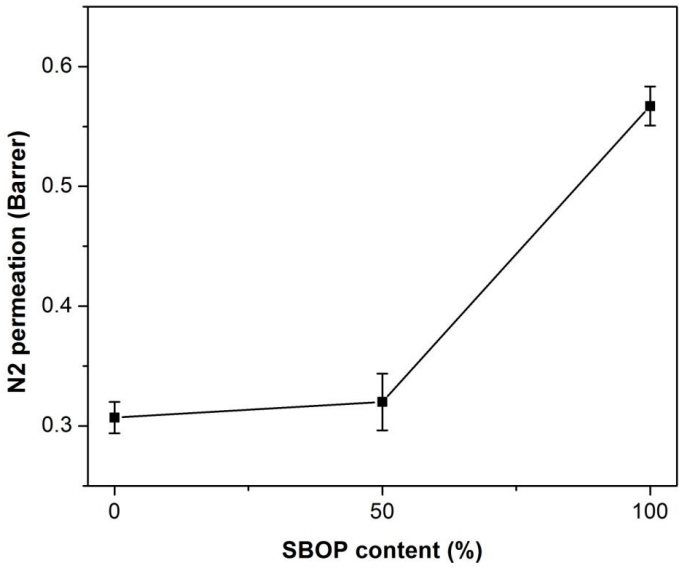

Figure 5.5: N_2 permeation of polyurethane thin films.

(Barrer is a non-SI unit of gas permeability, 1 Barrer=10^{-10} (cm^3 O_2) cm cm^{-2} s^{-1} $cmHg^{-1}$, here '$cm^{-3}O_2$' is a molar quantity of O_2)

5.3 Approaches for N_2 Permeation Improvement

5.3.1 Polymer Cohesive Energy Density

With other factors equal, gas permeation decreases with increasing structural symmetry and cohesive energy density of the polymer. [75]Compared to the chemical structure of petroleum-based polyol and SBOP, SBOP has less structural symmetry than petroleum-based polyols. But in the highly cross-linked polymers, such structural symmetry difference is not significant. Further study is conducted on investigating cohesive energy density of polyurethane thin films.

Polymer cohesive energy density is related to its solubility parameter. The solubility parameter is defined as the square root of the cohesive energy density in the amorphous state at 25 ℃. [52, 76] The solubility parameter of polyurethane thin films was determined at room temperature by equilibrium swelling method. The swelling study was conducted in different solvents whose solubility parameter (δ) ranged from 9.21 to 14.28 $(Cal/cm^3)^{1/2}$, where the swelling equilibrium was reached. The polyurethane thin film (~1.5-2.0 mm thickness) was dried and weighed before being immersed into the solvent. The film was taken out at certain time intervals, wiped out the adhering solvent and weighed again. This was continued until the swelling reached the equilibrium. Mole percent uptake (Q_t) was used to quantify the sorption of penetrant molecules into polymer, equation 5.1 showed the calculation of Q_t.

$$Q_t = \frac{n_i}{m_i} \times 100 \qquad \text{Equation 5.1}$$

Where, n_i was the moles of solvent taken up at time t, m_i is the dry mass of the sample. Q_∞ was denoted as the mole percent uptake at equilibrium. [77-79] Figure 5.6 showed a representative plot of mole percent uptake as a function of time. The equilibrium swelling degree ($Q\infty$) was obtained from the plateau and plotted against various δ of the solvents. Figure 5.7 showed the plot of equilibrium degree of swelling as a function of solvent solubility parameter. The solubility parameter of polymer was obtained from the peak value from the plot. [77] From the plot, the solubility parameter of thin film from Control B is around 12 $(Cal/cm^3)^{1/2}$, as SBOP substitution increased, polymer's solubility parameter tended to decrease to around 10.8 $(Cal/cm^3)^{1/2}$. Therefore, soy-based polyurethane thin film had lower solubility parameter, thus also lower polymer cohesive energy density, which led to higher N_2 permeation.

Increasing the cohesive energy of soy-based polyurethane thin film is one approach to reduce N_2 permeation. Actually, a very good example was found in the first formulation in Chapter 2. By adding glycerol, foams from 100% SBOP had similar k value aging profile to those from Control A. However, in the second formulation, foams from 100% SBOP had much faster k value aging profile than those from Control B. It was expected from the formulation that the polymer cohesive energy difference between films of Control and SBOP was larger in the second formulation than that in the first formulation.

Soy-based polyol can be chemically modified to increase its polarity. As discussed in section 1.4, HCl, HBr can be used in the ring-opening step. The introduction -Cl, -Br

side groups into the polyol will increase the cohesive energy density and is supposed to reduce the gas permeation too. [75]

Table 5.3: Solubility parameter of organic solvents used in swelling test.

Solvent	Chloroform	Tetrahydrofuran	Dichloromethane
δ $(Cal/cm^3)^{1/2}$	9.21	9.52	9.93
Solvent	Pyridine	N, N-dimethylformamide	Methanol
δ $(Cal/cm^3)^{1/2}$	10.61	12.14	14.28

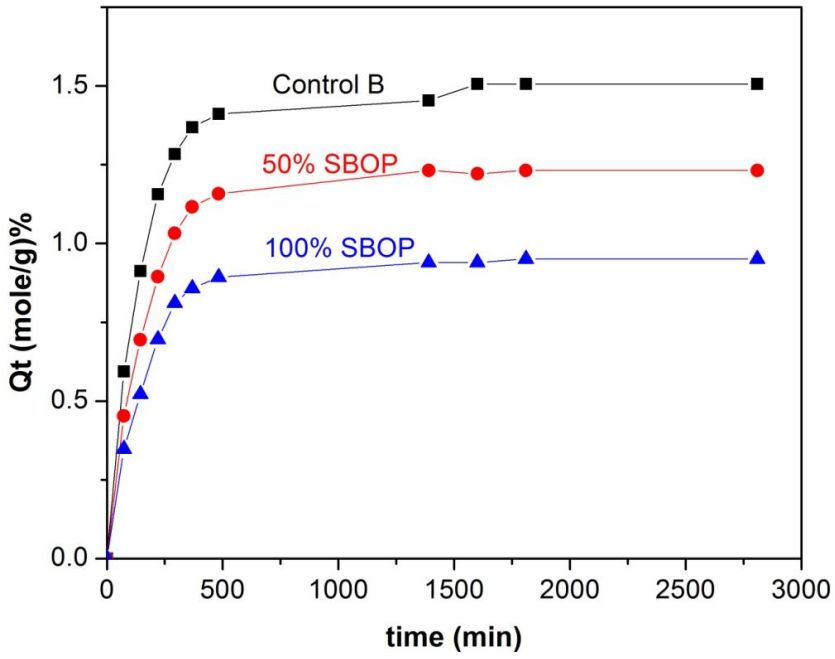

Figure 5.6: The sorption curve showing the mole percent uptake of polyurethane thin film as a function a time in DMF (δ=12.14 $(Cal/cm^3)^{1/2}$).

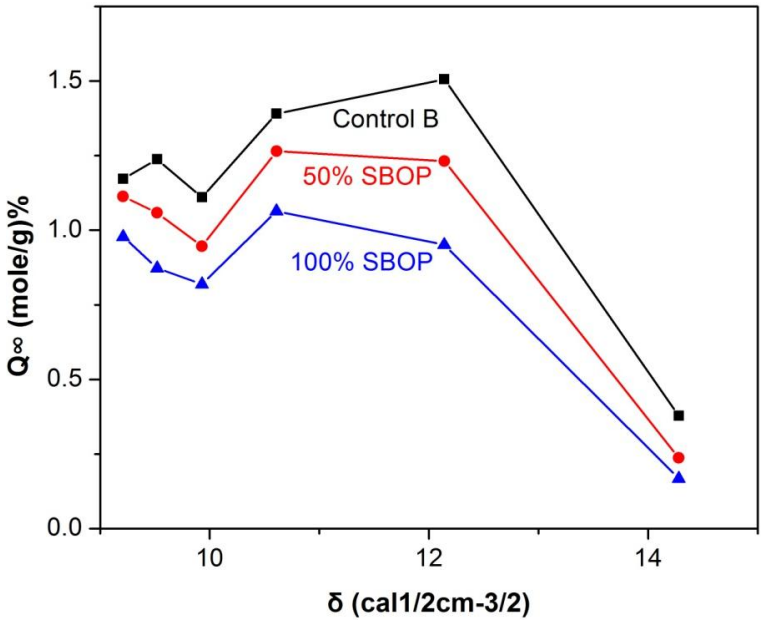

Figure 5.7: The plot of the equilibrium degree of swelling vs. solvent solubility parameter.

5.3.2 Free Volume Theory

In the free volume theory, the actual volume of polymer can be expressed as the sum of the volume occupied by the molecules (V_{occ}) and the free volume (V_f). Figure 5.8 shows the two dimensional schematic of chain packing showing the free volume in an amorphous polymer. The typical size of V_f is about 0.5-0.7 nm. Figure 5.9 is the scheme of the V_f concept. The key idea of V_f is that it decreases when cooling from liquid state. When the temperature reaches T_g of the sample, V_f reaches its minimum value. Below T_g, since the molecular motions are frozen out, the sample can no longer contract.

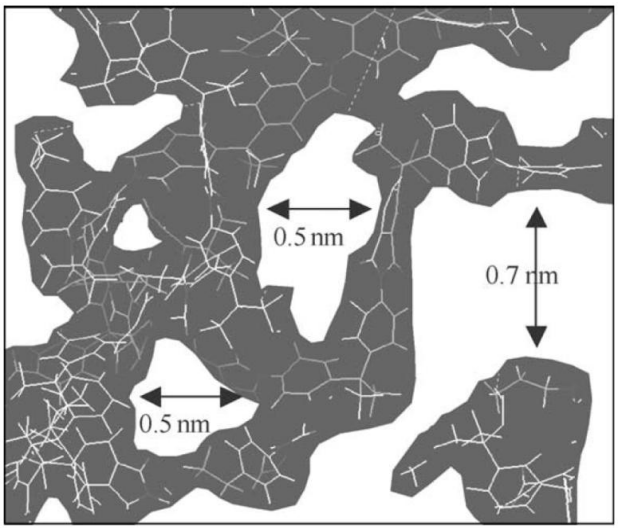

Figure 5.8: Two dimensional schematic of chain packing in an amorphous polymer showing free volume as white margins. [80]

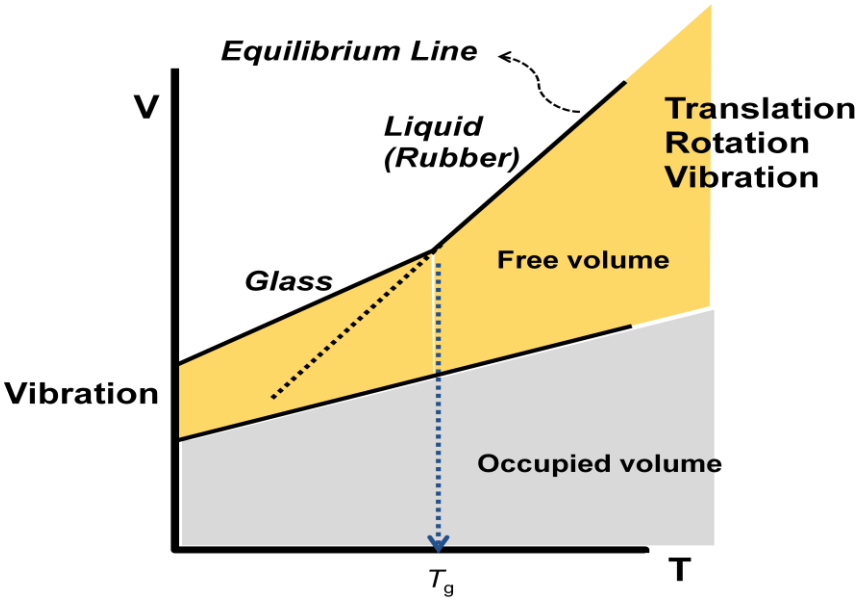

Figure 5.9: Schematic representation of the actual volume, occupied volume and free volume as a function a temperature. [81]

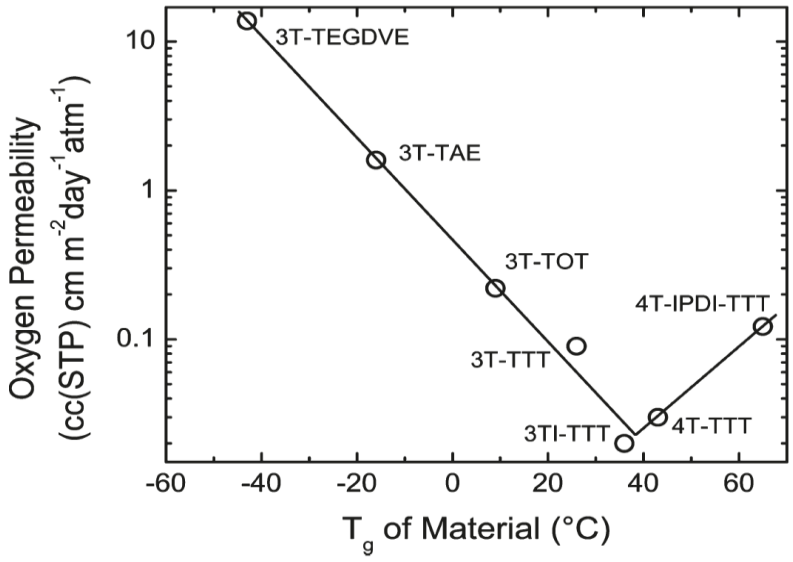

Figure 5.10: Relationship between polymer T_g and O_2 permeability. [82]

It has been shown that V_f has a close relationship with T_g. For a glassy polymer, when T_g of the polymer is higher than the gas permeation measurement temperature (T_{test}), the polymer with higher T_g will have larger V_f. [80, 81] Polymer with larger V_f will be easier for gas molecules to permeate. Kwisnek and co-workers have shown that O_2 permeability increases with increasing T_g for a series of glassy polymer [82] (See Figure 5.10). In the N_2 permeation study on the polyurethane thin films, same trend have been observed (see Figure 5.11).

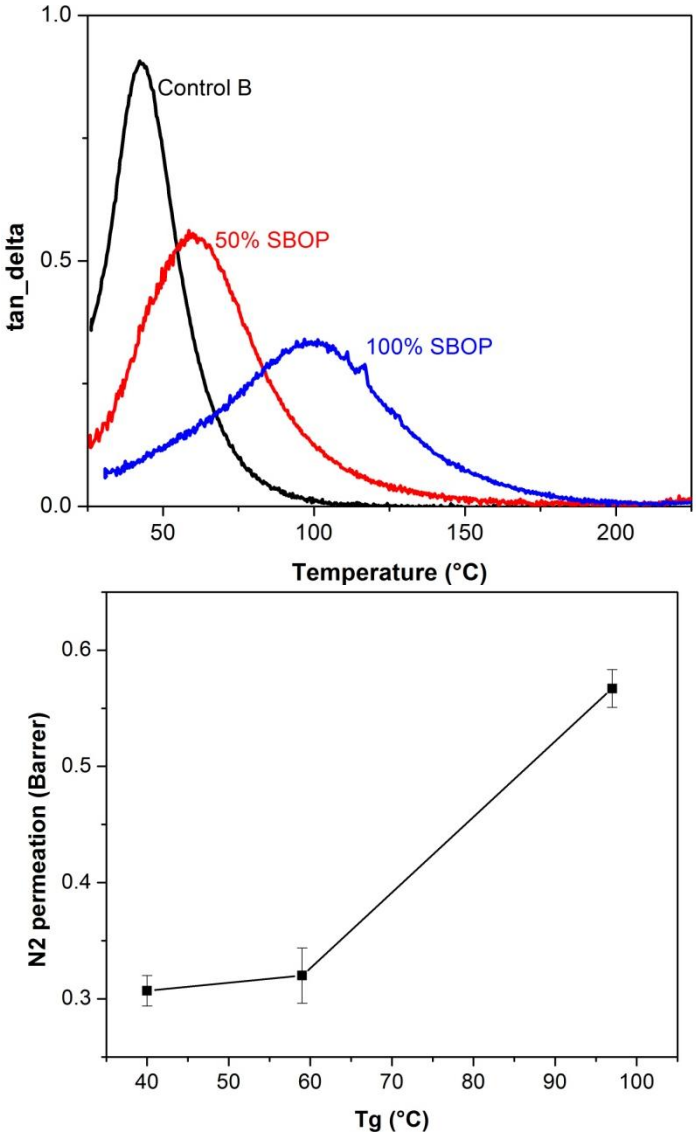

Figure 5.11: (top) Determination of T_g; (bottom) N_2 permeation vs. T_g.

By substituting SBOP, the T_g of polyurethane thin film increases with increasing amount of SBOP. And the N_2 permeation increases with increasing T_g. According to the free volume hypothesis, strategy can be taken to reduce T_g in order to reduce the N_2 permeation. Early work on soy-based polyurethane flexible foam from Zhang has shown that foams from castor oil have higher T_g than petroleum-based foams, but lower T_g than

that from SBOP. It is expected that polyurethane thin film from castor oil will have lower T_g than SBOP. However, castor oil has a much smaller OH number (163 mKOH/g) and lower f_n (f_n=2.7) [83], partially substitution of castor oil into SBOP is considered. N_2 permeation and T_g should be measured on the polyurethane thin films from SBOP with partially castor oil substitution.

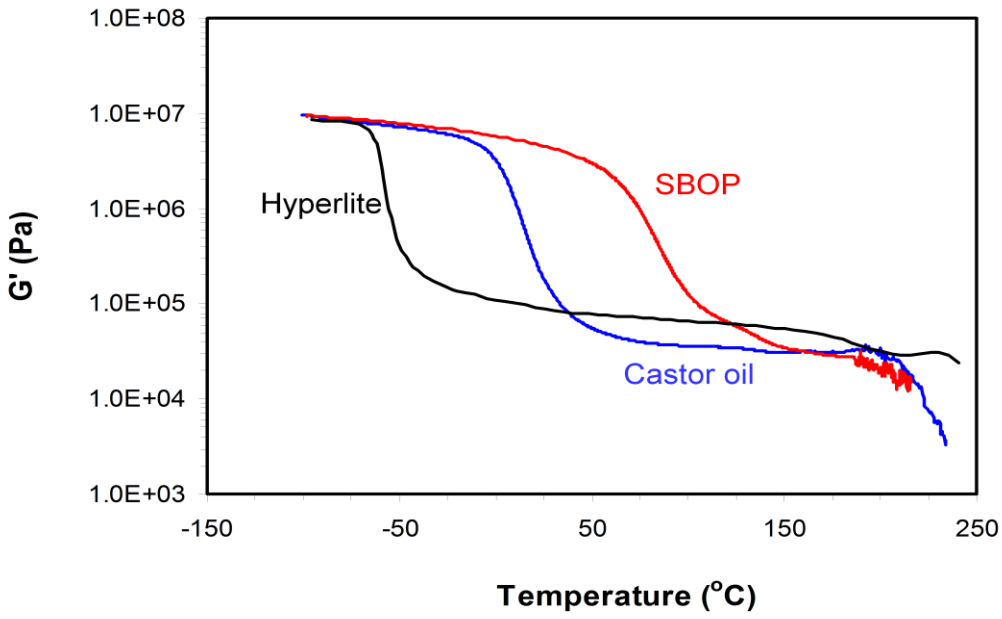

Figure 5.12: Plot of G' for flexible foams from (Hyperlite) petroleum-based polyol, castor oil and SBOP. [46]

5.3.3 Clay/polyurethane Composites

Clays such as vermiculite, graphene are often used as the reinforcing nano-materials to improve mechanical properties, dimensional stability, gas barrier and flame resistance of host polymers. [74] Ward and co-workers have prepared a polymer film filling with vermiculite. They found that the gas permeability had reduced for more than two orders

of magnitude by adding 3.0% wt of vermiculite in solvent cast films. [84] Gas barrier properties of vermiculite I butyl rubber/vermiculite nanocomposites coatings are also reported by Takahashi and co-workers. Gas permeability of various gases is found to be decreased greatly in high loading vermiculite coatings. [85]

Vermiculite will be used as the gas barrier to reduce N_2 permeation of polyurethane thin film from SBOP. Primary study has been done by adding 0.5% wt vermiculite into films made from SBOP. It is found that the N_2 permeation of vermiculite reinforced polyurethane thin film drops dramatically from 0.567 barrer to as low as 0.345 barrer. This is a really promising result. More reproducible work and further characterization such as XRD, DSC and RSA need be done to further investigate the effect of the vermiculite in gas permeation.

5.4 Summary

Mechanism behind foam aging is deeply studied in this chapter. Over time, due to the partial pressure difference between the cells and atmosphere, air will diffuse into the cells and CO_2 and n-pentane will diffuse out of the cells. Because the diffusion of air is much faster than n-pentane, the k value of air is also much higher than that of n-pentane and CO_2, the air diffusion dominates in the k value aging process. Considering that all the foams had comparable cell morphology, polyurethane thin films were made to perform the gas permeation test. It was shown that faster k value aging of soy-based foams is due to the higher N_2 permeation. Three approaches are proposed to reduce N_2 permeation. One is to increase the interaction between gas molecules and polymer by increasing

polymer cohesive energy. The introduction of polar groups like –Cl and –Br will effectively increase the polymer cohesive energy. Another way is to control the free volume of the polymer matrix to restrict gas molecules to permeate. Polymer free volume is closely related to its T_g, lower T_g tends to have smaller free volume. Castor oil can be partially substituted into SBOP to reduce T_g of polyurethane thin film. The last approached discussed is the addition of the vermiculite as the gas barrier. Primary study has shown a very promising result. By adding only 0.5% wt vermiculite, N_2 permeation has reduced by nearly 40%.

References:

[1] Singh, H.; Sharma, T. P.; Jain, A. K. *J. Appl. Polym. Sci*. **2007**, *106*, 1014.

[2] Randall, D; Lee, Steve. The Polyurethanes Book. **2002**. *John Wiley & Sons*, Ltd.

[3] IAL-Consultants, Alliance for the Polyurethanes Industry. 2004 End-use Market Survey on the Polyurethane Industry: **Oct. 2005**.

[4] Wirpsza, Z. translation editor, Kemp, T. J. *Polyurethanes: Chemistry, Technology and Applications*, **1994**.

[5] Hill, R. M. *Silicone Surfactants*; Marcel Dekker, Inc. **1999**.

[6] Mondal, P.; Khakhar, D. V. *Macromol. Symp.* **2004**, *216*, 241.

[7] Ionescu, M. *Chemistry and Technology of Polyols for Polyurethanes*, Smithers Rapra, **2005**.

[8] Szycher, Michael. *Szycher's Handbook of Polyurethanes*; CRC Press, **1999**.

[9] George W. *The ICI Polyurethanes Book*; John Willey & Sons. **1990**.

[10] Herrington, R.; Hock, Kathy. *Dow Polyurethanes: Flexible Foams*; **1997**.

[11] Petrovic, Z. S. *Polym. Rev*. **2008**, *48*, 109.

[12] Appelqvist LA. In: Robbenlen G, Downey R.K, Ashri A, editors. Oil crops of the world. Ed, New York: McGraw-Hill, **1989**.

[13] Carlson K.D, Chaudhry A, Bagby M. O. *J. Am. Oil. Chem. Soc*. **1990**, 67, 438.

[14] Finar I. L. Organic chemistry: The fundamental principles. *Longman Scientific & Technical*. **1986**.

[15] Solomons T. W. Graham. Organic chemistry. *Wiley*. **1984**.

[16] Findley T. W., Swern D., Scanlan J. T. *J. Am. Chem. Soc*. **1945**, 67, 412.

[17] Sinadinovic-Fiser S, Jankovic M, Petrovic Z. S. *J. Amer. Oil Chem. Soc*. **2001**, 78, 725.

[18] Petrovic Z. S, Guo A, Zhang W. *J. Polym. Sci., Part A: Polym. Chem.* **2000**, 38, 4062.

[19] Petrovic Z. S, Guo A, Javni I. US Pat. 2000/6, 107, 433.

[20] Petrovic Z. S, Javni I, Guo A, Zhang W. US Pat. 2002/6, 433, 121.

[21] Petrovic Z. S, Zhang W, Javni I. *Biomacromolecules*. **2005**, 6, 713.

[22] Tran P, Graiver D, Narayan R. *J. Amer. Oil Chem. Soc*. **2005**, 82, 653.

[23] Guo A, Demydov D, Zhang W, Petrovic Z. S. *J. Polym. Environ*. **2002**, 10, 49.

[24] Frankel E. N, Thomas F. L. *J. Am. Oil Chem. Soc.* **1972**, 49, 10.

[25] Kandanarachchi P, Guo A, Petrovic Z. S. *J. Mol. Catal. A: Chem*. **2002**, 184, 65.

[26] Lysenko Z, Schrock A. K, Babb D. A, Sanders A, Tsavalas J, Jouett R, Chambers L, Keillor C, Gilchrist J. H. WO Patent 096882; **2004**.

[27] Hou C. T. *Adv Appl. Microbiol*. **1995**, 41, 1.

[28] Tanaka, R.; Hirose, S.; Hatakeyama, H. *Bioresour. Technol.* **2008**, *99*, 3810.

[29] Lyon, C. K.; Garrett, V. H.; Franker, E. N. *J Am. Oil Chem. Soc* **1974**, *51*, 331.

[30] Hu, Y. H.; Gao,Y.; Wang, D. N.; Hu, C. P.; Zu, S.; Vanoverloop, L.; Randall, D. *J. Appl. Polym. Sci* **2002**, *84*, 591.

[31] Guo, A.; Javni, I. Petrovic, Z. *J. Appl. Polym Sci* **2000**, *77*, 467.

[32] Guo, A.; Zhang, W.; Petrovic, Z. S. *J. Mater. Sci* **2006**, *41*, 4914.

[33] Petrovic, Z. S.; Guo, A.; Javni, I.; Cvetkovic, I.; Hong, D. P. *Polym. Int.* **2008**, *57*, 275.

[34] Narine, S. S.; Kong, X.; Bouzidi, L. *J. Am Oil .Chem .Soc* **2007**, *84*, 65.

[35] Tu, Y.; Kiatsimkul, P.; Suppes, G.; Hsieh, F. *J. Appl. Polym Sci* **2006**, *105*, 453.

[36] Banik I, Sain M. M. *J. Reinf. Plast. Compos*. **2008**, 27, 357.

[37] Chang, L.; Xue, Y.; Hsieh, F. *J. Appl. Polym Sci* **2001**, *81*, 2027.

[38] Breger, D. *Journeys in Microspace: the Art of the Scanning Electron Microscope* Columbia University Press. **1994**.

[39] Bard, A. J.; Mirkin, M. V. *Scanning Electrochemical Microscopy* Marcel Dekker. **2001**.

[40] Hafner, B. *Scanning Electron Microscopy Primer*, Characterization Facility, University of Minnesota-Twin Cities, **2007**.

[41] Hilyard N. C, Cunningham A. Low Denisty Cellular Plastics: Physcial Basis of Behaviour. Chapman & Hall, 1994.

[42] Harikrishnan, G.; Macosko, C. W.; Choi, J. H.; Bischof, J. C.; Singh, S. N. *J Cell Plast*, **2008**, *44*, 481.

[43] Zhang, L.; Jeon, H. K.; Malsam, J.; Herrington, R.; Macosko, C. W. *Polymer*, **2007**, *48*, 6656.

[44] Morrison, F. A. *Understanding Rheology* Oxford University Press. **2001**.

[45] Macosko, C. W. *Rheology: principles, measurements, and applications* VCH. **1993**.

[46] L. Zhang, Ph. D Thesis, University of Minnesota, **2008**.

[47] Macosko C. W. *RIM, fundamentals of reaction injection molding*. New York: Hanser Publishers. **1989**.

[48] Hager K. F, Brandien J. E. *J Cell. Plast*. **1968**, 4, 298.

[49] Vespoli N. P, Alberino L. M. *Polym. Proc. Eng*. **1985**, 3, 127.

[50] Bogdan, M.; Hoerter, J.; Moore. F. O. *J. Cell. Plast*. **2005**, *41*, 41

[51] Thoen, J. A.; Gum, W.F.; Riese, W.; Ulrich, H. *Rigid cellular plastics*. p. 290 in Reactive Polymers, Hanser, Munich , **1992**.

[52] Hiemenz C. P, Lodge P. T. *Polymer Chemistry*. CRC Press. **2007**.

[53] Personal communication with Don Ference from Cargill, 2009.

[54] Kollmeier H. J, Schator H, Zaeske P. *Proceedings of the SPI 26th Annual Technical/Market Conference 1981, San Francisco*, Society of the Plastics Industry, New York, **1982**, pp. 219-220.

[55] Lim H, Kim S. H, Kim B. K. *eXPRESS Polymer Letters*. **2008**, 2, 194.

[56] Han M. S, Choi S. J, Kim J. M, Kim Y. H, Kim W. N, Lee H. S, Sung J. Y. *Macromol. Res.* **2009**, 17, 44.

[57] Eilbracht C, Hohl P. *J. Cell. Plast*. **2005**, 41, 323.

[58] Rosen M. J. *Surfactants and Interfacial Phenomena*. John Wiley & Sons, Inc. **2004**.

[59] Griffiths P. R. *Fourier Transform Infrared* Spectrometry John Wiley & Sons, Inc. **2007**.

[60] Christy A. A. *Modern Fourier Transform Infrared Spectroscopy* Elsevier. **2001**.

[61] Schmitt T. M. *Analysis of Surfactants*. Marcel Dekker, Inc. **2001**.

[62] http://www.wcaslab.com/tech/tbftir.htm

[63] Rutnakomoituk M, Ngamdee P, Phinyocheep P. *Polymer*. **2005**, 46, 9742.

[64] Chen S, Hua Z, Fang Z, Qi G. *Polymer*. **2004**, 45, 6519.

[65] Inoue T, Ohmura H, Murata D. *J. Colloid. Interface Sci.* **2003**, 258, 374.

[66]Huibers P. D. T, Shah D. O, Katritzky A. R. *J. Colloid. Interface Sci*. **1997**, 193, 132.

[67] Alsoy S. *J. Cell. Plast*. **1999**, 35, 247.

[68] Modesti M, Lorenzetti A, Dallacoua C. *Polym. Eng. Sci.* **2004**, 44, 2229.

[69] Olsson M. E, Jarfelt U. *J. Cell. Plast*. **2002**, 38, 177.

[70] Wilkes K. E, Gabbard W. A, Weaver F. J. For presentation at the Polyurethanes Conference 2000, Boston, MA.

[71] Bartlett P. L, Creazzo J. A, Hammel H. S. *J. Cell. Plast*. **1994**, 30, 126.

[72] Pye D. G, Hoehn H. H, Panar M. *J. Appl. Polym. Sci*. **1976**, 20, 1921.

[73] Jeong H. K, Krych W, Ramanan H. Nair S, Marand E, Tsapatsis M. *Chem. Mater*. **2004**, 16, 3838.

[74] Kim H. Ph. D Thesis, University of Minnesota, **2009**

[75] Comyn J. *Polymer Permeability*. Elsevier Applied Science Publications, London and New York. **1985**.

[76] Van Krevelen D. W. *Properties of Polymers*. Elsevier Science Publishing Company Inc. **1990**.

[77] Somani K. P, Patel, N. K, Kansara S. S, Rakshit A. K. *J. Macromol. Sci. Part A Pure Appl. Chem*. **2006**, 43, 797.

[78] Desai S, Thakore I. M, Sarawade B. D. *Polym. Eng. Sci*. **2000**, 40, 1200.

[79] George S. C, Thomas S, Ninan K. N. *Polymer*. **1996**, 37, 5839.

[80] Hill A. J, Freeman B. D, Jaffe M, Merkel T. C, Pinnau I. *J. Mol. Struct*. **2005**, 739, 173.

[81] Fox T. G, Flory P. J. *J. Appl. Phys*. **1950**, 21, 581.

[82] Kwisnek L, Nazarenko S, Hoyle C. E. *Macromolecules.* **2009**, 42, 7031.

[83] Appelqvist L. A. In: Robbenlen G, Downey R. K, Ashri A, editors. *Oil crops of the world*. Ed, New York: McGraw-Hill, **1989**.

[84] Ward W. J, Gaines G. L, Alger M. M, Stanley T. J. *J. Membr. Sci*. **1991**, 55, 173.

[85] Takahashi S, Goldberg H. A, Feeney C. A, Karim D. P, Farrell M, OLeary K, Paul D. R. *Polymer*. **2006**, 47, 3083.

Appendix A Needle Probe Method for Thermal Conductivity Measurement of Rigid Polyurethane Foams

Harikrishnan et. al have reported a simple and rapid technique based on a transient measurement using a needle probe. [1] The needle probe is widely used in the measurement of k value and thermal diffusivity of liquids and solids. [2] Using a needle probe, the time required to get the data is very short and the data accuracy is within 5%. [2] In this technique, [1] a short pulse of energy is discharged into a needle probe embedded inside the sample. The rate of pulse penetration depends on the thermal conductivity of the sample. The temperature decays as a function of time and is measured and used to calculate the sample's k value. This method does not require large sample size which is very suitable for small sample size from lab scale experiments. Usually, the heating area is just 2-3 times of the thermistor which is about 15mm. The equipment setup is simple, cheap and easy to operate. The values of k value obtained from this technique are found to be comparable to those from the standard test measurement. [1] Measurements are done by inserting the needle probe into the sample center. The measurement is based on the Wheatstone bridge circuit. R_2 and R_3 should be set to be equal and large enough to avoid large current flow. In the experiment, $R_2 = R_3 = 20\ k\Omega$. The resistance of the probe R_p is measured and set to be equal to R_1 by adjusting a zero voltage across the bridge before the measurement. A short pulse of energy is applied to the sample through the needle probe. After the completion of the pulse, the acquisition of the bridge voltage and the voltage cross the thermistor is obtained. [1] The change of the voltage across the bridge indicates the change of R_p due to the temperature change in the foam. Using the program

labview to convert the signal of voltage change to temperature change, k value over time is plotted. k value of the foam is the k value at which it reaches a plateau. Figure A-1 is the scheme representing the pulse/temperature measuring circuit. Scheme for the needle probe is shown in Figure A-2. The complete setup of k value measurement from needle probe method used in the lab can be found in Figure 2.2.

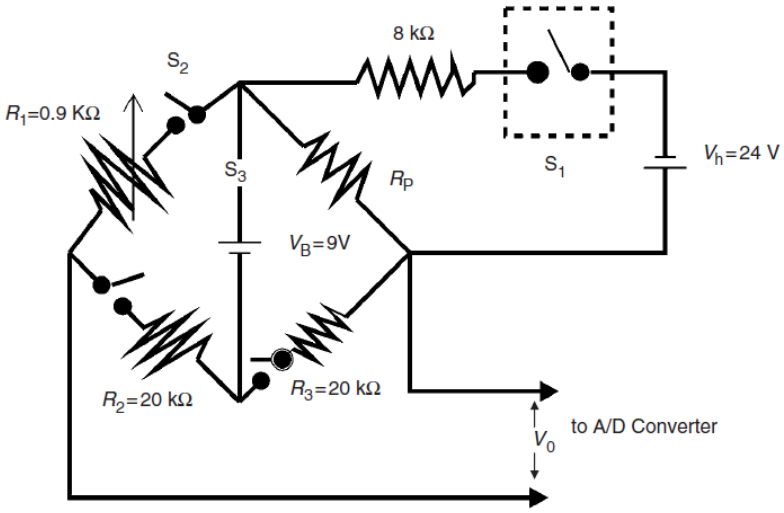

Figure A-1: Pulse/temperature measuring circuit.

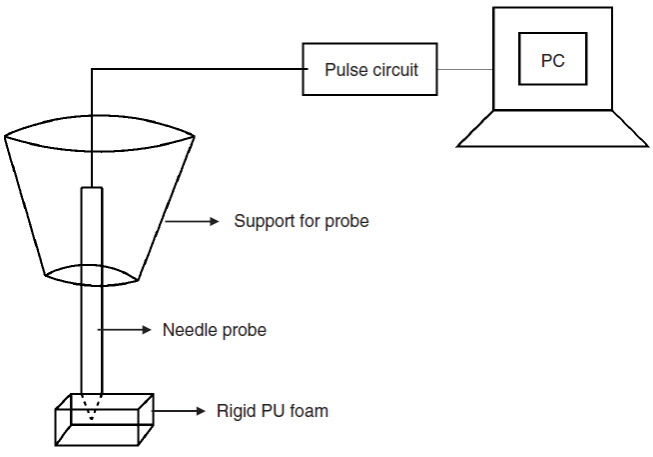

Figure A-2: Needle probe setup for k value measurements.

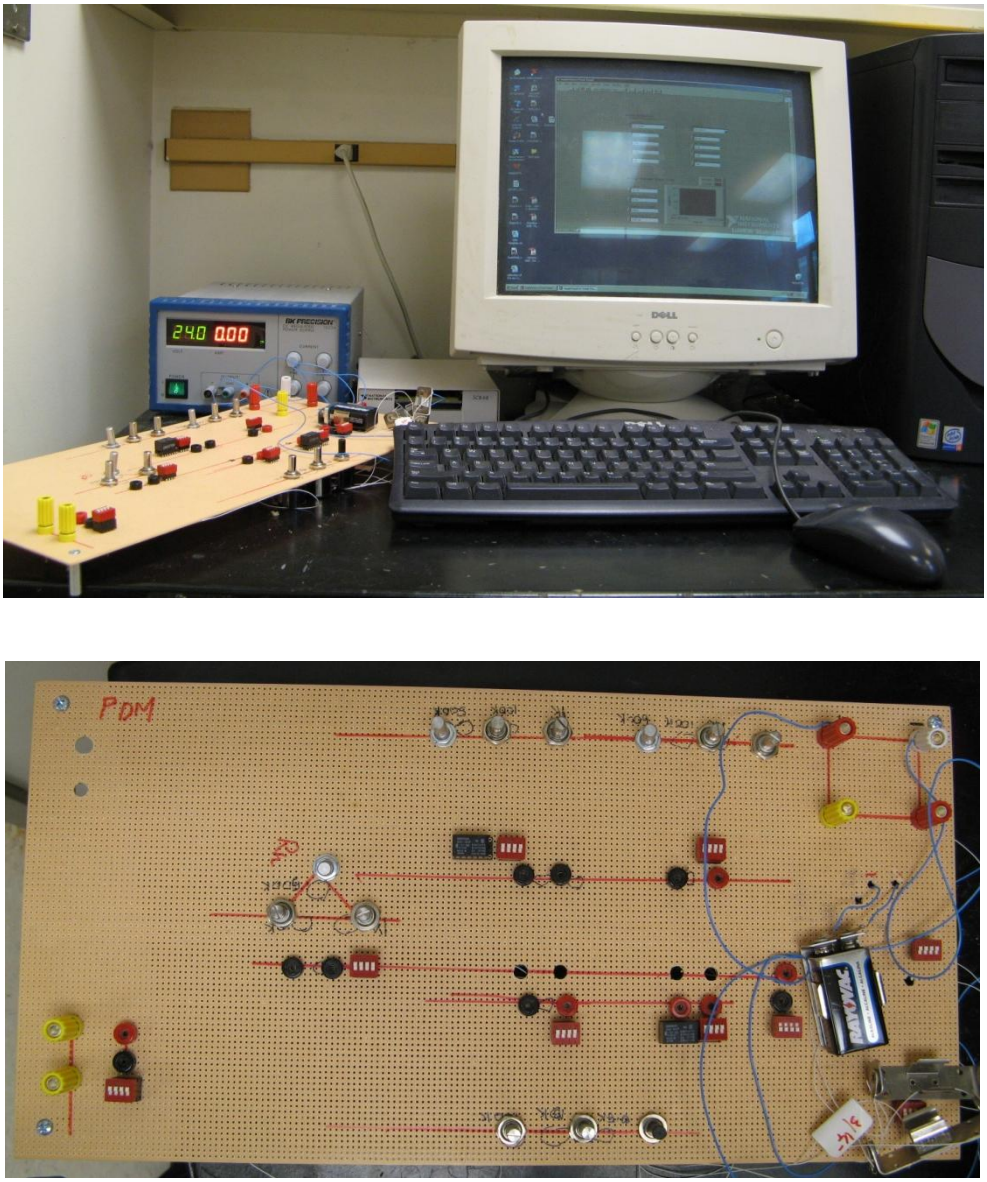

Figure A-3: (top) Complete setup of k value measurement from needle probe method, from left to right: circuit board, power supply, computer (with labview program); (bottom) closer look on the circuit board.

Appendix B Thermal Conductivity Measurement from AR-G2 [3]

Thermal conductivity (k value) measurement from AR-G2 is based on a steady state method. In such a method, a typical k value measurement is based on the rate of steady state heat transfer across the foam with known thickness, which is induced by two different known temperatures between two opposite surfaces of the foam. There are mainly two differences when measuring the k value using AR-G2 rather than the typical plates. Figure B-1 shows the k value measurement setup using AR-G2. The sample is cut into a foam disk with thickness ranging from ½ to 3 inches and a larger diameter than the EHP Heat Spreader. Before placing the foam disk against the peltier plate, a thin layer of thermal conductive paste is put on both sides of the disk to ensure good contact between foam sample and the plates. A 25mm EHP tool with UTS is placed against the foam disk on the other side. The peltier plate is kept at a constant temperature of 35 ℃ and the temperature of the upper surface of the foam disk is monitored by UTS. The foam sample and geometry are surrounded by a large PS foam cup with the bottom removed to reduce external heat transfer. However, there is still some external heat transfer even with the protection. Equations B-1 and B-2 are the basic equations for heat calculation. From the equations we could see that $q_{conduction}$ must be known in order to measure k value for unknown samples. However, q_{total} and q_{lost} are still unknown in the measurement. For a first approximation, we can assume that q_{total} and q_{lost} keep constant for all materials. So if we measure a known k value material, $q_{conduction}$ can be obtained. Measuring the temperature difference and gap, k value of an unknown sample is calculated from

Equation B-2. A typical temperature profile of upper surface of the sample was shown in Figure B-3.

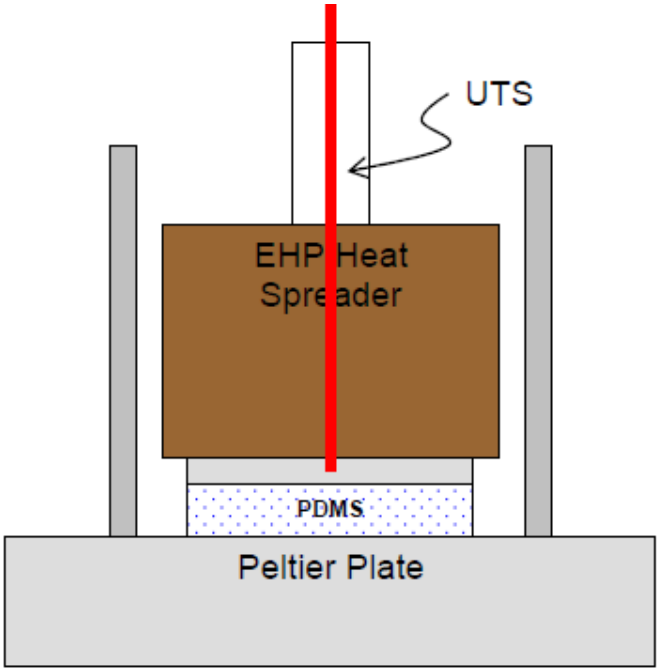

Figure B-1: k value measurement setup using AR-G2.

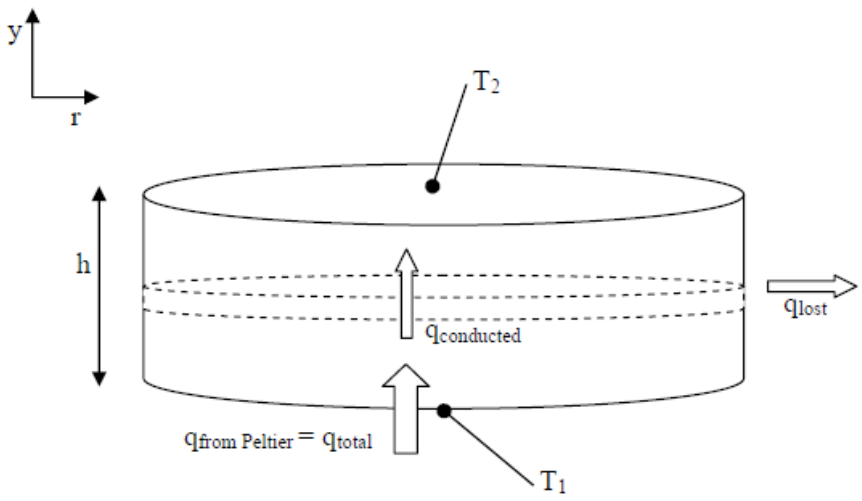

Figure B-2: Scheme of the heat transfer in the sample.

$$q_{total} = q_{conduction} + q_{lost} \qquad \text{Equation B} - 1$$

$$q_{conduction} = -k \cdot \frac{dT}{dy} = -k \cdot \frac{T_{final} - T_{initial}}{h} = q_{total} - q_{lost} \qquad \text{Equation B} - 2$$

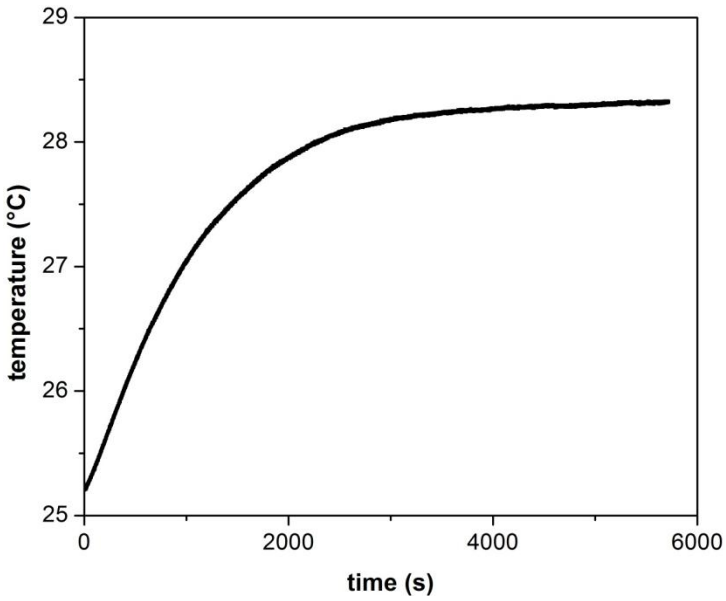

Figure B-3: Temperature profile of the upper sample surface.

Calibration was done on a polyurethane rigid foam sample with a known k value measured by needle probe method. Different thicknesses (1/2, 1 and 1 ½ inches respectively) of foam disks were cut and tested using the AR-G2. The temperature of peltier plate was kept at 35 ℃ and temperature of upper sample surface was monitored for 1.5 hours. The plot of $q_{conduction}(k\Delta T/h)$ vs. h was used as the calibration curve. The k value of the unkown sample was calculated from equation B-2.

The process of foam k value aging was monitored using AR-G2 with the above calibration curve. Foam disks were cut and cured at 70 ℃ in the oven. The samples were taken out and k value was then measured. Table B-1 listed the parameters and calculated k value from the measurement using the AR-G2. From the discussion from Chapter 2 to Chapter 4 that, k value increased as aging time increased. However, the calculated k value did not show a trend for k value aging.

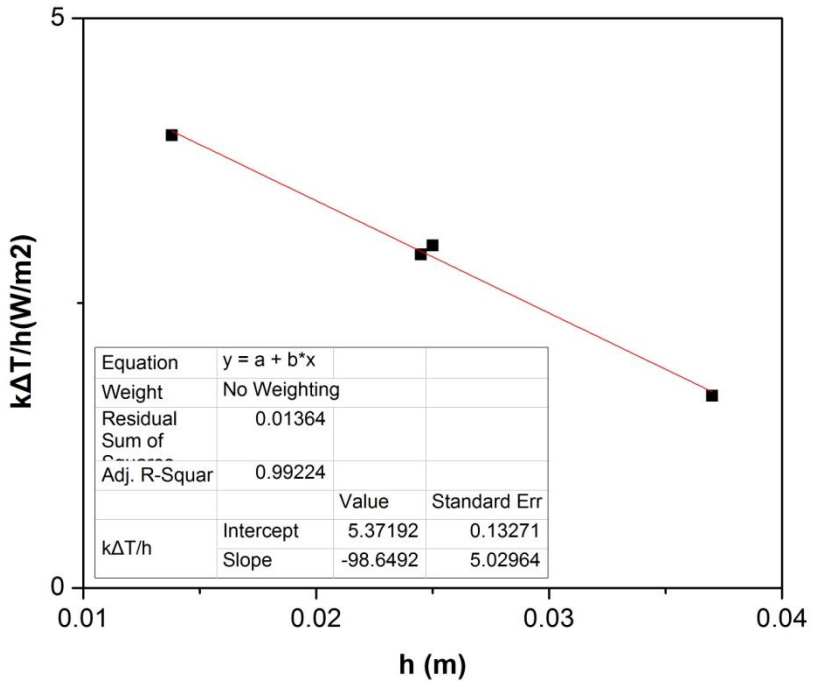

Figure B-4: Calibration curve of k value measurement using AR-G2.

Table B-1: Sample parameters and calculated k value from AR-G2 (Control B sample).

Aging time (h)	Thickness (m)	T_{final}-$T_{initial}$ (℃)	Calculated k value (mW/(m K))
3	0.0105	2.635	17.3
7	0.0135	2.290	23.8
31	0.015	3.400	17.2

Appendix C Mini Polyurethane Rigid Foam

In Chapter 2 and 4, polyurethane rigid foams were made from total reaction mixture of about 90 g. But for the foam kinetics study, total reaction mixture was about 25g. Mini-polyurethane rigid foams were made to study the feasibility of using less amount of reaction mixture for foam kinetics study. In this study, polyurethane rigid foams were synthesized from formulation B with reaction mixture of about 25 g. Foam density, k value and cell morphology (characterized using optical microscopy) were characterized and compared to the foams made from reaction mixture of about 90 g.

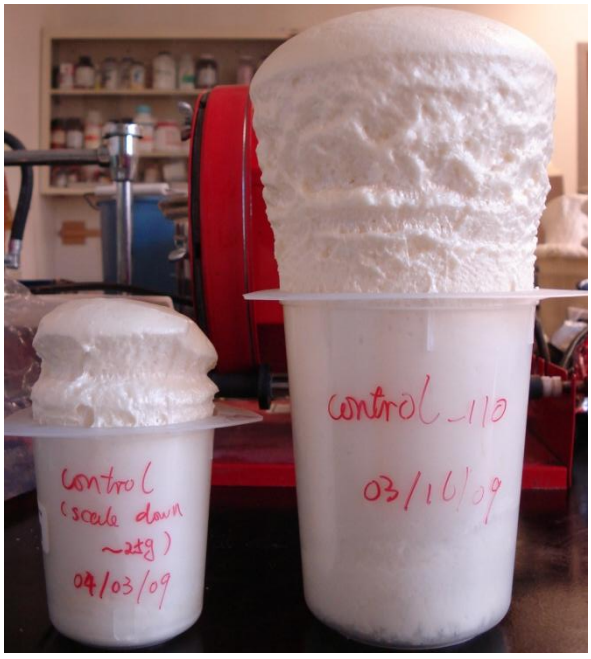

Figure C-1: Foam appearance: (left) mini-Control B, (right) Control B.

Table C-1: Properties summary of mini-polyurethane rigid foams and polyurethane rigid foams.

Foam type	Density (kg/m^3)	k value (mW/(mK))
Control B	39.5 ±0.8	24.4 ±0.04
Mini-Control B	40.5 ±0.9	23.8 ±0.06

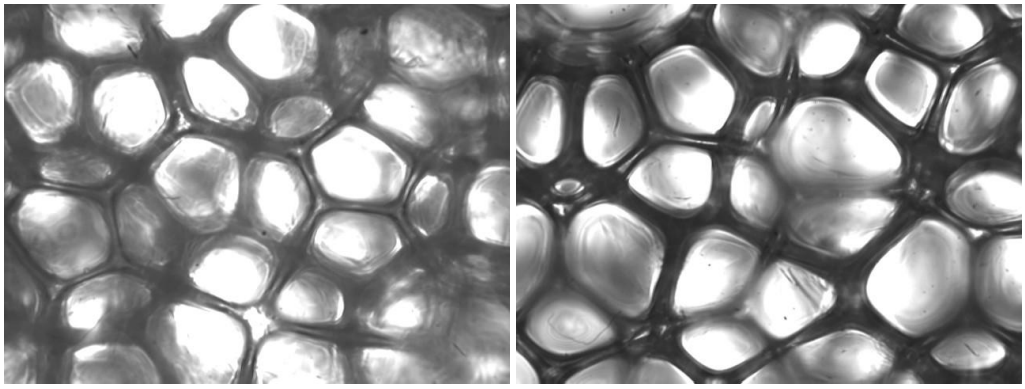

Figure C-2: Optical microscopy images (20x): (left) Control B; (right) mini-Control B.

It was shown from Table C-1 that mini-foams had comparable foam appearance, density and k value. Mini-foams also had comparable cell morphology with foams from reaction mixture of 90 g. Therefore, foam kinetic study on reaction mixture of 25 g can be used to study the foam kinetic of reaction mixture of 90 g.

Appendix D Gas Composition Analysis using Gas Chromatography

k value change of polyurethane rigid foams over time was due to the gas composition change. In Chapter, gas permeability analysis was done on polyurethane thin film to eliminate the complexities caused by cell morphology. However, gas permeability analysis must be done on foam samples in order to further study the gas composition change during foam aging process. Gas chromatography can be used to analyze the gas composition. [4]

Foam slice samples with the dimension of 2.5”×2.5”×0.5” were taken from the center of the foam in order to avoid the border effect. The samples were compressed completely to destroy the cell structures and the escaping gas was introduced into the GC to be analyzed. In order to perform quantitative analysis, small amount of methane which was about 3 ml was introduced into the gas mixture as the external standard. Both flame ionization detection (FID) and thermal conductivity detector (TCD) were used to analyze the gas. FID was sensitive primarily to methane and pentane, while TCD was used to detect air. Figure D-1 showed the GC spectrum from FID (top) and TCD (bottom). The peaks in the FID spectrum were corresponding to methane and pentane respectively, the peak in the TCD spectrum showed the trace of air. Parameters were to be adjusted to separate O_2 and N_2.

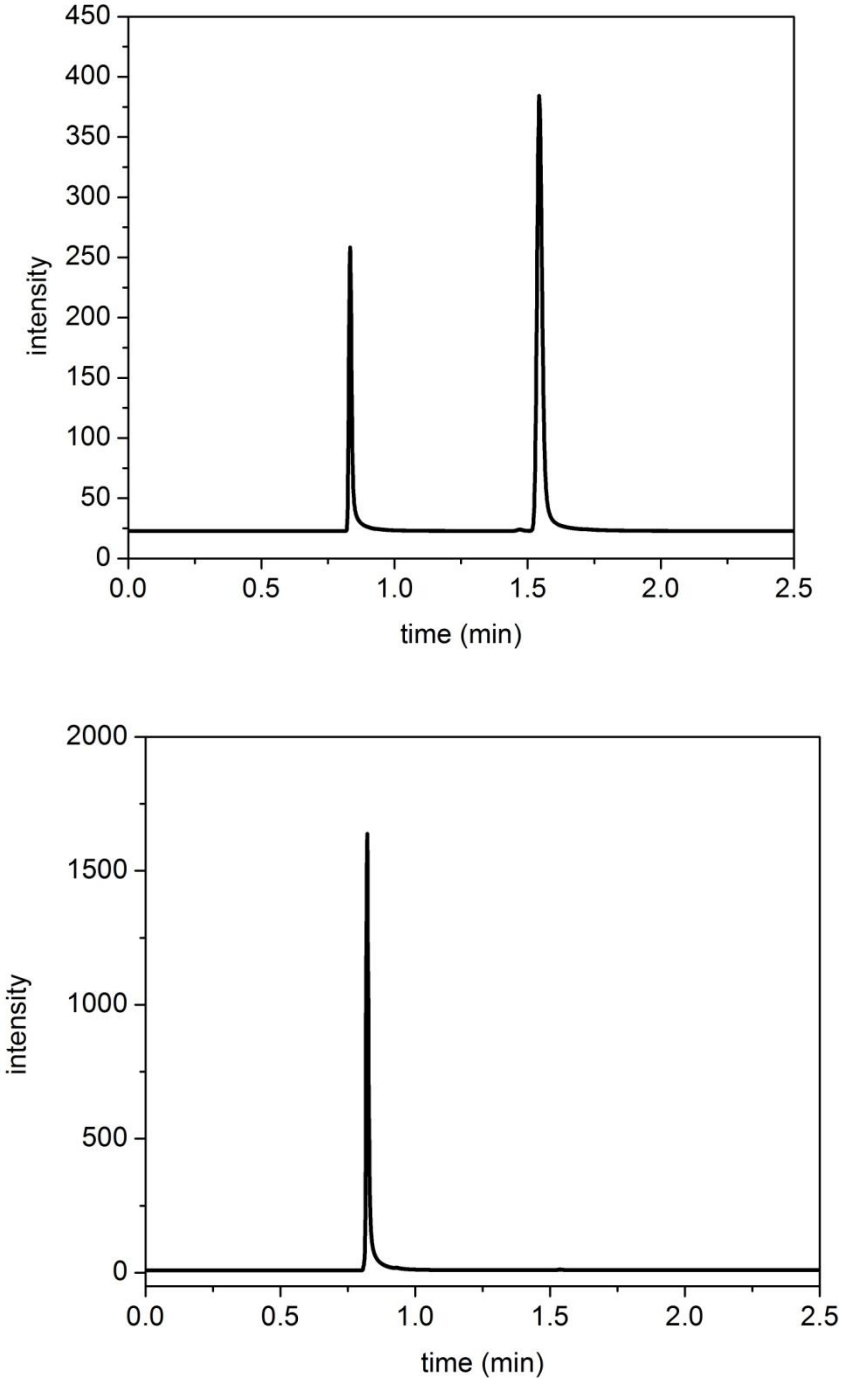

Figure D.1: GC spectrum: (top) FID showed trace of methane and pentane; (bottom) TCD showed trace of air.

References:

[1] Harikrishnan, G.; Macosko, C. W.; Choi, J. H.; Bischof, J. C.; Singh, S. N. *J Cell Plast*, **2008**, *44*, 481.

[2] Asher, G. B.; Sloan, E. D.; Graboski, M. S. *Int J Thermophys* **1986**, *7*, 285.

[3] AR-G2 thermal conductivity option manual from TA Instrument.

[4] Modesti M, Lorenzetti A, Dallacoua C. *Polym. Eng. Sci.* **2004**, 44, 2229.